Design and verification of discontinuity regions in reinforced concrete structures with the strut and tie method

Stress redistribution due to cracking and plastic deformation

Kempengren, Kent

2023

Document Version:
Publisher's PDF, also known as Version of record

Design and verification of discontinuity regions in reinforced concrete structures with the strut and tie method

Stress redistribution due to cracking and plastic deformation

KENT KEMPENGREN | FACULTY OF ENGINEERING | LUND UNIVERSITY

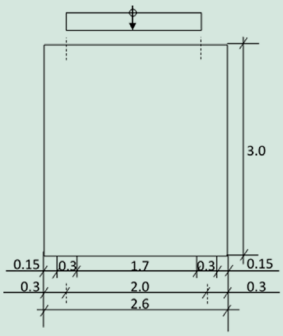

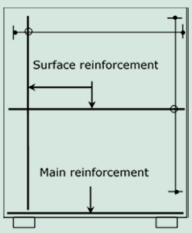

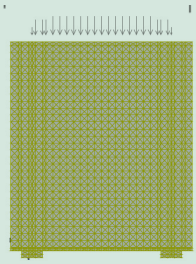

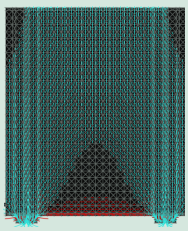

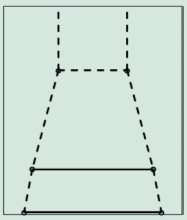

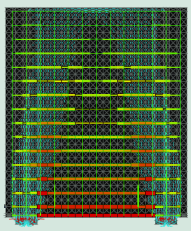

Design and verification of discontinuity regions in reinforced concrete structures with the strut and tie method

Design and verification of discontinuity regions in reinforced concrete structures with the strut and tie method

Stress redistribution due to cracking and plastic deformation

Kent Kempengren

LUND
UNIVERSITY

LICENTIATE DISSERTATION
by due permission of the Faculty of Engineering, Lund University, Sweden.
To be defended at lecture hall V:D, V-Huset, John Ericssons väg 1, Lund, on
Thursday, the 14th of December 2023 at 10:00.

Faculty opponent
Dr. Morgan Johansson

Organization: LUND UNIVERSITY	**Document name:** LICENTIATE DISSERTATION
	Date of issue: 14 December 2023
Author: Kent Kempengren	Sponsoring organization: AFRY

Title and subtitle: Design and verification of discontinuity regions in reinforced concrete structures with the strut and tie method - Stress redistribution due to cracking and plastic deformation

Abstract: Linear and nonlinear FE-analyses are used increasingly in design and verification of continuity and discontinuity regions in reinforced concrete structures. This has been made possible by the increasing access to various calculation programs on the market with their increasingly user-friendly interfaces. These linear and nonlinear FE-analyses require knowledge of the input data. The inputs are models of the realities and can relate to the selection of structures, geometries, materials, loads, boundary conditions, etc., all of which have decisive influence on the results. By results in this context is meant, for instance, the load effects used as a basis for design and detailing in connection with new structures, or used in analyses for verification purposes and studies of load-bearing capacity and load carrying mechanism of existing structures. It is obvious that helpful tools are needed to evaluate and interpret these results and ensure that they are accurate.

Such tools, based on stress fields and strut and tie models, exist and are available. Guidelines for how to use them have been around for a long time, and the recommendations have been to base them on linear-elastic, uncracked analyses, i.e. to ignore the effects of cracking and plastic deformations. In recent years, there has been increasing use of systematized and automated processes for producing stress fields and strut and tie models based on nonlinear FE-analyses. However, the use of these automated processes must not replace a basic understanding of the impact of various factors on the redistribution of the stress fields and of how to choose these stress fields most suitably for different types of reinforced concrete structures in order to meet the requirements of both the ultimate and the serviceability limit state, as well as obtaining an economical and practical arrangement of the reinforcement.

This licentiate thesis concerns simply supported deep beams loaded with a uniformly distributed load at the top with the aim to produce a well-functioning FE-model, to obtain a basic understanding of the stress redistribution that takes place when loading up to the point of failure and to show the consequences of alternative strut and tie models in terms of fulfilment of various requirements. The studies are conducted in a model world and are thus performed by examining, with the help of nonlinear FE-analyses, the impact of the conditions that are present. The major conclusions that can be highlighted are as follows:

- Large stress redistributions occur during cracking already before the reinforcement yields.
- A strut and tie model following the linear elastic stress field clearly underestimates the load-bearing capacity in the ultimate limit state and overestimates the stress in the reinforcement during the service state.
- The ultimate and the serviceability limit state can be dealt with, in terms of optimal utilisation, by use of different strut and tie models not following the elastic stress field.
- A strut and tie model utilising the compressive strength of the concrete in the horizontal strut at the upper edge of the deep beam can be used for determining the load-bearing capacity in the ultimate limit state.
- In order to determine the stress in the reinforcement used to calculate the crack width in the serviceability limit state a strut and tie model that not follows the linear stress field can be used. It can then be recommended to use a stress redistribution corresponding to an increase in the inner lever arm, compared to the one for the linear elastic stress field. The increase can cautiously be chosen to be 25 percent of the difference between the inner lever arm for the maximum stress redistribution, that is full utilisation of the compressive capacity of the concrete, and the inner lever arm for the linear elastic stress field. A larger stress redistribution might be possible, but this requires data from more studied cases.

It should be noted that the conclusions above apply under the conditions given in the studies, especially the conditions regarding low reinforcement ratio. The conclusions do not contradict results obtained, for corresponding structures, by other researchers. However, if this is in agreement with the general opinion among practicing designers, is a different matter. There are a lot of indications that earlier recommendations, such as use of the linear elastic stress field in both the ultimate and the serviceability limit state often are applied without further reflection, which would mean that the users should update their knowledge in the area. This shows that there is a need for the transfer of state-of-the-art through the various channels that exist between research at universities and application in society.

Key words: Nonlinear FE-analyses, Stress fields, Strut and tie method, Stress redistribution, Discontinuity region

Classification system and/or index terms (if any):

Supplementary bibliographical information: ISRN LUTVDG/TVBK-22/1057-SE		Language: English
ISSN and key title: 0349-4969, Report TVBK-1057		**ISBN:** 978-91-87993-23-7
Recipient's notes:	**Number of pages**:125	Price:
	Security classification:	

Signature Date 2023-10-22

Design and verification of discontinuity regions in reinforced concrete structures with the strut and tie method

Stress redistribution due to cracking and plastic deformation

Kent Kempengren

LUND
UNIVERSITY

Front cover: Illustrate for a deep beam, geometry, reinforcement, FE-model, stresses in the concrete using linear analysis, strut and tie model and stresses in the concrete and in the reinforcement using nonlinear analysis. Stresses calculated by use of the program EvalS.

Faculty of Engineering
Department of Building & Environmental Technology
Division of Structural Engineering

Report: TVBK-1057
ISBN: 978-91-87993-23-7
ISSN: 0349-4969
ISRN: LUTVDG/TVBK-22/1057-SE

Printed in Sweden by Media-Tryck, Lund University
Lund 2023

Dedicated to my beloved wife, Marie

Contents

Acknowledgement

My interest in research began before I finished my Master's degree and this interest has remained throughout my time thus far in my profession. There are countless evenings in which I have deepened myself in technical problems that have arisen during the working day. My interest in the strut and tie method began quite early. I appreciated its clear and pedagogical way of describing how a structure carries its loads. What finally determined the direction of my research was literature written by, and discussions I had with, Professor Björn Engström, of the subject.

The work presented in the thesis would not have been possible without the financial support I received from AFRY. For this I am very grateful. In addition, Scanscot Technology has sponsored the research project by giving me free access to the FE-program BRIGADE, for which I am also very grateful.

I want to thank my supervisor Professor Annika Mårtensson for her ability to drive me forward in the process. Thanks also to my assistant supervisor Oskar Larsson Ivanov for his input during my work on the articles and the thesis. I want also to thank my assistant supervisor Professor Sven Thelandersson both for his initial support and his continued encouragement. I thank also Associate Professor Kamyab Zandi for his input on issues related to FE-modeling. I would like to thank all of you for the guidance you have given me along the way to this licentiate degree. I look forward to continued cooperation with you.

I would like also to address special thanks to Professor Björn Engström, who unfortunately is no longer with us, for his deep commitment to and knowledge of the subject. The fact that, despite his being a very busy man, he still took the time he did and became very much involved in the project was invaluable for me.

I would also like to thank Tomas Ekström, AFRY, and Linus Andersson, Scanscot Technology, for their participation in the reference group and their accessibility throughout of the project.

Not least important has been the working climate and spirit I have had around me. For this, I would like to thank my colleagues at the Division of Structural Engineering and the Section of Bridge and Plant Design at AFRY.

All of this work would not have been possible without the support that I received from family and friends, and not least from my wife Marie. You have encouraged and supported me the whole time, despite my late evenings and nights in front of the computer and studying the literature. Thank you, my love.

Summary

Linear and nonlinear FE-analyses are used increasingly in design and verification of continuity and discontinuity regions in reinforced concrete structures. This has been made possible by the increasing access to various calculation programs on the market with their increasingly user-friendly interfaces. These linear and nonlinear FE-analyses require knowledge of the input data. The inputs are models of the realities and can relate to the selection of structures, geometries, materials, loads, boundary conditions, etc., all of which have decisive influence on the results. Results are for example the load effects used as a basis for design and detailing in connection with new structures. It can also be analyses for verification purposes and studies of load-bearing capacity and load carrying mechanism of existing structures. It is obvious that helpful tools are needed to evaluate and interpret these results and ensure that they are accurate.

Such tools, based on stress fields and strut and tie models, exist and are available. Guidelines for how to use them have been around for a long time, and the recommendations have been to base them on linear-elastic, uncracked analyses, i.e. to ignore the effects of cracking and plastic deformations. In recent years, there has been increasing use of systematized and automated processes for producing stress fields and strut and tie models based on nonlinear FE-analyses. However, the use of these automated processes must not replace a basic understanding of the impact of various factors on the redistribution of the stress fields and of how to choose these stress fields most suitably for different types of reinforced concrete structures in order to meet the requirements of both the ultimate and the serviceability limit state, as well as obtaining an economical and practical arrangement of the reinforcement.

This licentiate thesis concerns simply supported deep beams loaded with a uniformly distributed load at the top with the aim to produce a well-functioning FE-model. The aim is also to obtain a basic understanding of the stress redistribution that takes place when loading up to the point of failure. The consequences of alternative strut and tie models in terms of fulfilment of various requirements are also studied. The studies are conducted in a model world and are thus performed by examining, with the help of nonlinear FE-analyses, the impact of the conditions that are present.

The major conclusions that can be highlighted are as follows:

- Large stress redistributions occur during cracking already before the reinforcement yields.
- A strut and tie model following the linear elastic stress field clearly underestimates the load-bearing capacity in the ultimate limit state and overestimates the stress in the reinforcement during the service state.

- The ultimate and the serviceability limit state can be dealt with, in terms of optimal utilisation, by use of different strut and tie models not following the elastic stress field.
- A strut and tie model utilising the compressive strength of the concrete in the horizontal strut at the upper edge of the deep beam can be used for determining the load-bearing capacity in the ultimate limit state.
- In order to determine the stress in the reinforcement used to calculate the crack width in the serviceability limit state a strut and tie model that not follows the linear stress field can be used. It can then be recommended to use a stress redistribution corresponding to an increase in the inner lever arm, compared to the one for the linear elastic stress field. The increase can cautiously be chosen to be 25 percent of the difference between the inner lever arm for the maximum stress redistribution, that is full utilisation of the compressive capacity of the concrete, and the inner lever arm for the linear elastic stress field. A larger stress redistribution might be possible, but this requires data from more studied cases.

It should be noted that the conclusions above apply under the conditions given in the studies, especially the conditions regarding low reinforcement ratio. The conclusions do not contradict results obtained, for corresponding structures, by other researchers. However, if this is in agreement with the general opinion among practicing designers, is a different matter. There are a lot of indications that earlier recommendations, such as use of the linear elastic stress field in both the ultimate and the serviceability limit state often are applied without further reflection, which would mean that the users should update their knowledge in the area. This shows that there is a need for the transfer of state-of-the-art through the various channels that exist between research at universities and application in society.

Sammanfattning

Linjära och olinjära FE-analyser används allt mer vid dimensionering och verifikation av kontinuitets- och diskontinuitetszoner i armerade betongkonstruktioner. Detta har möjliggjorts av en ökad tillgång till olika beräkningsprogram på marknaden med allt mer användarvänliga gränssnitt. Dessa linjära och olinjära FE-analyser kräver kunskap om den givna indatan. Indatan är modeller av verkligheten och kan avse val av bärverk, geometrier, material, laster, randvillkor, m.m., vilka alla har ett avgörande inflytande på resultatet. Med resultat menas i detta sammanhang, t.ex., lasteffekter som används som underlag för dimensionering och detaljutformning vid nykonstruktion. Det kan också vara analyser för verifikation och studier av bärförmåga respektive bärande mekanism hos befintliga konstruktioner. Det är uppenbart att användbara verktyg behövs för att tolka, utvärdera och för att försäkra sig om riktigheten av dessa erhållna resultat.

Denna typ av verktyg, baserade på spänningsfält och fackverksanalogier, finns och är tillgängliga. Riktlinjer för hur dessa ska användas har funnits under en längre tid och rekommendationerna har då varit att utgå från linjärelastiska ospruckna analyser, d.v.s. att bortse från effekter av uppsprickning och plastiska deformationer. Nu på senare år har det skett en ökad användning av systematiserade och automatiserade processer för framtagning av spänningsfält- och fackverksmodeller baserade på olinjära FE-analyser. Användningen av dessa automatiserade processer får dock inte ersätta en grundläggande förståelse för olika faktorers inverkan på spänningsfältens omfördelning och för hur man lämpligast väljer dessa spänningsfält för olika typer av armerade betongstrukturer. Väsentligt är att det finns en förståelse på hur dessa val påverkar uppfyllandet av krav såväl i brott- som bruksgränstillståndet samt för att erhålla en ekonomisk och praktisk inläggning av armeringen.

Licentiatavhandlingen behandlar fritt upplagda höga balkar belastade med en jämnt utbredd last i överkant och målet är att ta fram en välfungerande FE-modell. Avhandlingen ska också bidra till en grundläggande förståelse för spänningsomfördelning vid belastning upp till brott samt visa på konsekvenser av alternativa fackverksmodeller avseende uppfyllande av olika krav. Studierna bedrivs i en modellvärld och utförs sålunda genom att undersöka inverkan av givna förutsättningar med hjälp av olinjära FE-analyser.

De större slutsatserna som kan lyftas fram är följande:

- Stora spänningsomfördelningar inträffar under uppsprickning innan armeringen flyter.
- Att följa det linjärelastiska spänningsfältet underskattar kraftigt bärförmågan i brottgränstillståndet och överskattar armeringsspänningarna i bruksstadiet.
- För att optimera bärförmågan i brott- och bruksgränstillståndet används med fördel olika fackverksmodeller i de olika gränstillstånden.
- En fackverksmodell som utnyttjar betongens tryckhållfasthet för den horisontella tryckströvan i överkant av den höga balken kan användas för att bestämma bärförmågan i brottgränstillståndet.
- För att bestämma spänningen i armeringen som används för att beräkna sprickbredden i bruksgränstillståndet kan en fackverksmodell som inte följer det linjärelastiska spänningsfältet användas. Det kan då rekommenderas att använda en spänningsomfördelning motsvarande en ökning av den inre hävarmen, jämfört med den för det linjärelastiska spänningsfältet. Ökningen kan med försiktighet väljas till 25 procent av skillnaden mellan den inre hävarmen för maximal spänningsomfördelning, det vill säga fullt utnyttjande av betongens tryckhållfasthet, och den inre hävarmen för det linjärelastiska spänningsfältet. En större spänningsomfördelning kan vara möjlig, men detta kräver data från fler studerade fall.

Slutsatserna ovan gäller under de förutsättningar som getts i studien, speciellt förutsättningarna avseende lågt armeringsinnehåll. Slutsatserna står inte i motsats till resultat erhållna av andra forskare för motsvarande konstruktioner. Huruvida detta är i överensstämmelse med den allmänna uppfattningen bland praktiserande konstruktörer kan dock diskuteras. Mycket tyder på att tidigare rekommendationer, såsom att t.ex. använda det linjärelastiska spänningsfältet i både brott- och bruksgränstillståndet ofta fortfarande tillämpas utan närmare eftertanke, vilket innebär att den rådande kunskapen bland användare behöver uppdateras. Detta visar på att det finns ett behov av överföring av den senaste kunskapen inom området via de olika kanaler som finns mellan forskning på universiteten och tillämpning i samhället.

1. Introduction

1.1. Background and problem statement

The development and use of numerical methods such as linear and nonlinear FE-analyses in two or three dimensions has increased and will surely increase in the future. The models employed can be complex with regard to the geometry, materials, boundary conditions and loads involved. This complexity makes demands on how the calculations are communicated to facilitate understanding in the review process. There is therefore a need for guidance in how to present the calculation report and how to verify the calculations. The need of this has become increasingly apparent, one example in the literature of efforts to help in this respect being Ekström, et al. [1], whose aim is to provide guidance for review of advanced computer-based calculations in this area.

It is, of course, also important when using FE-calculation programs to be able to interpret and assess the accuracy of the output. It is particularly difficult to interpret the results of linear analyses for a cracked concrete structure because the influence of reinforcement is not considered, and a cracked reinforced concrete structure does not have a linear response. Thus, the output of such analyses does not adequately describe the behaviour of the structures involved. The evaluation of the results of an advanced structural analysis is facilitated by an understanding of how equilibrium in cracked reinforced concrete in a given structure can be secured by means of reinforcement when exposed to loads.

Strut and tie method is a method that can be used for design purposes and for verification of cracked reinforced concrete. It is a pedagogical tool that illustrates how a structure carries a specific load. The method is logical, and leads to an increased conceptual understanding of the mode of operation of cracked reinforced concrete. The method is described, for example, in EN 1992-1-1 [2], sec. 5.6.4 and sec. 6.5.

There are examples in practical design operations in which use of strut and tie models in the design process would have prevented the high cost that the collapse of a structure can bring about. Such a case is the collapse of the Sleipner A 1991 oil platform, see Figure 1. The entire oil platform, worth approximately $ 700 million, collapsed during the towing to an oil field. An inadequate computer analysis with

use of a poor finite element mesh and an insufficient anchorage of the reinforcement (T-headed bar) in a critical zone led to the collapse. A separate investigation also documented a size effect in shear failure resulting in a reduced shear capacity by about 40%. If strut and tie models had been used for the details, the collapse could have been prevented. In the case in question a completely new platform was designed by hand without the help of computers.

More examples exist where the application of simple strut and tie models would have prevented extensive damage with huge costs as a result. Such examples not infrequently concern partially loaded areas that create transverse tension. This is relevant when the support areas, for different reasons, do not have the same dimensions as the structure in general, such as in the case of prefabricated columns with cut-outs at the bottom. From a strut and tie model it would have been clear if there was a need for additional reinforcement to carry the transverse tensile forces. The principle of the strut and tie method is generally applicable to concrete structures, and it is a useful complement to linear and nonlinear FE-analyses.

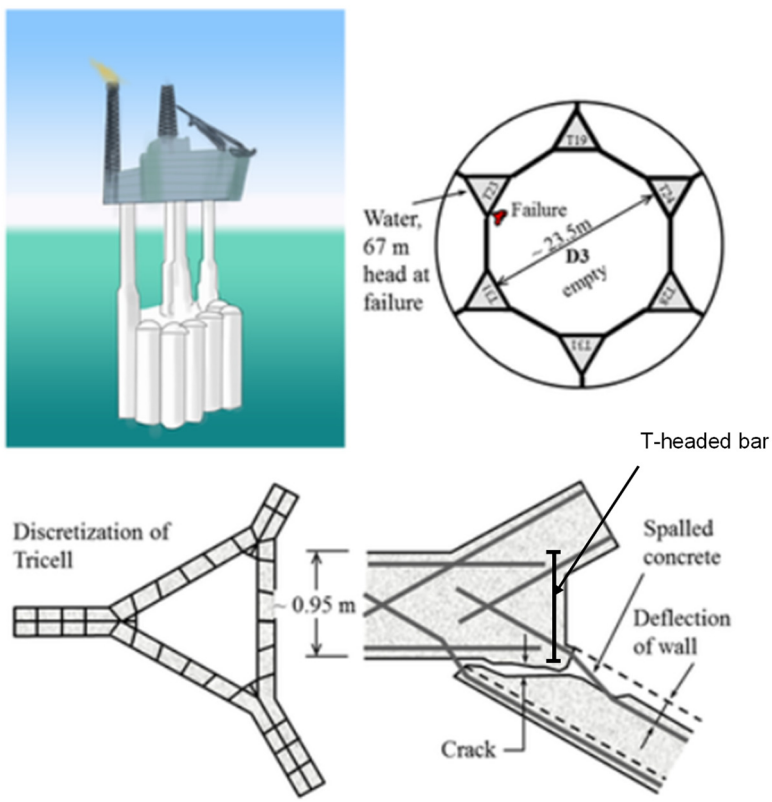

Figure 1
Failure of Sleipner A Oil Platform, Norway 1991

A problem in analysing a concrete structure that cracks with use of linear FE-analysis is that the analysis procedure itself results in stresses occurring in a homogeneous material (uncracked concrete) that carries tensile forces that should instead be carried by the reinforcement alone. A linear FE-analysis does not describe the behaviour of a cracked concrete structure. This means that tensile stresses at each point of the cracked concrete structure cannot be adequately assessed. Because of this the reinforcement is generally not included in the model used for the linear analysis. Instead, the reinforcement is designed in a separate program for the loads obtained in the analysis in the ultimate and serviceability limit state. In this design program the reinforcement is assumed to carry the tension stresses alone and it is assumed to yield in the ultimate limit state regardless of the deformation found in the analysis.

When the concrete is cracked equilibrium is achieved by means of reinforcement. Reinforced concrete is a composite and has a nonlinear mode of action, but linear FE-analysis presupposes there to be linear action in a homogeneous material. All of this can be solved by using nonlinear FE-analysis to study the impact of cracking and of different reinforcement layouts.

The use of the strut and tie method as a complement to FE-analysis clarifies the behaviour of a cracked reinforced concrete structure and contributes to the fulfilment of safety requirements in the ultimate limit state and of functioning in the serviceability limit state. Despite the simplicity of the strut and tie method, it is relatively complex due to the choices required concerning the stress fields (struts and ties), which affect and are affected by the arrangement of the reinforcement and thus the structure's response in terms of resistance, ductility and serviceability. The conditions for these choices also differ between different discontinuity regions, making the method difficult to generalize. Various alternative reinforcement arrangements, for one and the same structure, can be selected to help ensure the equilibrium of cracked concrete. The choice made has consequences with regard to the behaviour of the structure in service and ultimate state. In addition to this practical and economic considerations regarding arrangement of the reinforcement are of importance. Increased knowledge of the consequences of various alternative reinforcement arrangements, especially concerning stress redistribution, makes it possible to assume strut and tie models that better describe the behaviour of cracked reinforced concrete.

Strut and tie models are chosen based on assumed stress fields for which the compressive struts are the resultants of the compressive stresses. For an uncracked concrete structure, a stress field has the same appearance regardless of the load value. The value of the stresses increases linearly with the load. A strut and tie model that has been chosen for a cracked reinforced concrete structure and follows the linear elastic stress field, is assumed to require less stress redistribution than a model

that follows a stress field that deviates from the linear elastic stress field. The question can then be to what extent one can deviate from the linear elastic stress field while still fulfilling different important requirements. Such requirements can be function in serviceability limit state or avoiding premature failure before the stress redistribution that is needed has been reached in ultimate limit state. Stress redistribution takes place through cracking and plastic deformation. Premature failure occurs if the plastic deformation capacity is less than that which is needed for reaching the assumed stress field. Today, there is still limited knowledge of the stress redistributions due to cracking and plastic deformation that is available for discontinuity regions.

1.2. Aim and purpose

The aim of this thesis is to contribute to knowledge concerning stress redistribution due to cracking and plastic deformation, as well as of contributing to the implementation of the strut and tie method as a method to be used increasingly in the design and verification of reinforced concrete structures.

Simple recommendations for guidance purposes can facilitate the choice of suitable strut and tie model and help provide conditions for better optimizing a structure in terms of the functions desired. Today, such recommendations are relatively sparse, are not easy to use and are somewhat inaccessible for daily use.

The overall aim of this licentiate thesis is to summarize the state of art regarding the strut and tie method and to investigate certain basic principles regarding stress redistributions and the fulfilment of requirements in the ultimate and serviceability limit state for simply supported deep beams loaded with a uniformly distributed load.

The more specific aims are the following:

- To produce a functioning model for the nonlinear FE-analysis of simply supported deep beams.
- To obtain a basic understanding of the stress redistribution in simply supported deep beams when loaded to failure.
- To show the consequences of the use of alternative strut and tie models regarding their fulfilment of requirements in the ultimate and serviceability limit state for simply supported deep beams.

1.3. Research questions

The primary research questions dealt with in this licentiate thesis concern simply supported deep beams loaded with a uniformly distributed load. These questions are in particular the following:

- To what extent can one deviate from the linear elastic stress field in the discontinuity region while still fulfilling the functional requirements involved and avoiding premature failure?
- How large can the degree of stress redistribution due to cracking and plastic deformation be?
- What are the conditions for choosing different stress fields for design in the ultimate and serviceability limit state?
- What effects do geometry, material, reinforcement content and reinforcement arrangement, respectively, have on the stress redistribution and the crack development that takes place?

1.4. Limitations

The analyses carried out are performed with use of FE-calculations, conducted in a model world, so to speak. Practical tests are not performed. All the nodes are assumed to be secured from failure and the anchorage provided is regarded as being sufficient, the failure that occurs being assumed to be compressive failure in the struts or tensile failure in the ties.

1.5. Research approach

In this thesis, a discontinuity region corresponding to a deep beam was studied with use of nonlinear FE-analysis. For the same geometry in each case, the impact of different reinforcement arrangements was analysed. The reinforcement arrangements chosen were regarded as being simple and practical, being straight bars without bends placed parallel to one another or orthogonal to the edges of the structure. Nonlinear FE-analyses were performed for the deep beam at increasing load and responses such as crack development together with crack width, stress redistribution, deformation capacity and load-bearing capacity were monitored continuously and recorded. Regarding the idealization and modelling of the

structure, the interaction between concrete and the reinforcement was assumed to follow a given bond slip function and the support reaction was assumed to be uniformly distributed over the width of the support. The consequences of choosing different strut and tie models with their resulting reinforcement arrangements were assessed on the basis of the response in FE-analyses.

The research was carried out at the Division of Structural Engineering at LTH. During the project, discussions was also held with the Division of Structural Engineering, Chalmers University of Technology. The major steps in the project are described below.

1. Literature studies

   In an introductory phase, the available knowledge and theory concerning discontinuity regions, the strut and tie method, the stress field method, stress redistribution and the deformation capacity in discontinuity regions were studied. Answers to questions such as where topic-wise the research front within this area today is located were sought and relevant published articles and reports within this area were read.

2. The basis for FE-analyses

   At this stage, a specific discontinuity region, its geometry and different reinforcement arrangements were chosen for further study. FE-analysis requires knowledge of input data such as the type of analysis conducted (static, quasi-static (loading rate)), the load displacement response (load- or displacement controlled), the material relationships, the interaction of concrete and reinforcements, the boundary conditions and the mesh. Here, the effects on the results of calculations that different choices of input data have were investigated, comparisons being made with similar modelling reported in the literature. Problems of convergence are quite common in nonlinear analyses. This and other problems that can arise in an analysis can be avoided by use of well-chosen input data and solution technique. If the investigation as a whole is properly planned, the results obtained should in the best way possible describe the behaviour of the structure.

3. FE-analyses

   Here nonlinear FE-analyses were performed in a study concerning the cases chosen in step 2. The output of load-displacement relations, inner lever arms, concrete and reinforcement stresses, crack widths and load-bearing capacity are dealt with and are reported in diagrams.

4. Comparisons of the strut and tie method with FE-analyses and conclusions based on studies of the literature.

A study based on the results of the previous stage was carried out, one that compared the results of calculations using the strut and tie method with results obtained by FE-analyses.

1.6. Outline of the thesis

A brief description of the layout of the parts of the dissertation in addition to what has been presented thus far is as follows:

- Chapter 2: Strut and tie method – State of the art

  Here, a historical account of the strut and tie method and other similar methods, such as truss analogy and the stress field method, is presented. The method of topology optimization is also included here as well as methods of systemization that can make the design and assessment of cracked reinforced concrete structures more effective.

  The chapter also takes up the theory of the strut and tie method. Specifically, it deals with the difference between B- and D-regions, and the fact that the strut and tie method complies with plastic analysis, the assumptions upon which the method is based also being outlined. Furthermore, the chapter addresses stress redistribution and its importance for the behaviour in service and ultimate state.

- Chapter 3: Deep beam studies

  The chapter contains two studies. Study 1 investigates the effects of the amount and arrangement of the reinforcement on the load-bearing capacity, the different stress fields, the stress redistribution that occurs, and the crack width. The study concerns a deep beam that has six different reinforcement arrangements, these being subjected to a uniformly distributed load. The structural behaviour involved is investigated by use of nonlinear FE-analysis.

  Study 2 investigates the effects of alternative strut and tie models and reinforcement arrangements in the design of a simply supported deep beam. The beam is limited to a particular set of geometric conditions, a uniformly distributed load being placed on top of the structure. The results from the different models are compared with the responses obtained in nonlinear FE-analyses.

- Chapter 4: Conclusions

  Here, the conclusions arrived at are presented and discussed.

- Chapter 5: Further research

  The chapter suggests further research that is of interest.

1.7. Publications

The following papers have been published by the author:

Nonlinear FE-analysis of stress redistribution in a deep beam
K. Kempengren
Conference paper. Presented at the fib symposium in 2017, in Maastricht, the Netherlands.

Strut and tie Method – A powerful method to use in continuity and discontinuity regions in reinforced concrete structures in the design process
K. Kempengren
Conference paper. Presented at the XXIII Nordic Concrete Research Symposium in 2017, in Aalborg, Denmark.

2. Strut and Tie Method – State of the art

2.1. Introduction

In the design of concrete structures, the main objectives are the achievement of resistance, proper functioning and durability. There are different methods of achieving this. It is advantageous for designers regarding their understanding of the behaviour of the structure that the models involved are consistent, readily understood, and based on uniform theoretical principles. This thesis concerns use of the strut and tie method, a method that is characterized by being both consistent and easy to understand. A brief summary of the theory behind it and its basics characteristics are presented below. The method is closely related to the shear conception, truss analogy and the stress field method. In order to create an overall picture of the state of the art, the truss analogy and the stress field method are therefore also treated.

2.2. Strut and Tie Method

2.2.1. General

The strut and tie method is a practical design method, one often considered to be quite pedagogical and rather easy to understand. In Schlaich and Weischede [3] it is evident that the method can be used as a tool in design. In 1987 Schlaich, et al. [4] presented a comprehensive description how to use the method. The strut and tie method can be seen as a generalization of the truss analogy for beams, and it has been suggested to be a consistent approach to design all types of concrete structures and their parts, this based on the fact that concrete structures carry their loads through compressive fields linked with tensile fields, consisting either of reinforcing steel, prestressing steel or concrete tensile stress fields. The strut and tie model is an idealisation of the current stress fields in which the struts, ties and nodes represent the force resultants of the compression fields, the tension fields and their connections within the stress fields involved, see Figure 2, where struts are represented by dashed lines and ties by solid lines.

Figure 3 illustrate the behaviour and the transition from bending and shear (continuity region) to direct compression (discontinuity region) for a load approaching the support. The closer to the support the load is the more of the load goes directly there.

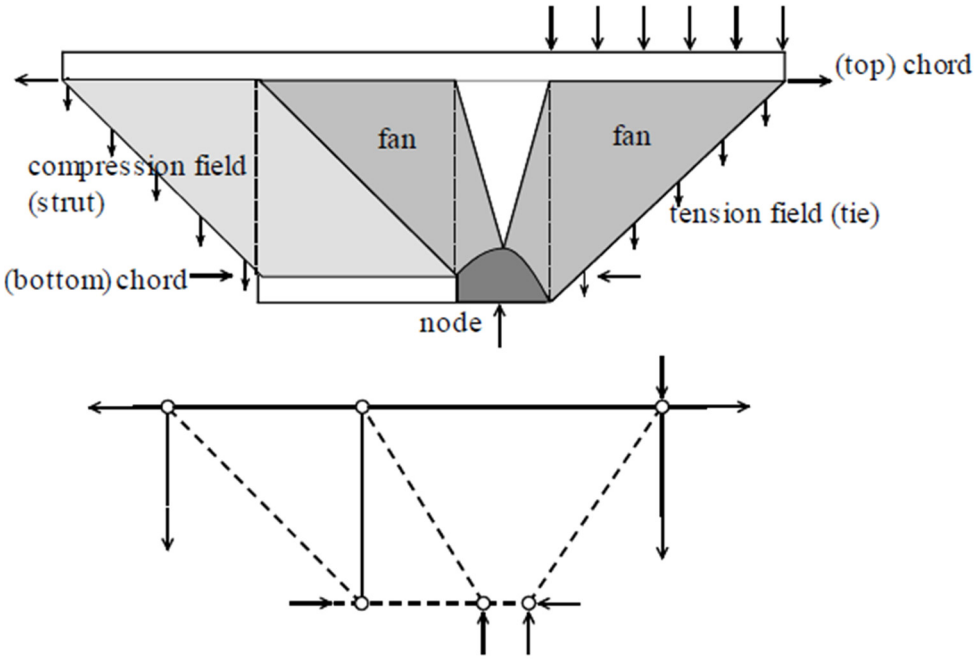

Figure 2
Components of the stress field and the strut and tie method and the statically equivalent truss models. According to the convention struts are represented by dashed lines and ties by solid lines. The struts and ties are inserted between the node points. Reproduced from fib Bulletin 66, Model Code 2010 volume 2, page 77 - “Fig. 7.3-35: Basic Elements for stress field analysis as well as for strut-and-tie modelling and statically equivalent truss models” with permission from the International Federation for Structural Concrete (fib). fib Bulletin 66 [5].

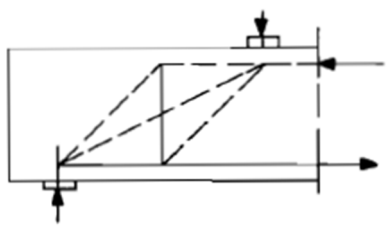

Figure 3
A load carrying system involving the direct thrust and truss analogy. Reproduced from CEB-FIP Model Code 1990, page 159 - “Fig. 6.3.8c: improvement by sharing load between a direct thrust and a lattice system" with permission from the International Federation for Structural Concrete (fib). CEB-FIP Model Code 1990 [6].

The two methods, the strut and tie method and the stress field method, represent basically the same physical behaviour, complementing each other and having their various clear advantages in practical applications. The strut and tie method is best used in deciding where the main reinforcement should be placed, and the stress field method being particularly useful for checking the compression field, designing details and determining where there is a need of distributed minimum reinforcement for crack control.

The strut and tie method can be used both in the ultimate limit state and in the serviceability limit state. For purposes of simplicity and from a practical point of view, the proposal of Schlaich, et al. [4] was to use the same model for both states following the elastic stress field and the theory of plasticity. It was also said that if the aim was to determine the actual ultimate load, another stress field, one not following the linear elastic stress field, could be chosen instead. It is important then to take account of the plastic deformation capacity.

In EN 1992-1-1 [2], sec. 5.6.4 (2), the following is stated:

> Verifications in SLS may also be carried out using strut-and-tie models, e.g. verification of steel stresses and crack width control, if approximate compatibility for strut-and-tie models is ensured (in particular the position and direction of important struts should be oriented according to linear elasticity theory).

The text in EN 1992-1-1 [2] is only a recommendation for choice of the strut and tie model in the serviceability limit state. If it can be shown that other stress fields are appropriate for design in the serviceability limit state, it is permissible to use these stress fields. Nothing is said in EN 1992-1-1 [2] regarding the choice of stress fields in the ultimate limit state.

2.2.2. Briefly about theory and basics of the strut and tie method

What is addressed in this chapter is based on material presented in Schlaich, et al. [4], Schaefer [7], Schaefer [8], FIP Report [9], fib bulletin 16 [10] and fib Bulletin 61 [11].

A concrete structure and its parts can be divided into B-regions (B as in Beam, Bernoulli, which represents the continuity region) and D-regions (D as in Disturbed, Discontinuity), see Figure 4. Characteristic of B-regions is that the stress distribution across the cross section of the structure is linear (plane sections remain plane under loading). For discontinuity regions this is not the case, the strain distribution instead being nonlinear. The discontinuities involved can be both geometric and static (load dependent). A discontinuity results in a disturbance that is equalized within the discontinuity region. In the neighbouring B-region the effect

of the disturbance is gone. Continuity regions can be analysed by use of beam theory. For discontinuity regions, on the other hand, the design methods are not as obvious.

In designing discontinuity regions with use of the strut and tie method, it is advisable to perform the calculations required in the following steps, referred to by Schlaich, et al. [4], that have come to represent the primary application of the method:

1. Structural analysis used to calculate the support reactions and the section forces.
2. Identification of discontinuity regions. See the examples in Figure 4 and 5.
3. Decide upon the linear stress distribution to have at the boundaries between discontinuity and continuity regions.
4. Estimate the stress field in the discontinuity regions with use of the load path method or elastic linear FE-analysis. See the example shown in Figure 6.

   In the figure:

   - F_c = Horizontal compression strut.
   - $F_{c\theta}$ = Inclined compression strut.
   - F_t = Tension tie.
   - θ = Angle for the inclined compression strut.
   - σ_x = Horizontal stress in the concrete.
   - b = Width of the deep beam.
   - h = Height of the deep beam.
   - l = Distance between the centre of the support.
   - z = Inner lever arm.
   - q = Uniformly distributed load at the top of the deep beam.
5. Create a suitable strut and tie model for representing the stress field. See the example given in Figure 6.
6. Calculate the forces in the struts and ties.
7. Create the design and the control of the reinforcement, the struts and the nodes, respectively.

The work of Schlaich, et al. [4], was important for development of the method.

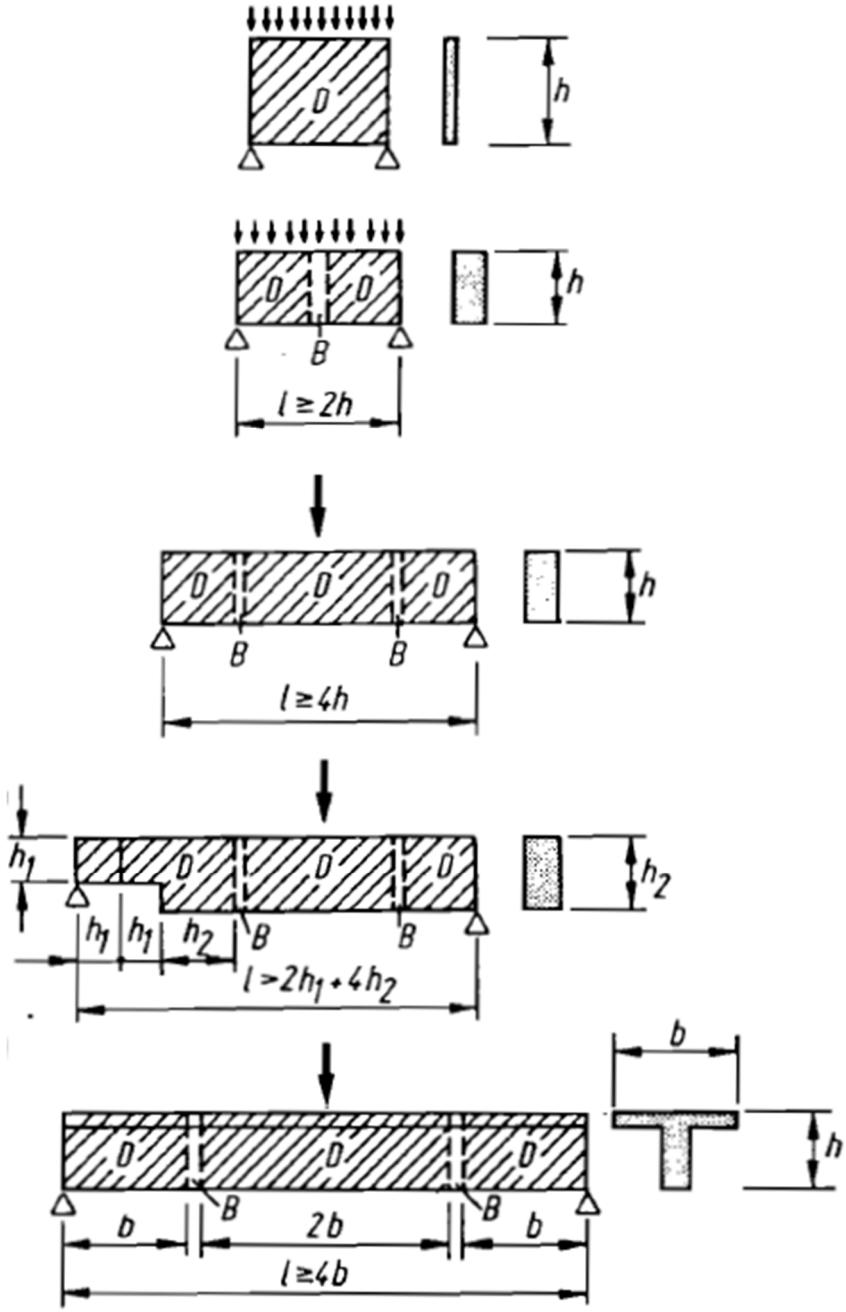

Figure 4
D=Discontinuity regions, B=Continuity region. Reproduced with permission. Schlaich, et al. [4].

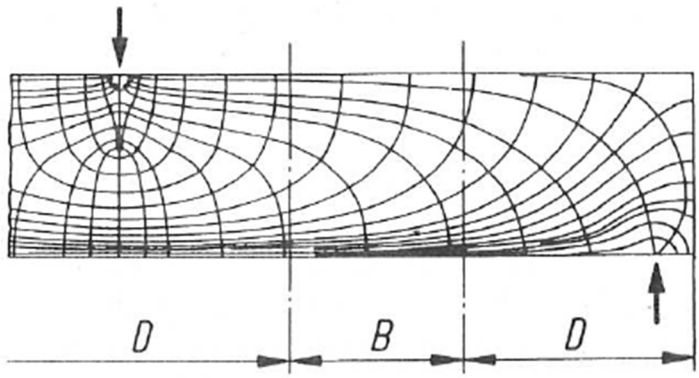

Figure 5
Stress trajectories in a B-region and near regions of discontinuities (D-regions). Reproduced from fib Bulletin 3, Structural Concrete, Textbook on Behaviour, Design and Performance Updated knowledge of the CEB/FIP Model Code 1990, Volume 3, page 143 - "Fig. 7.3-3: Stress trajectories in a B-region and near Discontinuities (D-regions)" with permission from the International Federation for Structural Concrete (fib). Schaefer [8].

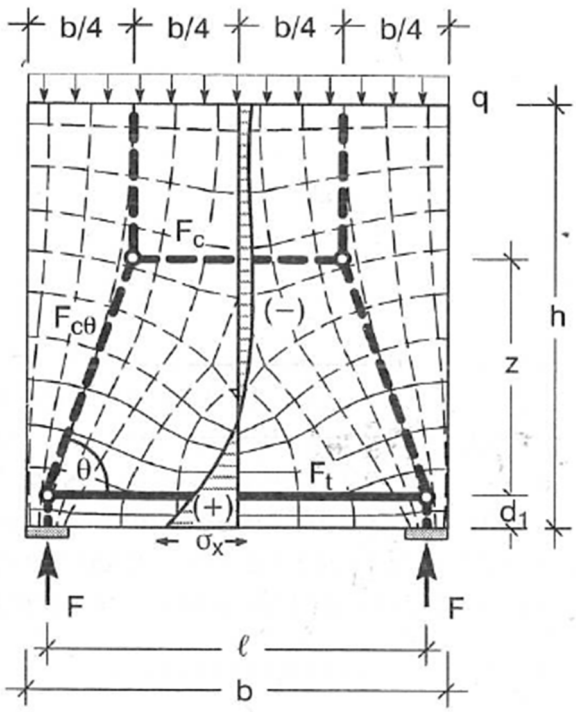

Figure 6
Linear elastic stress trajectories and the strut and tie model. Reproduced from fib Bulletin 3, Structural Concrete, Textbook on Behaviour, Design and Performance Updated knowledge of the CEB/FIP Model Code 1990, Volume 3, page 153 - "Fig. 7.3-10: Orienting the strut-and-tie model of a deep beam at the theory of elasticity. Linear elastic stress trajectories, stress distribution in the middle section and related strut-and-tie model" with permission from the International Federation for Structural Concrete (fib). Schaefer [8].

For a continuity region there is no need of establishing a complete truss model. Thus, in a continuity region between discontinuity regions there is no need for an adaptation of the angle θ to obtain a truss in the continuity region that fits with the truss that crosses the boundary of each D-region, see Figure 7. A continuity region should be designed for the angle θ between the concrete compression strut and the beam axis perpendicular to the shear force, used in the design for shear. Discontinuity regions separated by continuity regions are not affected by the conditions inside the continuity regions. The important thing here is that the boundary conditions are clear. Other prerequisites apply to structures that in their entirety are discontinuity regions. It is important here to develop complete models that are in equilibrium with the loads that are applied.

As was indicated above, the strut and tie method can be used, in continuity and discontinuity regions, for different structures or parts of structures, simulating the resultants of the stress fields in a concrete structure. It is generally used for cracked reinforced concrete in the ultimate limit state in discontinuity zones. It is suitable for identifying areas in which there is tension and a need of reinforcement, and also areas where can be anchorage problems of the reinforcement. The model is made up of struts, ties and nodes that represent compressive stresses in the concrete, tensile stresses in the concrete or tensile stresses carried by the reinforcement and nodes connecting the struts and the ties. The strut and tie method complies with plastic theory, it follows the lower bound theorem (static theorem) and always provides a load-bearing capacity that is less than or equal to the failure load.

The method assumes that:

- Stress fields are in equilibrium with loads.
- No stresses exceed yielding.
- The deformation capacity is unlimited.

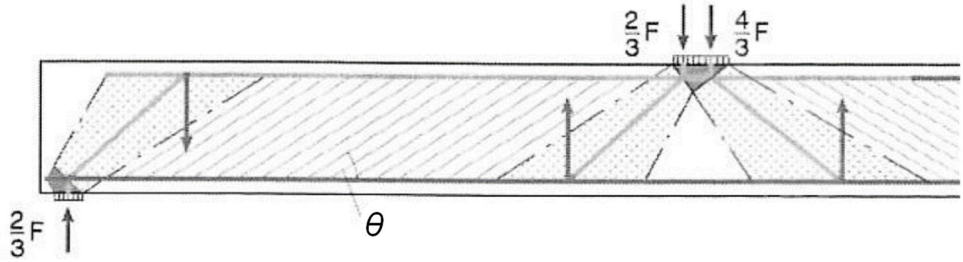

Figure 7
Part of a beam with stress fields and truss models. The boundary between the B- and D-regions are indicated by dotted lines. The strut angle in the B-region is indicated by θ. The strut angle in the continuity region do not have to fit with the ties that crosses the boundaries. Reproduced from fib Bulletin 61, Design examples for Strut-and-Tie models 2011, page 203 - “Fig. 16-4: Truss model and stress fields for a beam with a cantilever" with permission from the International Federation for Structural Concrete (fib). fib Bulletin 61 [11].

A strut and tie model in a discontinuity region describes one of many possible failure mechanisms (stress fields), fulfilling the equilibrium conditions, see Figure 8. The final stress field that maintains equilibrium and for which failure occurs is governed by the reinforcement arrangement, since this affects the distribution of stiffness. This final stress field is achieved by successive stress redistribution, due to the cracking and yielding, from a stress field corresponding to uncracked concrete (linear elastic stress distribution), into a stress field corresponding to that of the capacities of the input material, provided sufficient deformation capacity exists.

In choosing a strut and tie model that complies with the linear elastic stress field applicable to uncracked concrete, a stress field representing one of the many possible failure mechanisms in the structures, it is assumed that there is only a minor need for stress redistribution. Linear elastic FE-analysis and the load path method are two possible approaches that can be used to develop a strut and tie model from the linear elastic stress field. In a linear elastic FE-analysis, stress trajectories showing the orientation of the principal stresses involved is employed. In the load path method, a streamlined load path through the structure, representing the location of the stress field load resultant, is connected to the corresponding reaction having the same load value. Load lines cannot intersect. At the point where the load lines change direction, additional forces are required. Based on load lines, alterations in their direction and complementary forces, an idealized model involving straight struts (that carry the uniaxial compression) and ties (that carry the uniaxial tension) connected in nodes (having bi- or tri-axially stressed volumes in which the load paths are deflected and in which ties are anchored beyond) is created, see Figure 6.

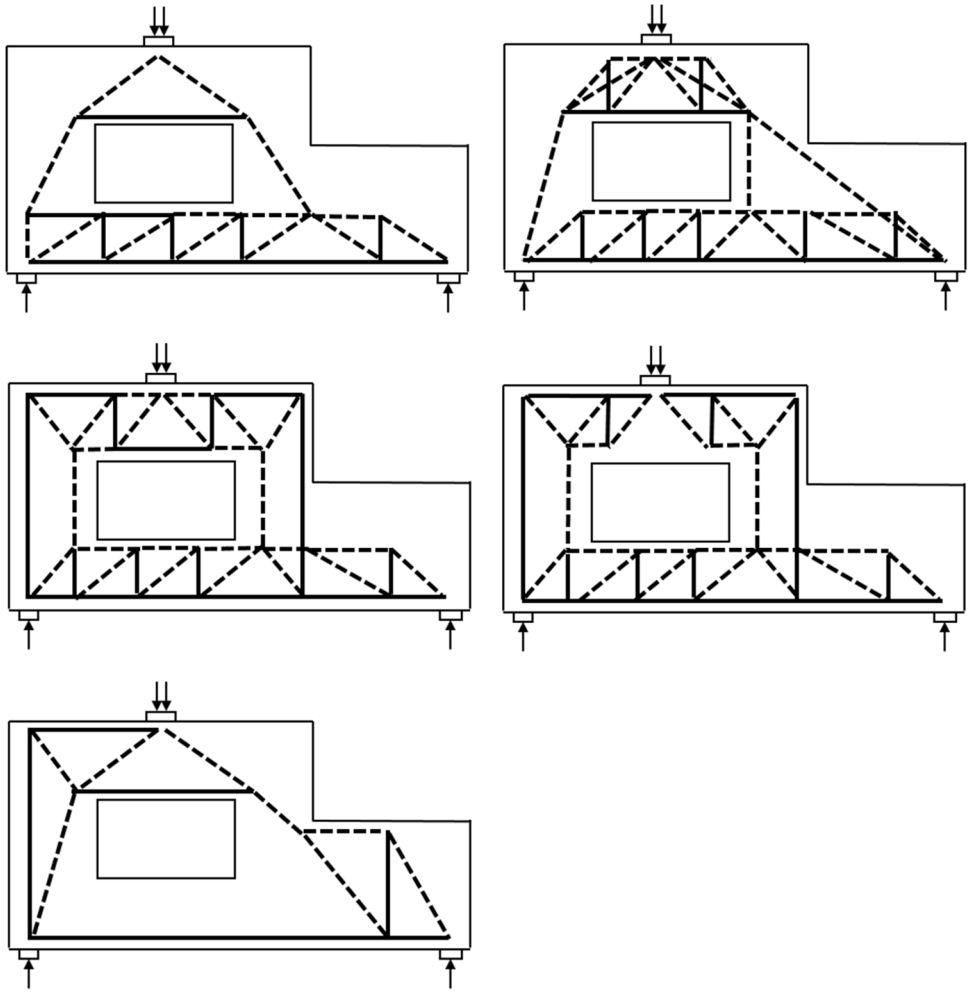

Figure 8
Different possible strut and tie models for carrying the same load. Based upon Reineck [12].

The strut and tie method assumes that in theory there is an unlimited deformation capacity. In practice, it is sufficient that the deformation capacity exceeds the deformation that is required to enable a stress redistribution. This stress redistribution is needed to fulfil an assumed final stress field used in the strut and tie model for the design of the structure in the ultimate limit state. During the stress redistribution, before the final stress field has been reached, no unforeseen failures should occur. A failure should preferably be ductile, which is the case if failure occurs when the reinforcement reaches its ultimate strain. This can be compared with the ultimate compressive strain for concrete which is about 2% of the ultimate strain for reinforcement. This leads to a brittle fracture in concrete subjected to

compression. Accordingly, compression failure in the concrete should be avoided, that is the concrete compression capacity should never be fully utilised in the design. One way to avoid this is to ensure that the loading and support surfaces are sufficient in area to keep the compressive stresses low. Instead minimizing the width of these surfaces requires knowledge of the deformation capacity that is available. It is important to be observant regarding the occurrence of tensile strain in the area of compression struts since it reduces the compressive strength of the concrete.

Another type of failure that affects the available deformation capacity is anchorage failure. An incomplete anchoring of the reinforcement in the nodes, where compression struts and reinforcement ties meet, results in the ties being unable to carry the force for which they are designed. In order to ensure that an anchorage failure does not occur, the equilibrium control in the nodes should best be refined by use of local stress field models.

This makes clear the importance of knowledge concerning the stress redistribution and deformation capacity being available when use is made of the strut and tie method for design and for assessing cracked reinforced concrete structures.

2.3. Truss analogy

It can be difficult to determine who was the first to present certain new ideas, as can be seen in connection with the truss analogy. In 1892, Francois Hennebique patented a design method (the Hennebique System) that added shear reinforcement in beams. The method was later discussed by Ritter [13], who explained the theory for the flow of forces in a cracked concrete structure with use of a truss analogy involving vertical reinforcement (stirrups) connecting the longitudinal reinforcement on the bottom side with the flexural compression zone at the top side of a structure. Diagonal pressure at an inclination of 45° connected the top and the bottom of the vertical reinforcement. In the model, reinforcement was assumed to have an effect similar to that of ties and compression zones, an effect similar to that of struts. In Figure 9 the horizontal strut at the top is omitted.

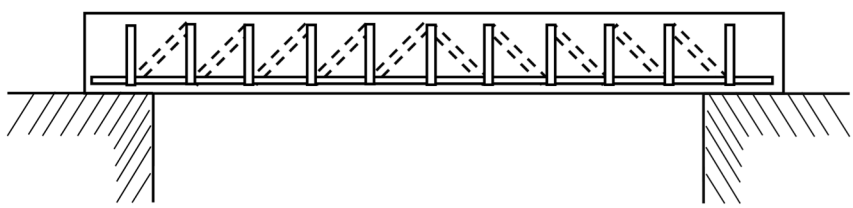

Figure 9
A truss model according to Ritter based upon ideas of Hennebique's. Based upon Ritter [13].

In 1909 Mörsch [14] explained the truss analogy more thoroughly. He showed that inclined compression struts do not have to go between the top and the bottom of the nearest stirrups, see Figure 10a. In later editions of his text, Mörsch [15] presented a more detailed model, one in which concrete resists the shear force by means of continuous compression fields rather than by means of compression struts, see Figure 10b. In both Ritter's and Mörsch's model the angle between the compression diagonal and the horizontal plane is 45°. This angle remains after cracking of the concrete, under the assumption that there is no tensile stress in the concrete. Mörsch discussed the choice of the inclination of the diagonal compressive stress. He saw no practical way of determining this slope mathematically, and suggested a conservative value for it, one of 45°.

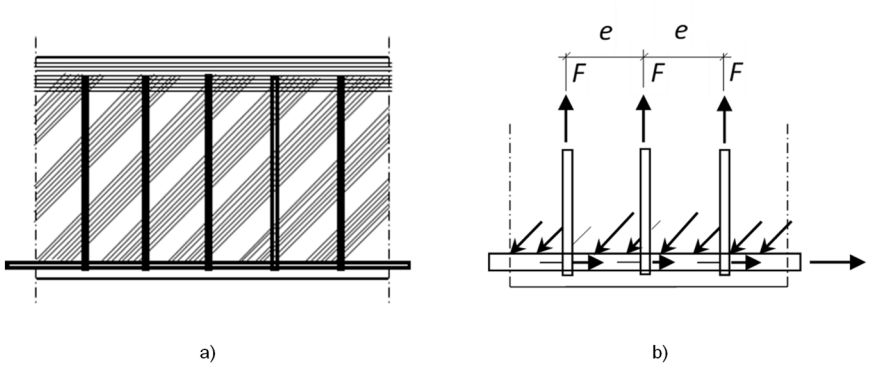

Figure 10
a) Compressive struts. b) Compression field. Based upon Mörsch [14] and Mörsch [15].

Mörsch's theory and his suggestion that cracked beams could be designed by use of a truss model is still accepted and has been the basis for theories developed later that have led to new models and to the design rules used today. Many reinforced concrete beams were tested in the first decades of the 20th century. The tests showed that there was a difference between the predicted strain and the smaller measured strain in the stirrups. This was assumed to be due to the choice of a compressive strut inclination of 45°, a value that is conservative and decreases if the tensile stresses in the concrete are accounted for. If an angle of 45° is valid, then a beam without transverse reinforcement should not be able to carry a shear force. The experiments did not confirm this instead they showed that failure did not occur before diagonal cracks had formed. In order to take the positive impact of concrete tensile stresses into account, the first ACI Code in 1910 determined that the concrete contributed to the shear capacity. Another way to do this is to assume an angle of less than 45°. In using the variable-angle truss model, the designer can choose an angle, θ, between 31° and 59°, see Figure 11.

In the figure:

- R = Inclined compression force.
- N_v = Longitudinal component of the inclined compression force.
- σ_2 = principal compressive stress.
- $A_w f_w$ = Tensile force in stirrup.
- M = Bending moment.
- V = Shear force.
- z = Inner lever arm.
- s = Distance between stirrups.
- b = Width of the beam.

The model was introduced in CEB-FIP [16].

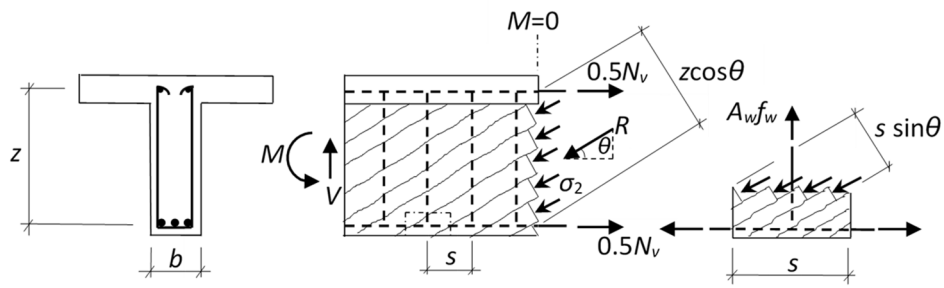

Figure 11
Equilibrium for the variable-angle truss model. Based upon Collins and Mitchell [17].

The inclination of the diagonal compressive struts, θ, is an important variable for determining the shear strength of a beam. In 1929 Wagner [18] studied the post-buckling shear resistance of thin-webbed metal girders. He assumed that the angle of inclination of the diagonal tensile stresses corresponds to the angle of inclination of the principal tensile strain, an assumption later known as tension field theory, see Figure 12. The problem is equivalent to that of concrete, except that it concerns tension instead of compression.

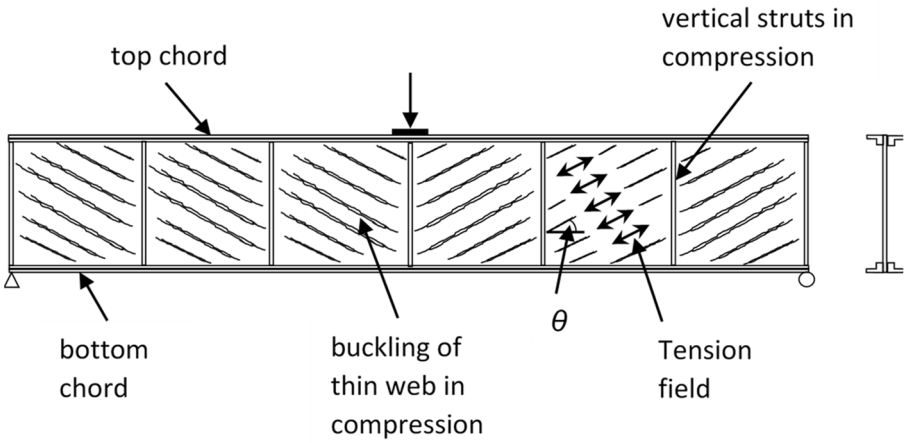

Figure 12
Tension fields due to shear in a thin-webbed metal girder. Based upon Wagner [18].

This analogue was used by Mitchell and Collins [19] and by Collins [20] when they proposed a method, Compression Field Theory, for finding the shear strength of a beam. The method assumes that concrete does not carry tension after cracking. The angle of the diagonal compression field that carries the shear and the compressive strength of the concrete are important for the method. They found that the principal compressive strength depends upon the associated principal tensile strain. Later on, Vecchio and Collins [21] improved their own method in accounting for tensile stresses in the concrete between the cracks in it. The method was termed "Modified Compression Field Theory", see Figure 13. In the figure σ_1 and σ_2 denote the principal stresses in the concrete.

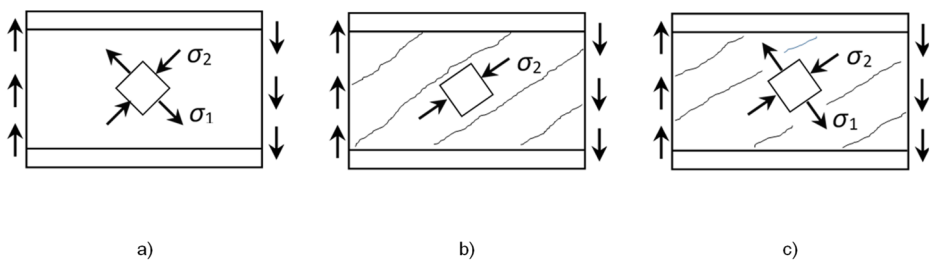

Figure 13
Stress fields in web of reinforced concrete beam: a) Before cracking, $\sigma_1=\sigma_2$, $\theta=45°$ (slope for compressive stresses). b) Compression field theory, $\sigma_1=0$. c) Modified compression field theory, $\sigma_1\neq0$. Based upon Collins and Mitchell [17].

The theories connected with the truss model and the knowledge gained by use of the model have served as input info in the concept of stress fields.

2.4. Stress field model

Leonhardt and Walther [22] conducted tests on deep beams differing in geometries and loads. Such as simply supported deep beams loaded on the top with uniformly distributed loads. Among other things they investigated the horizontal concrete stresses in the midspan of uncracked concrete structures involving various ratios of span to height, l/d, see Figure 14. In the figure σ_u and σ_o denote the horizontal stresses in the concrete at the bottom and top of the structure. The figure clearly shows the transition from the linear stresses that characterize beams generally, to the nonlinear stresses that apply to discontinuity regions, such as deep beams. The figure is used here only to graphically illustrate the change in the horizontal stresses in the concrete.

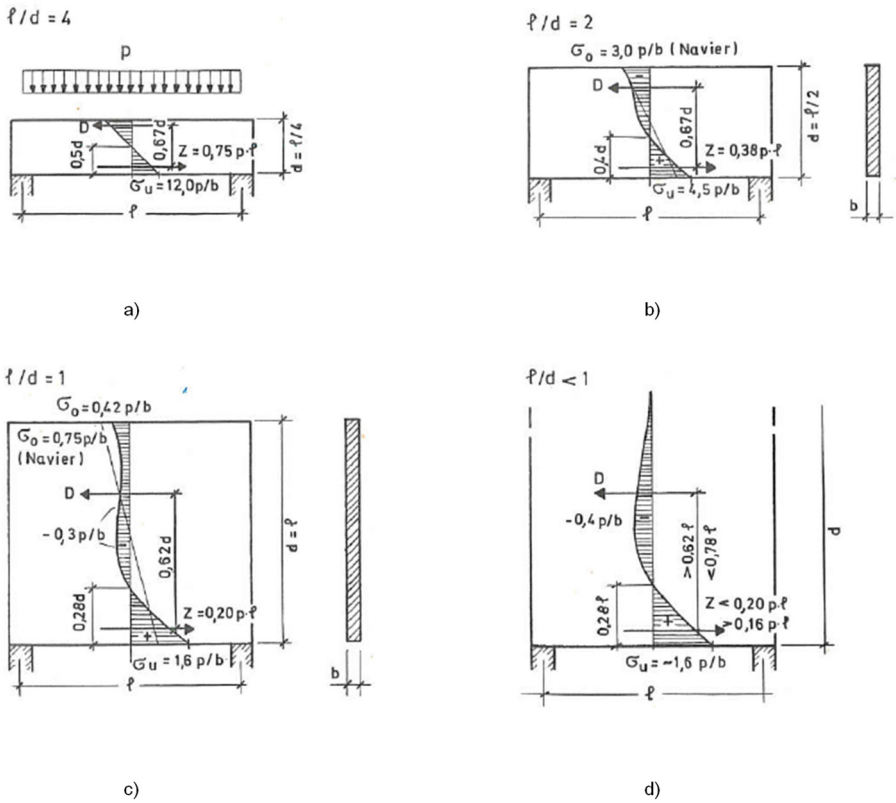

Figure 14
Inner lever arm and tensile forces in midspan of a simply supported deep beam loaded with a uniformly distributed load on the top of the structure. Reprinted by permission from Springer Nature: Springer-Verlag, Vorlesungen uber Massivbau, Zweiter Teil, Sonderfälle der Bemessung im Stahlbetonbau, Zweite Auflage by Fritz Leonhardt, Eduard Mönnig, Copyright 1975. Leonhardt and Mönnig [23].

Leonhardt and Walther [22] also showed how the value of the inner lever arm increased when the concrete cracked. Stresses according to elastic theory for deep beams, were far from the stresses measured in the service state and the ultimate state. For the specimen WT1-b shown in Figure 15, this can be observed in Figure 16. That figure shows the horizontal concrete compressive stresses in the middle of the span for increasing load. One can note that the concrete cracks for a total load of P = 30 Mp and after that the compression zone moves high up in the deep beam.

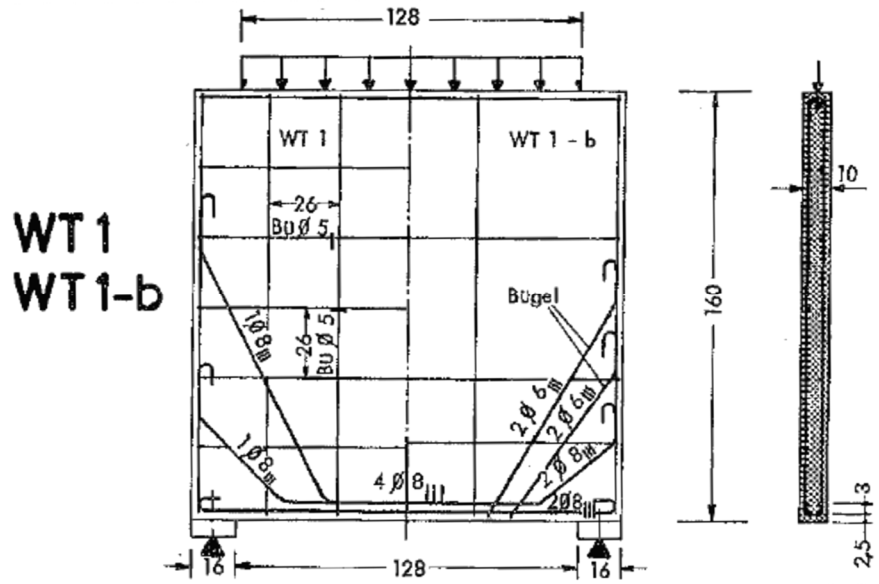

Figure 15
The figure shows two different specimens, WT1 and WT1-b, that was studied by Leonhardt and Walther. The dimensions in the figure are in cm. Copyright 1966 Wilhelm Ernst & Sohn Verlag für Architektur und technische Wissenschaften GmbH & Co. KG. Reproduced with permission. Leonhardt and Walther [22].

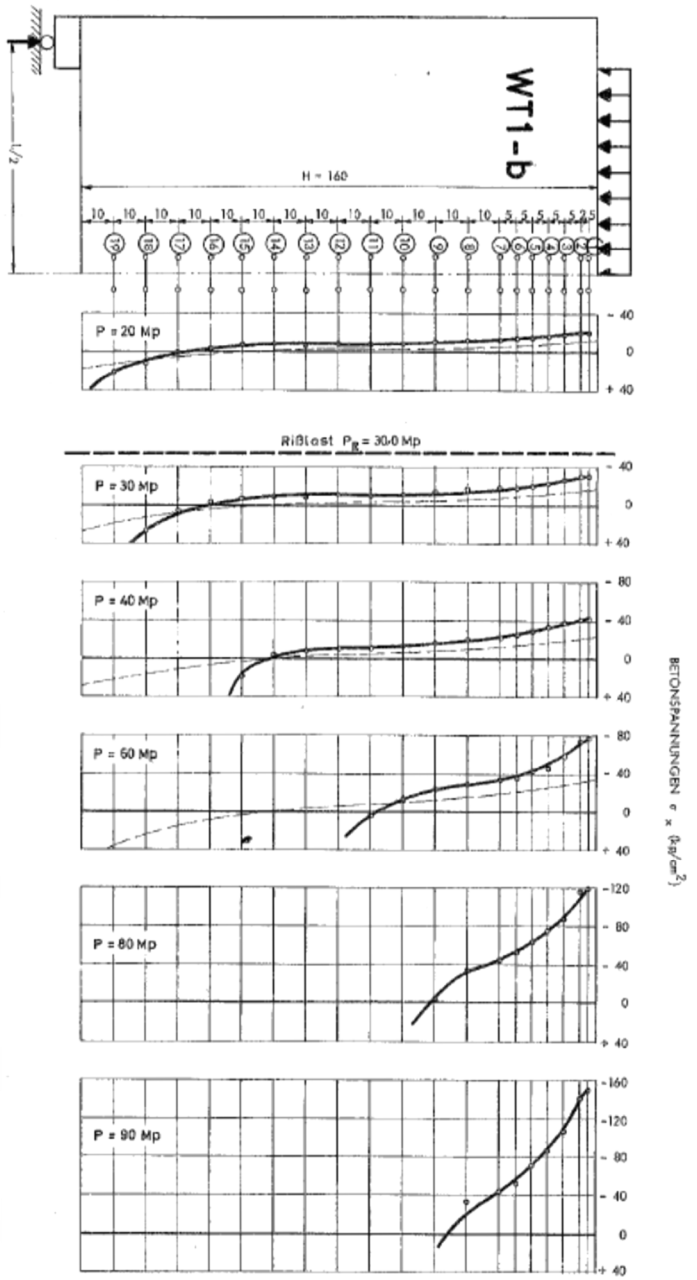

Figure 16
Horizontal concrete stresses σ_x distributed over the height for a total load of P on top of the studied specimen. Negative values of the stresses indicate compressive stresses. The unit for load is Mp and for stress kp/cm^2. Leonhardt and Walther [22].

In their tests, they noticed that final failures occurred for different reasons, such as:

- Yielding of the reinforcement.
- High concrete compressive stresses above the support.
- High inclined concrete compressive stresses.

For a simply supported deep beam loaded at the top with a uniformly distributed load and with a ratio of 1 for height to total width they concluded that:

- The tensile force in the reinforcement was the same between the two supports and did not follow the moment curve.
- The main reinforcement and the additional surface reinforcement should be distributed in the tension zone so as to limit crack widths.
- If there is sufficient reinforcement, the greatest risk of failure is in the inclined concrete compressive zone and near the support. In this case when the ratio of height to total width is 1 and for cases in which the ratio of span to height is ≤ 1 the horizontal compressive stresses in the midspan are not critical.

Leonhardt and Walther relate to some extent to the concept of stress field, as can be seen in Figure 17, which shows examples of the conceptual idea of inner trusses for the approximate determination of the tensile force Z in cantilevered deep beams. The compressive struts in the figure have a certain width over which there is assumed to be a uniformly distributed stress field.

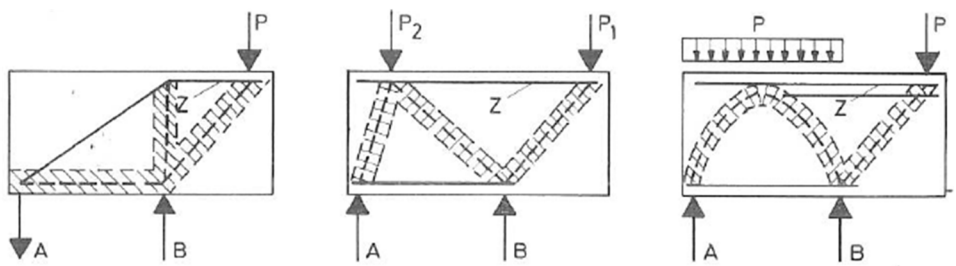

Figure 17
An inner truss with tensile force Z. Reprinted by permission from Springer Nature: Springer-Verlag, Vorlessungen uber Massivbau, Zweiter Teil, Sonderfälle der Bemessung im Stahlbetonbau, Zweite Auflage by Fritz Leonhardt, Eduard Mönnig, Copyright 1975. Leonhardt and Mönnig [23].

In the 1980's stress field models were studied by a number of researchers. Both the basic theory and how to use the method in the design of discontinuity regions were developed. Marti [24] showed that strut and tie models are only a simplification of the stress field, representing the resultant of the stress field. He dealt with many different discontinuities, whole structures such as deep beams, and parts of

structures such as nodal zones, struts, and the like. Muttoni, et al. [25] came with a basic document in 1996 concerning the design of concrete structures by use of stress fields. The authors' intention with the book was to provide a unified theoretical basis for the behaviour and strength of reinforced and prestressed concrete structures. The stress field method is based on the lower bound theorem of plasticity. Figure 18 shows the development of a stress field for several concentrated loads. Figure 19 shows a stress field for a distributed load (with an infinite number of concentrated loads). For slenderer beams, the slope of the compression diagonal could be too small. Two structural systems are therefore required for transmitting a concentrated load to the support, see Figure 20. Any admissible stress field can be selected in designing. Muttoni noted that working with force resultants or stress fields has various advantages. Figure 21 shows that the internal forces in the discontinuity region can be investigated using force resultants. Detailing of the reinforcement should, however, be carried out by use of stress fields. The figure stresses the fact that care should be taken regarding deviation of the longitudinal strut. The deviation can be brought about by use of concentrated or distributed stirrups.

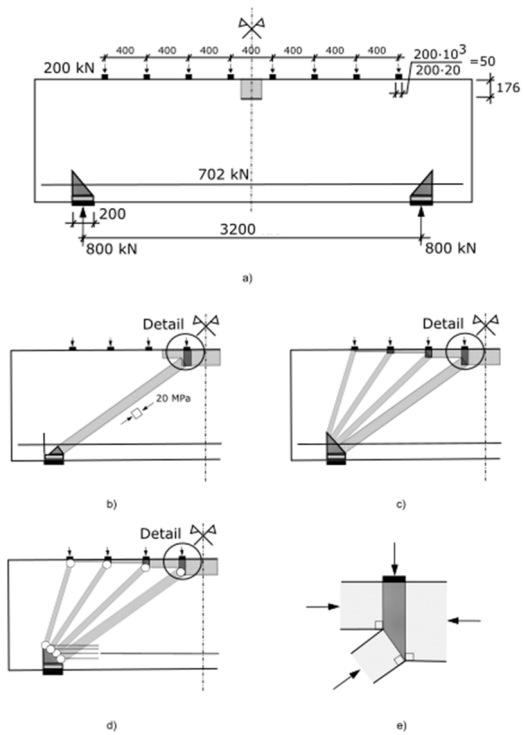

Figure 18
Development of a stress field through calculations. Dimensions are given in mm. The width of the deep beam is 200 mm. The effective concrete strength is 20 MPa. a) Beam and loading. b) First diagonal. c) Complete stress field. d) Resultants. e) Detail. Based upon Muttoni, et al. [25].

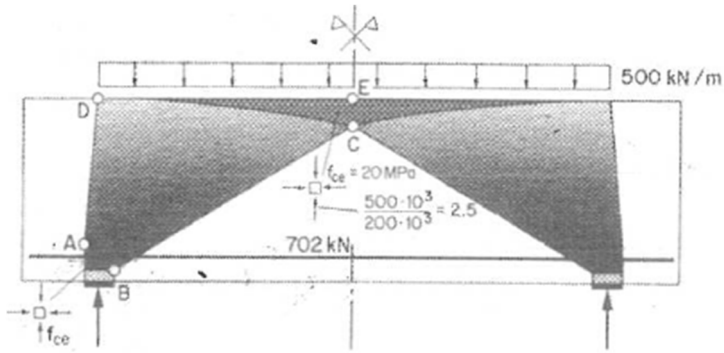

Figure 19
Stress field for a distributed load developed through calculations for an infinitely large number of concentrated loads analogous to Figure 18. Dimensions and material properties are the same as in Figure 18. The symbol f_{ce} denotes the effective concrete strength. Reprinted by permission from Springer Nature: Birkhäuser-Verlag, Design of Concrete Structures with Stress Fields by A. Muttoni, J. Schwartz, B Thürlimann, Copyright 1997. Muttoni, et al. [25].

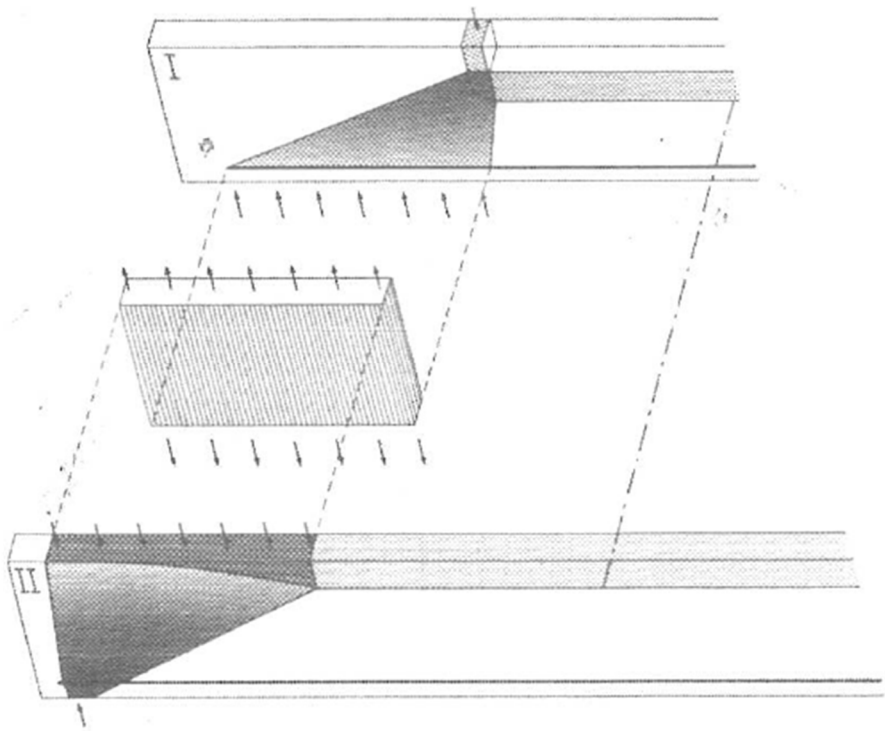

Figure 20
Combination of two structural systems I and II. The reactions of system I load system II by means of vertical stirrup reinforcement. Reprinted by permission from Springer Nature: Birkhäuser-Verlag, Design of Concrete Structures with Stress Fields by A. Muttoni, J. Schwartz, B Thürlimann, Copyright 1997. Muttoni, et al. [25].

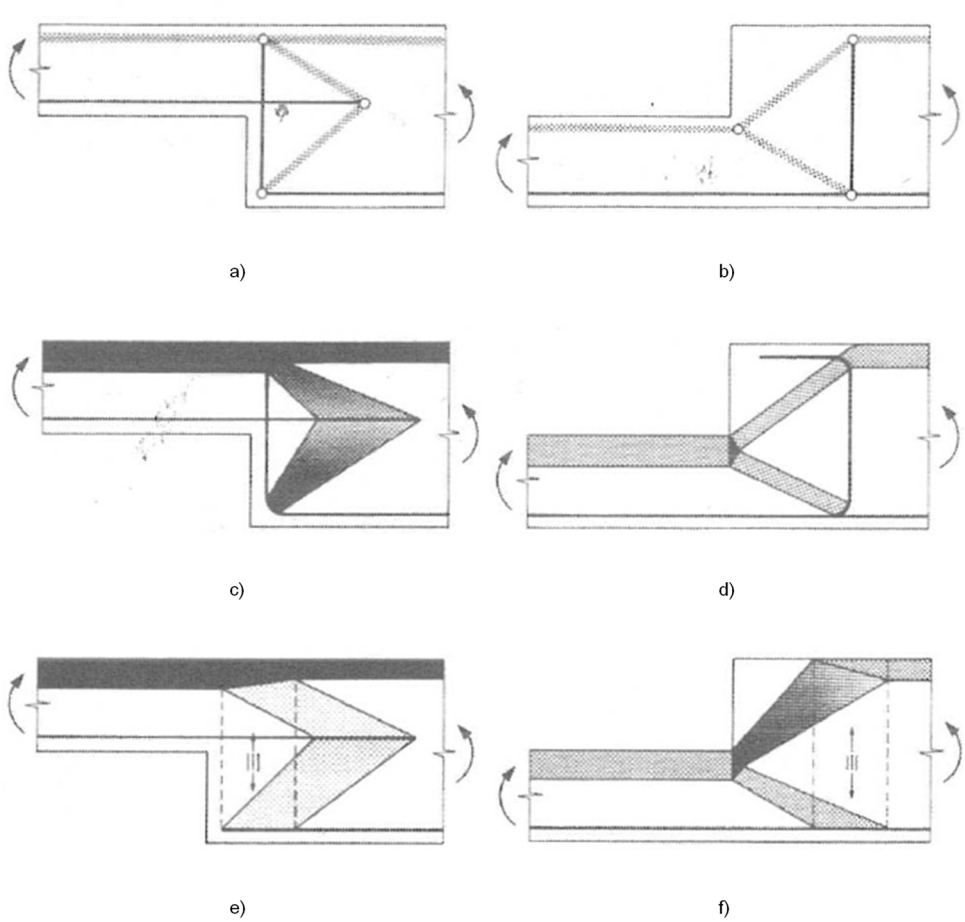

Figure 21
Resultants and stress fields: a) and b) Internal forces (resultants to stress fields). c) and d) Stirrup concentrating the deviation force. e) and f) Stirrups indicated by III distributing the deviation force. Reprinted by permission from Springer Nature: Birkhäuser-Verlag, Design of Concrete Structures with Stress Fields by A. Muttoni, J. Schwartz, B Thürlimann, Copyright 1997. Muttoni, et al. [25].

2.5. Codes and other technical and normative documents

A main innovative aspect of the CEB-FIP Model Code 1990 [6] was “Continuity and consistency of models for dimensioning”. Instead of separate verification in cross-sections, attending to critical regions and their global resistance was considered as being a step towards a consistent approach to the design of all types of concrete structures and their parts, as mentioned by Schlaich, et al. [4].

In 1999, FIP published recommendations entitled Practical Design of Structural Concrete FIP Report [9]. The recommendations were based on the CEB-FIP Model Code 1990 and explained the design and detailing of members by means of strut and tie models. The document constituted a consistent design and detailing tool of interest to consultants, contractors and authorities, for helping in the use of strut and tie models. This was also the wish of FIP Commission 3.

Updated knowledge of the CEB/FIP Model Code 90 (MC 90) was published in the Textbook on Structural Concrete, fib Bulletins 2 and 3, in which design with use of the strut and tie method is summarized in an extensive review of MC 90 by Schaefer [7] and Schaefer [8]. The second editions of Bulletins 2 and 3 were published in 2010 as Bulletins 52 and 54, see Schaefer [26] and Schaefer [27].

In 2002 fib published fib bulletin 16 [10]. The main objective of the bulletin was to demonstrate by use of practical examples the application of the 1996 recommendations, and especially to illustrate the use of strut and tie models for the design of discontinuity regions in concrete structures. As a continuation of fib Bulletin 16, fib Bulletin 61 [11] was published in 2011. Again, the bulletin's main objective was to demonstrate, by use of examples, the application of the FIP Recommendations "Practical Design of Structural Concrete", and especially to illustrate the use of strut and tie models in designing discontinuity regions in concrete structures. Another publication that came out in 2002 was Reineck [12], which presented examples for the use of strut and tie models, following Appendix A of ACI 318-2002, for the design of D-regions.

At the IABSE Collegium in Stuttgart 1991, Breen [28] "suggests a general framework for developing future professional practices, codes and standards, and educational approaches to structural concrete". He also proclaimed as a key topic for the conference "useful and transparent models, which can enhance the designer's realization of structural action". According to Schaefer, et al. [29], Breen [28] considered strut and tie modelling to be such a tool. The introduction of CEB-FIP Model Code 1990 [6] can be considered as a breakthrough for the thoughts discussed at the IABSE Collegium in Stuttgart.

In 2004 the Eurocode 2, EN 1992-1-1 [2], was published. It applies to the design of buildings and civil engineering works in plain, reinforced and prestressed concrete. Here the strut and tie method was described as a method that can be used for the design and detailing of both continuity and discontinuity regions. A review of EN 1992-1-1 [2] is ongoing and a release is currently scheduled for 2023.

A new Model Code, MC2010, fib Bulletin 65 [30] and fib Bulletin 66 [5], was published in 2010. "The objectives of MC2010 are to (a) serve as a basis for future codes for concrete structures, and (b) present new developments with regard to concrete structures, structural materials and new ideas in order to achieve optimum

behaviour". Work is in progress for producing an updated Model Code with the working title MC2020.

A new Bulletin, fib Bulletin 100 [31], concerning strut and tie models and stress fields was published 2021. The aim of the Bulletin is to show principles, development and application of strut and tie and stress field models. The following are examples of its contents:

- A guide for designers on how to create, apply and evaluate the strut and tie and stress field models.
- Design for new and assessment of existing structures.
- Use of the Levels-of-Approximation concept.
- Principles of computer modelling.
- Effects of load reversals.
- 3D-modelling.

2.6. Systematic procedures for strut and tie and stress fields models

The need of systematic computer-based procedures for establishing and calculating strut and tie and stress field models became apparent in the early 1990s.

The theories and concepts that computer-based methods uses, differ. Some researchers use the energetic criteria mentioned by Schlaich, et al. [4], in some form:

> In selecting the model, it is helpful to realize that loads try to use the path with the least forces and deformations. Since reinforced ties are much more deformable than concrete struts, the model with the least and shortest ties is the best.

One method that can be used for establishing a truss structure layout that has attracted considerable interest and developed rapidly in recent years is Topology optimization (TO) (for an overview, see for example Bendsoe and Sigmund [32]). This is a mathematical method that optimizes the material layout within a given domain of design and for a given set of loads, boundary conditions and constraints, with the goal of maximizing the performance of the system. The method has no predefined configurations within the domain, unlike shape-and-sizing optimization. It can be divided up into continuum and discrete types.

There are also simpler computer programs – an example of this is Eurocode Software AB [33] – the purpose of which is to systematize and facilitate the

development of strut and tie models and to calculate the forces in its components by means of equilibrium conditions.

Below, various tools for automating the development of strut and tie models and stress field models are outlined briefly.

Schlaich [34] presented a procedure for the design of reinforced concrete structures with use of truss models that are implemented in a program. The computational methods involved are based on the theory of plasticity. Different material models are available, elastic, elastic-plastic and rigid-plastic ones. The program minimizes the reinforcement needed and calculates the widths of the one-dimensional compressive stress fields for the forces in the compressive struts and with a stress limited to the compressive strength of the concrete. For the nodes, a statically permissible two-dimensional stress field is needed and is determined by use of a geometrical procedure. According to the author, the truss model approach based on the stress fields and covering the structure as a whole, is an alternative to ultimate load design.

Hajdin [35] presented a thesis having as its objective “the development of necessary fundamentals underlying the computer aided construction of stress fields for reinforced concrete walls”. The stress fields were constructed using constant stress triangle elements.

Ruckert [36], Ruckert [37] and Ruckert [38], Sundermann and Mutscher [39] and later Sundermann [40], used the criterion of optimizing/minimizing the internal energy of the total system giving the smallest possible stresses and strains. This was done for a model that was adapted through an iterative nonlinear FE-analysis finding the best geometry for increasing loads, see Figure 22. In this way, the state both of stresses and of displacements during the entire loading process up to the ultimate load could be determined. The structure goes to failure when the compressive strength of the concrete or the tensile strength of the reinforcement are reached. The program called for use of a given initial strut and tie model and recommended the one following a linear elastic stress field. The program calculated the forces and displacements for the ultimate and serviceability limit states. Ruckert verified his method by use of tests, obtaining satisfactory results.

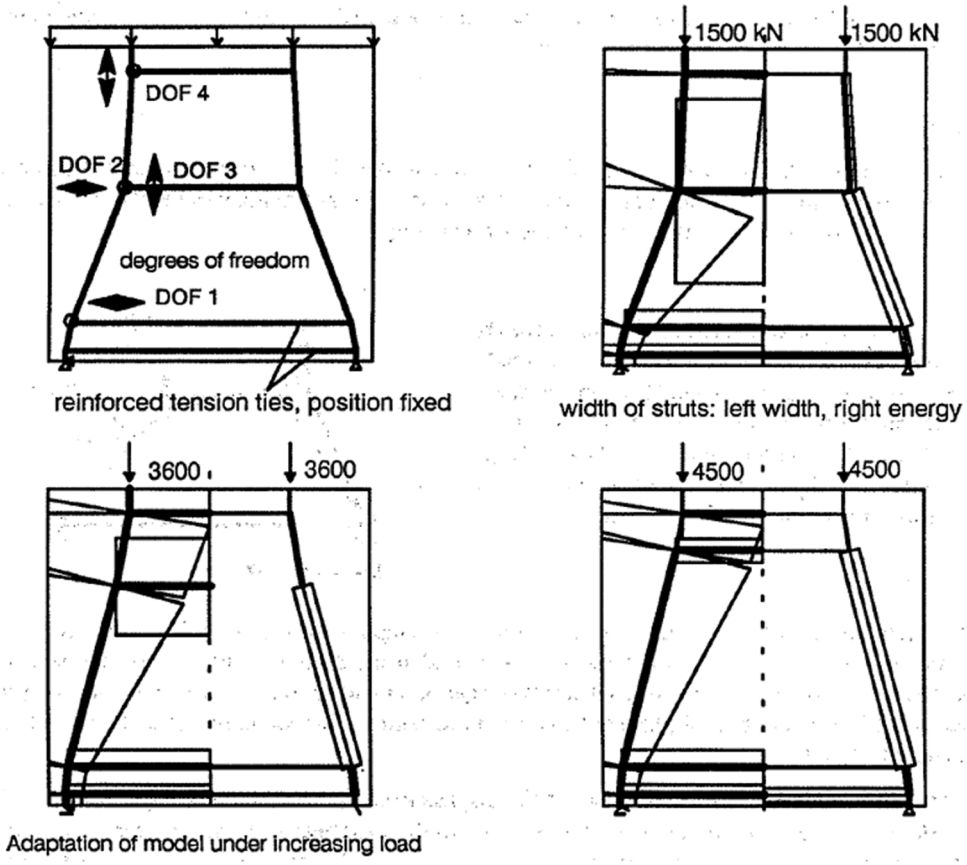

Figure 22
Adaptation of model under increasing load. DOF indicate directions in which the nodes are free to move. Widths on the left in the figures symbolize stresses and widths on the right symbolize energy. Reproduced by permission. Ruckert [36].

Xie and Steven [41] proposed an evolutionary procedure for optimization of the shape and layout of structures. During the evolution process, low-stressed material is increasingly eliminated from the structure. The procedure is as follows:

1. Run a FE-analysis.
2. Use a rejection criterion, such as von Mises stress, deleting all elements for which the stress is below a given value for a chosen rejection ratio times the maximum von Mises stress over the structure.
3. Repeat the FE-analysis and the element elimination cycle until a steady state for different rejection ratios is reached.

The authors' intention in use of the evolutionary procedure is to provide the design engineer with a guide regarding the optimum layout and shape of a structure under certain given loading conditions.

Figure 23 provides an example of a deep beam with a vertically concentrated load at the bottom centre of the structure. The procedure is simple but, according to Xie and Steven, agrees well with solutions obtained by analytical and other mathematically rigorous procedures.

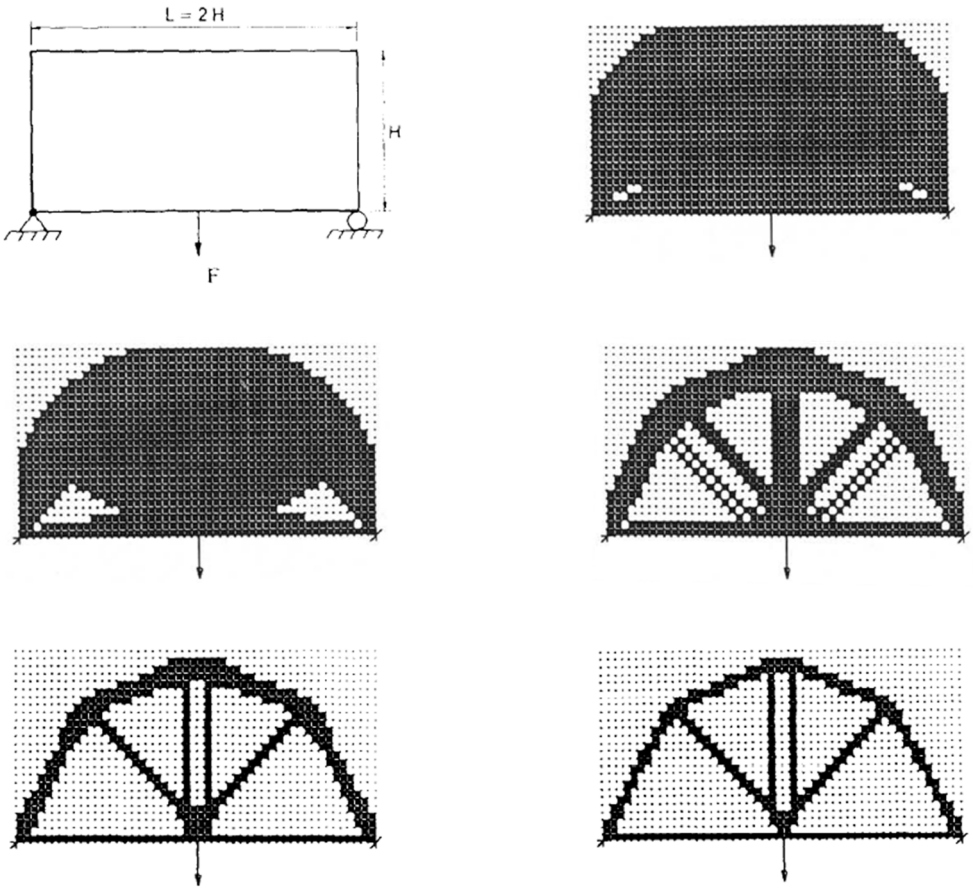

Figure 23
Structural optimization over time for a rectangular plate, resulting in the final truss type structure (dark colour). Reprinted from Computers & Structures Vol. 49, Y. M. Xie, G. P Steven, A simple evolutionary procedure for structural optimization, No. 5; pp. 885-896, 1993, Copyright 1994, with permission from Elsevier. Xie and Steven [41].

Bendsoe, et al. [42] provides a survey of classical truss topology methodology concerning discrete truss topology problems. According to Bendsoe, "Truss topology design for minimum external work (compliance) can be expressed in a

number of equivalent potential or complementary energy problem formulations in term of member forces, displacements and bar areas".

Kuchma and Tjhin [43] and Kuchma and Tjhin [44] discuss the strut and tie method with its advantages and disadvantages, possibilities for creating computer systematizing tools, and future research. They present their program CAST, a computer-aided strut and tie design tool for the interactive design of discontinuity regions in structural concrete. The authors point out that computer-based graphical design aids, rather than cumbersome hand-based design processes, are needed for exploiting the potential of the strut and tie method. It is, however, important that the programs are simple, efficient and transparent.

Elia, et al. [45] present an interactive procedure for designing strut and tie models. They used the Evolution Structural Optimisation (ESO) Method, see Xie and Steven [41], extending it in line with practical requirements. The authors conclude that according to this method, the difference in strain energy between the designed and the optimal strut and tie model is a measure of the consequences (in terms of congruence and crack width) that the structural engineer pays using his design choice taking into account a more practical reinforcement layout.

Salem [46] developed a micro truss model having small isotropic truss members, this automatically providing the macro truss strut and tie model. Full interaction between the reinforcement and the concrete is assumed, see Figure 24. The model can be used both for designing and for checking the nonlinear behaviour of reinforced concrete structures. The model was checked against published experimental results.

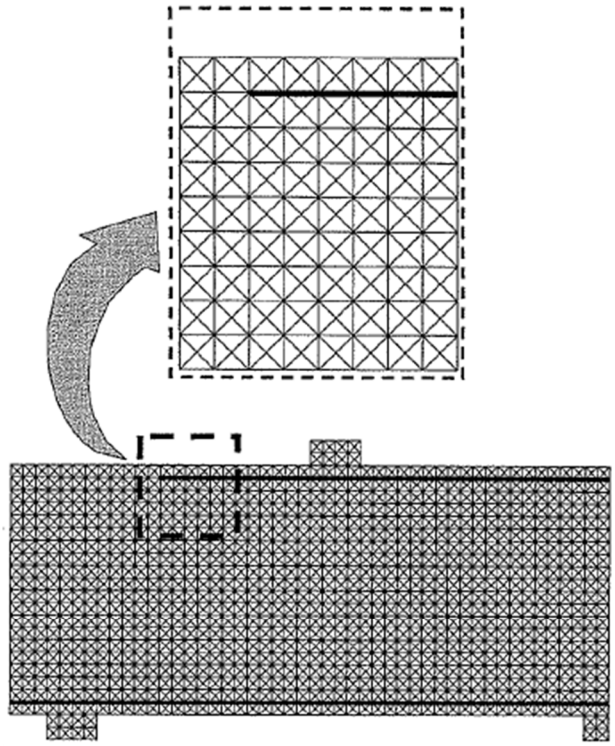

a)

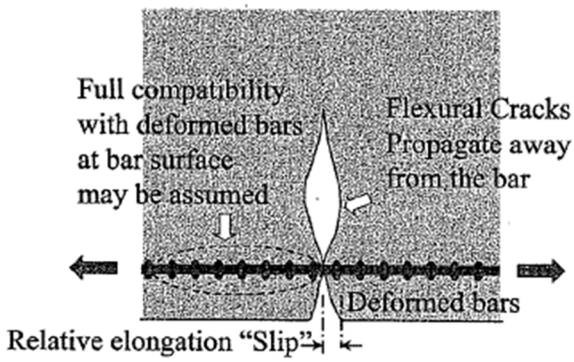

b)

Figure 24
a) Schematic diagram of the micro truss model. b) Full interaction between the concrete and the reinforcement was assumed in the model. Copyright by JCI. Reprinted by permission. Salem [46].

Lourenco, et al. [47] and Lourenco [48] presented an improvement of the procedures developed by Ruckert [36] and by Sundermann [40] "a consistent methodology for predicting nonlinear behaviour and design of structural concrete discontinuity regions". The methodology, Adaptive stress Field Models, uses the adaptive structures concept, i.e., the adjustment of stress fields during an increase in load based on use of stress field models and of the energetic criterion (energy minimization). The model is quite satisfactory for studying the behaviour in a service state, matters of ductility, for developing different strut and tie models and evaluating their effects. The behaviour of reinforced concrete tie elements follows the Tension Chord Model, presented by Marti, et al. [49]. The proposed technique is compared with the use of monotonic and pseudo-cyclic tests and nonlinear FE-analysis.

One of the simulations that Lourenco carried out was a follow-up of his results in regard to service behaviour, obtained in an analysis based on the same conditions that were applied to test specimens WT2 and WT3 in Leonhardt and Walther [22]. Lourenco uses two different strut and tie models, for the same geometry and load, see Figure 25. The two strut and tie models provide different values for the reinforcement involved, see Figure 26. In Figure 27a a simplified adaptive stress field model is shown. This model does not take account of the distributed reinforcement involved. The results of using such a model is a sudden increase in the inner lever arm directly after cracking of the concrete. In Figure 27b a refined adaptive stress field model considering the distributed reinforcement is shown, and it was this model that was used in the simulation. Figure 28 illustrates the configuration of the model before and after the first load step. The figure shows how the minimization process in the adaptive methodology changes the location of the nodes in the horizontal direction and how this affects the value of the forces in compressive struts and tensile ties. In Figure 29 the inner lever arm variation for the adaptive stress field model used in the simulation is presented. Lourenco shows, by calculating steel stresses and crack widths, that for the theoretical tests performed there was appropriate service behaviour and that the model that was used for the ultimate limit state could be employed for checking the service behaviour.

The bond-slip relationship used for concrete and reinforcement can be seen in Figure 30. Lourenco applied nonlinear material models for concrete and reinforcement, taken into account monotonic and reversal loads, see Figure 31.

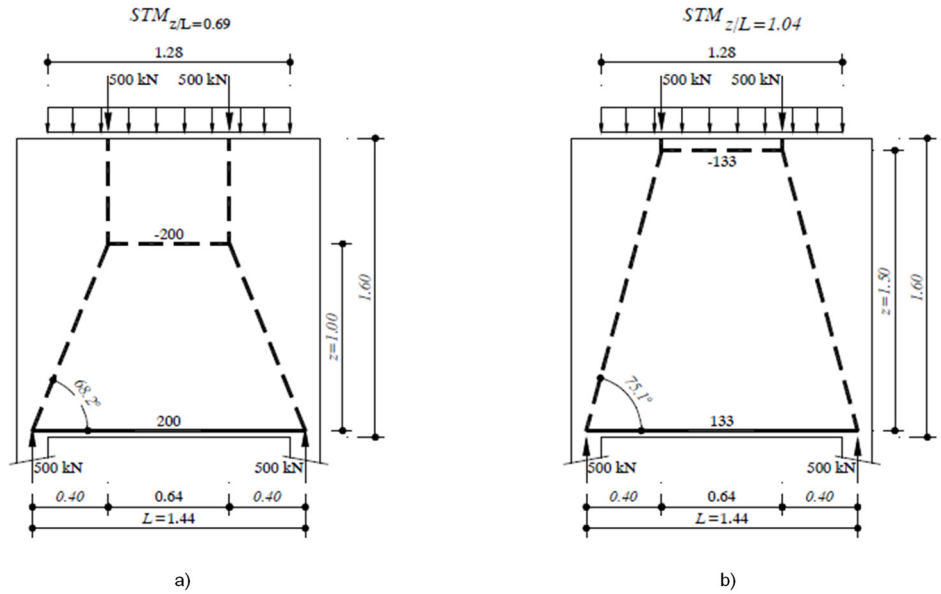

Figure 25
Designing strut and tie models: a) An elastic stress trajectory based model. b) A model assuming stress redistribution. Reproduced by permission. Lourenco [48].

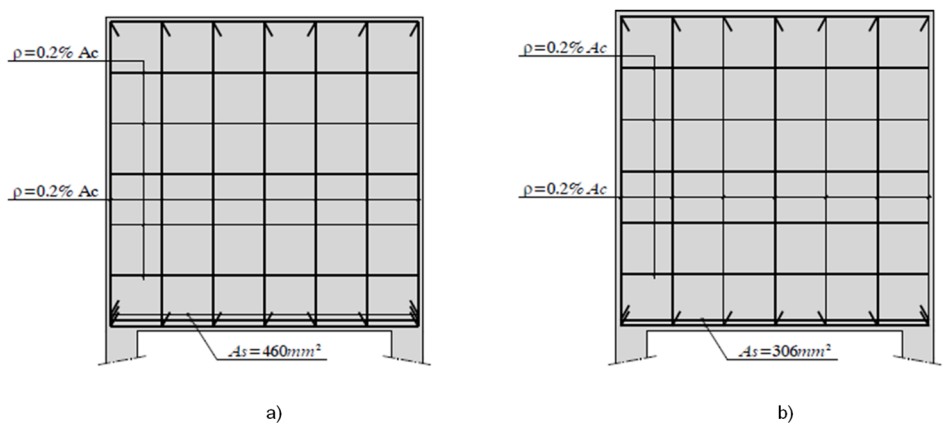

Figure 26
Deep beam reinforcement layout. Additional minimum web reinforcement of approximately ρ=0.2% was adopted: a) Main reinforcement of A_s = 460 mm² obtained for the model in Figure 25a. b) Main reinforcement of A_s = 306 mm² obtained for the model in Figure 25b. Reproduced by permission. Lourenco [48].

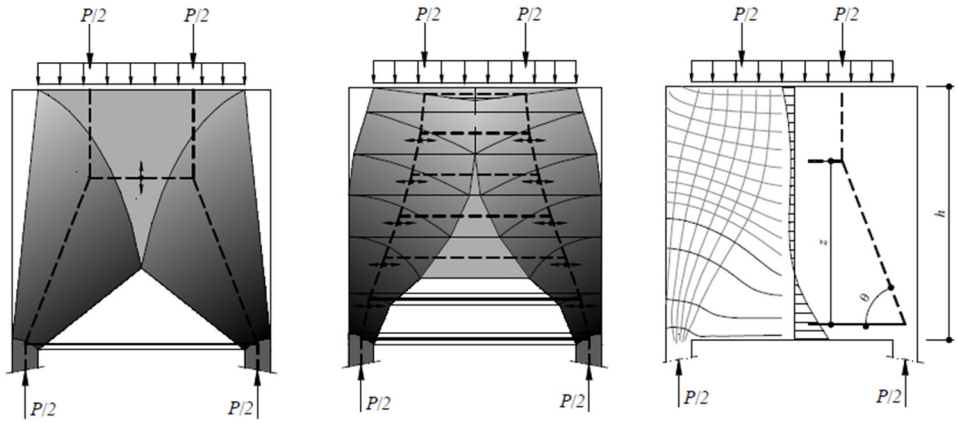

Figure 27
a) Simplified adaptive stress field model. Dark area indicate fan shaped compression stress fields and bright area indicate vertical and horizontal prismatic shaped compression stress fields. b) Refined adaptive stress field model. Dark area indicate fan shaped and horizontal prismatic compression stress fields and bright area indicate horizontal prismatic shaped compression stress fields. c) Elastic stress trajectories. Reproduced by permission. Lourenco [48].

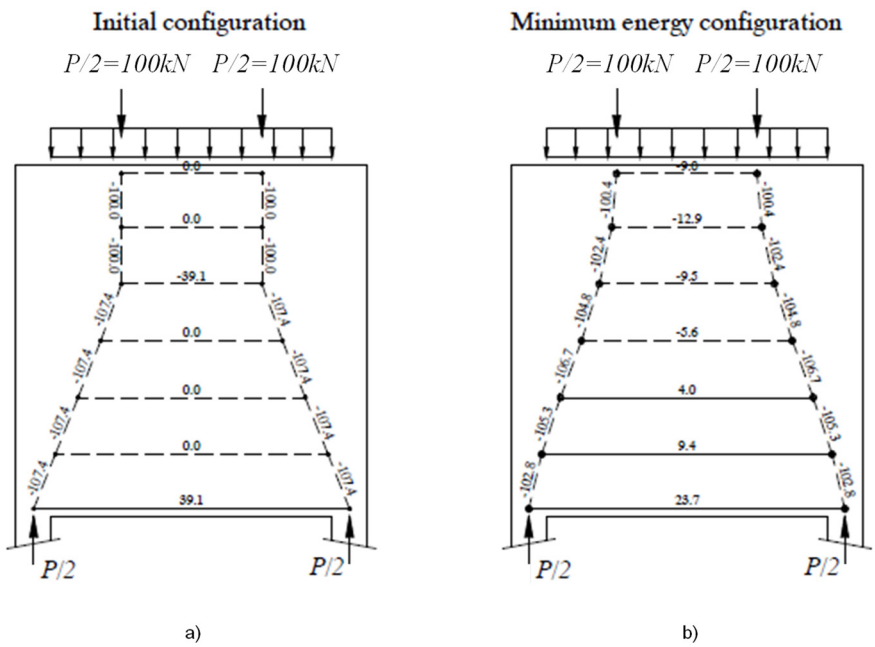

Figure 28
First load step for the adaptive stress field model. The concentrated loads on top of the structure are resultants to the uniformly distributed load. Reproduced by permission. Based upon Lourenco [48].

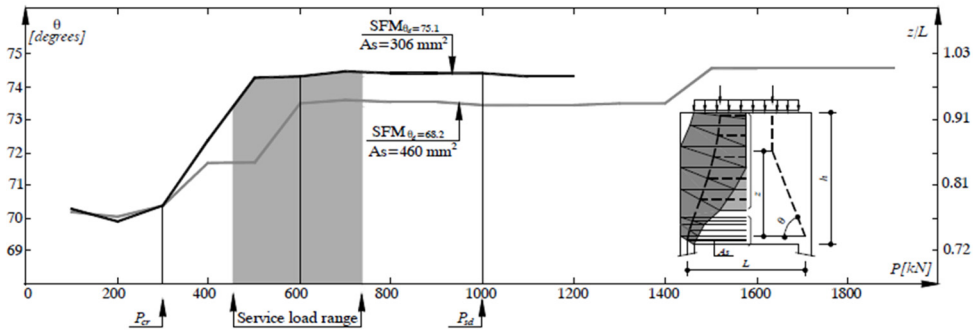

Figure 29
Inner lever arm distribution. The left vertical axis shows the angle between the inclined strut and the main reinforcement. The right vertical axis shows the relationship between the inner lever arm and the span. The horizontal axis shows the applied total load. The dark curve applies to the model in Figure 25a and the light curve applies to the model in Figure 25b. P_{cr} = 300 kN and P_{sd} = 1000 kN indicate crack load and design load, respectively. Reproduced by permission. Lourenco [48].

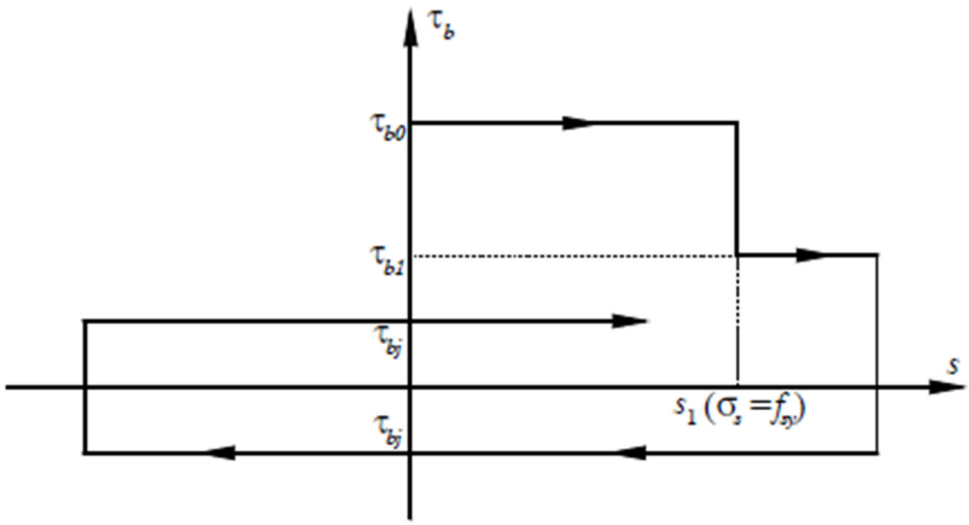

Figure 30
Bond-slip relationship for interaction concrete and reinforcement. The vertical axis shows the bond stress and the horizontal axis shows the slip between a reinforcing bar and the concrete. $\tau_{b0} = 2f_{ct}$ and $\tau_{b1} = f_{ct}$ for monotonic load before and after yielding, $\sigma_s = f_{sy}$, of the reinforcement steel, respectively. $\tau_{bj} = \tau_{b0}/8$ for reversal loads. Reproduced by permission. Lourenco [48].

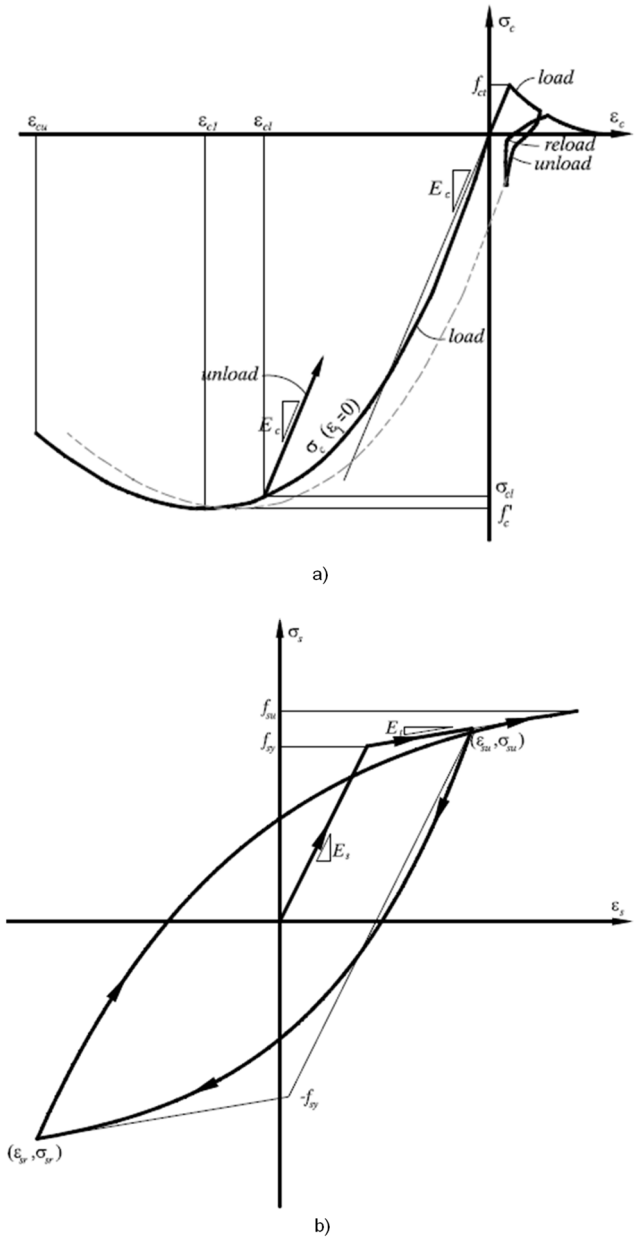

Figure 31
Constitutive relationship. The vertical axis shows stress and the horizontal axis shows strain: a) For concrete. b) For reinforcement. Reproduced by permission. Lourenco [48].

Vitone, et al. [50] used the strut and tie method and the load path method for assessment throughout the structural body state transformations, from the uncracked state to the ultimate limit state. The load path method can serve as a tool for evaluating the results from experimental tests and from numerical analysis.

Kostic [51] presented an automatic stiffness-based procedure, first proposed by Bendsoe, et al. [42] and Biondini, et al. [52], for the generation of strut and tie models. The procedure starts with a number of possible bars in a strut and tie model connected at joints. The least effective bars were removed, the remaining model being the one assumed to carry the load with the lowest degree of energy consumption. From the final strut and tie model an initial stress field was developed assuming the value of the concrete compressive strength, f_{cd}, in all compression field. In the next step the shape of the stress field was modified, without changing the positions of where the loads and reactions act. This modification was done to obtain node regions in a shape that resulted in a pseudo-hydrostatic state of stress, that is, all the compression fields are rectangular and perpendicular to the edges of the node. By doing this the check of the stresses in the concrete became very simple, according to the author. Figure 32 shows an example of an initial and a final strut and tie model. Using the final strut and tie model from Figure 32, Figure 33 shows the creation of stress fields.

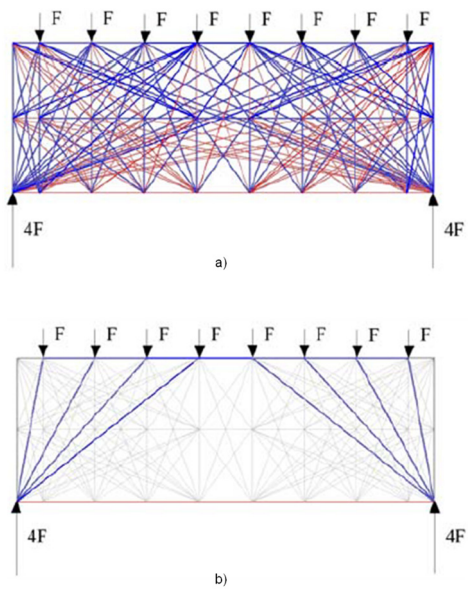

Figure 32
a) Initial strut and tie model. b) Final strut and tie model. The initial strut and tie model is greyed out. Reproduced from fib Proceedings - 6th International PhD Symposium in Civil Engineering, Zurich, August 23-26, 2006, page 83 - Computer-Based Development of Stress Fields, Neven Kostic, “Fig. 1: Strut-and-tie models for a deep beam" with permission from the International Federation for Structural Concrete (fib). Kostic [51].

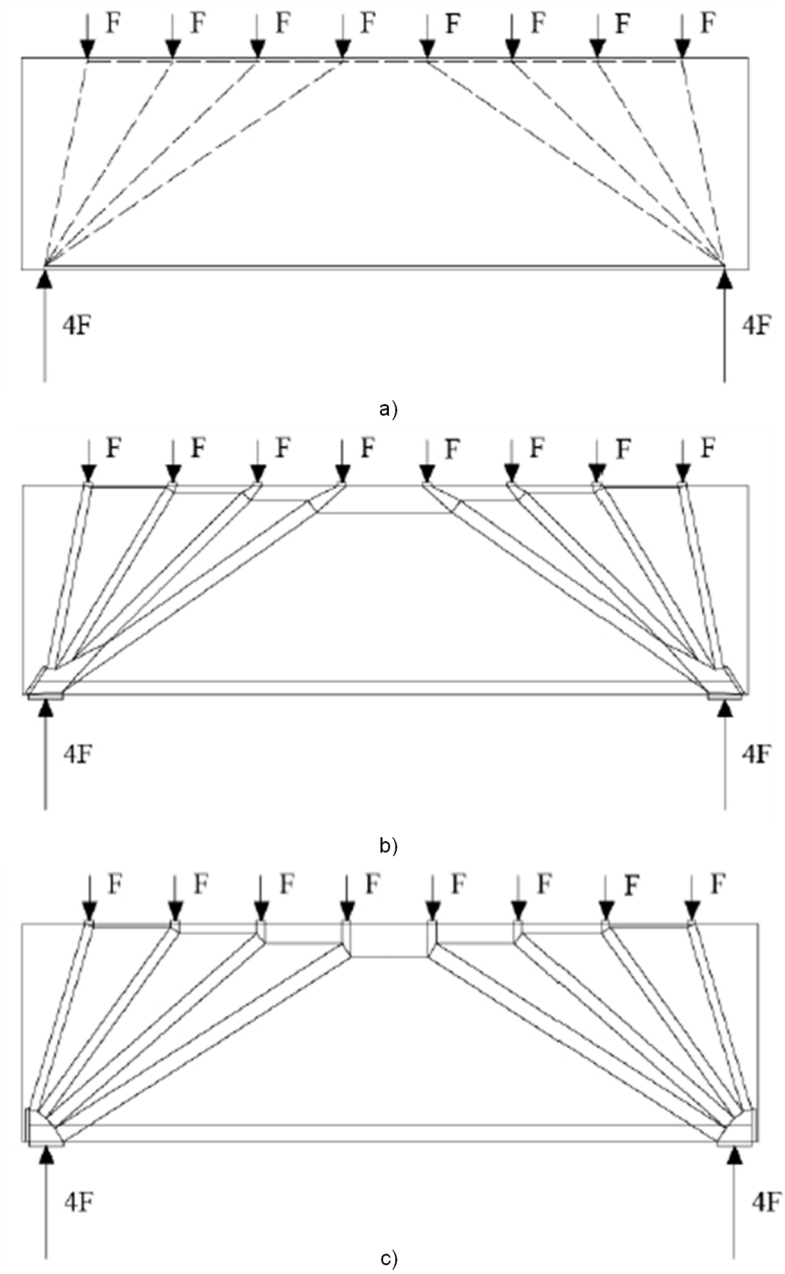

Figure 33
a) Final strut and tie model. b) Initial stress field. c) Stress field with pseudo-hydrostatic nodes. Reproduced from fib Proceedings - 6th International PhD Symposium in Civil Engineering, Zurich, August 23-26, 2006, page 84 - Computer-Based Development of Stress Fields, Neven Kostic, “Fig. 2: Stress field for deep beam as obtained by means of the proposed procedure" with permission from the International Federation for Structural Concrete (fib). Kostic [51].

Ruiz and Muttoni [53] presented a method using an Elastic-Plastic Stress Field (EPSF) for the automatic development of stress fields, using the finite element method, see Muttoni, et al. [54] for further details. Compatibility exists, the stress fields being calculated iteratively for each applied load step on the basis of the deformation field and the stress-strain relationships for the concrete and for the reinforcement. Full interaction with zero slip was assumed to take place between the concrete and the reinforcement. From the resulting stress field, strut and tie models can be developed if needed. The method is useful for practical design and also for the investigation of load carrying capacity. Figure 34 shows the material models for the concrete and for the reinforcement. When checking existing structures, the method is direct in the sense that the reinforcement already exists in the structure. For design, the author suggests a three-step approach:

1. A trial FE-model is first created. A reinforcement design is chosen, in accordance with experience, or a minimum reinforcement is chosen, one corresponding to what is required for crack control. The concrete is assumed to be elastoplastic and without tensile strength. The reinforcement is assumed to be linearly elastic.
2. From the load effects obtained from the FE-analysis, stress fields and, if necessary, strut and tie models are created. The reinforcement required is calculated as the ratio of the current force in the reinforcement to the tensile strength. A lesser reinforcement than one of a minimum value should not be chosen.
3. A new FE-analysis is then performed using adjusted values for the reinforcement. The reinforcement then assumes an elastoplastic stress-strain curve. Under these conditions, other necessary controls are performed. Some iterations may be needed to converge the results obtained into a final reinforcement design.

The method requires only a few material parameters as input data and primarily refers to studies of the ultimate limit state. A minimum amount of reinforcement is required because the concrete is assumed to have no tensile strength. The minimum reinforcement is needed for distributing cracks, for counteracting a brittle failure and to ensure proper functioning in the service state.

To be able to check serviceability limit state regarding crack widths and deflection the authors proposed to develop simple elastic-plastic stress fields accounting for the cracked behaviour of concrete. This check in serviceability limit state is possible because the material model used for the concrete to develop the EPSF is based on deformation and strain compatibility, i.e., equal deformation for adjacent material particles.

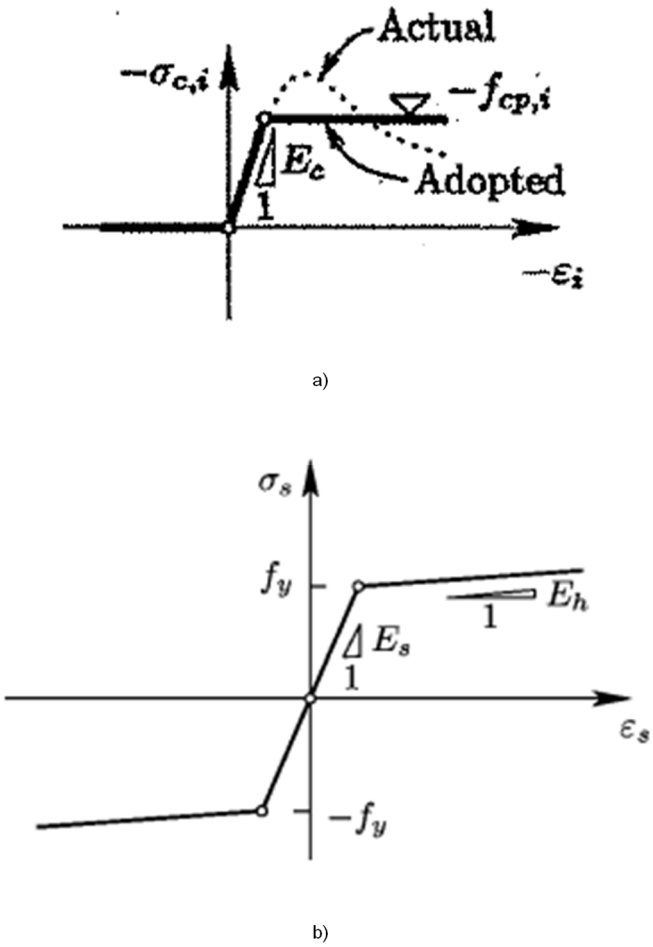

Figure 34
The figure shows the material models for concrete and reinforcement. a) Actual and adopted elastic-perfectly plastic stress-strain response for concrete. The letter i stands for the two principal stresses and strains. b) Elastic-plastic stress-strain respons with strain hardening for reinforcement. Authorized reprint from July-Aug 2007 ACI Structural Journal, Vol. 104 No. 4, Title No. 104-S48 “On Development of Suitable Stress Fields for structural Concrete.”. Ruiz and Muttoni [53].

Muttoni, et al. [55] discuss the difference between the approaches used in the design of new structures and the assessment of existing ones using EPSF (elastic-plastic stress field) in a clarifying way. Examples of design and assessment are given. Many comparisons are made with tests reported in the literature, good results being obtained in verifying the method. Figure 35 shows the linear elastic stress field and a strut and tie model based on it, and also an elastic-plastic stress field and the corresponding reinforcement, all of this for the same structural member. The

differences between a strut and tie model that follows the linear elastic stress field and a reinforcement layout calculated after a resulting elastic-plastic stress field are shown in the figure.

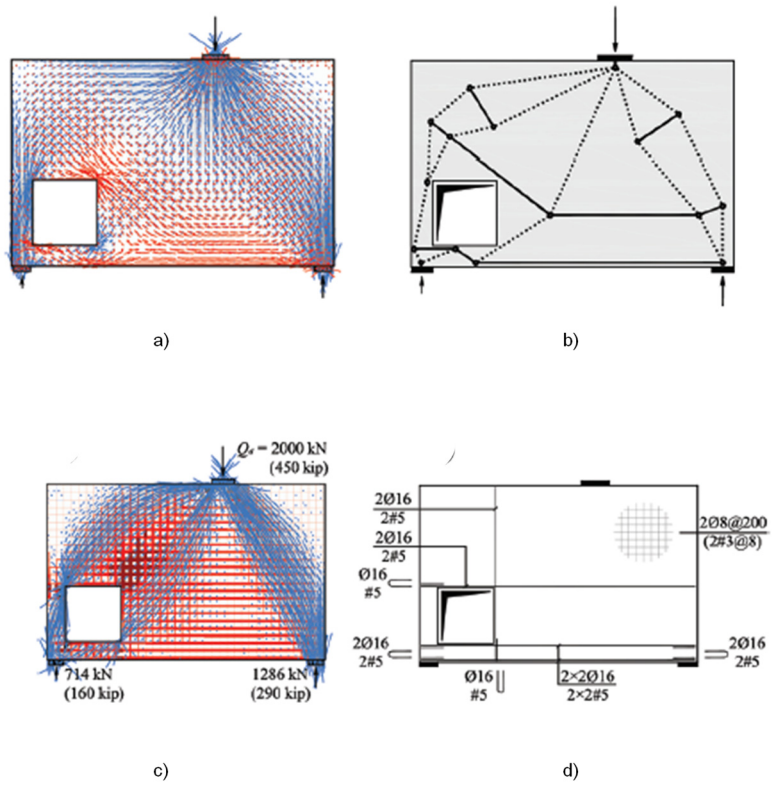

Figure 35
In Figure a) and c) shades of blue indicate compression and shades of red indicate tension. a) Linear elastic uncracked stress field. b) Strut and tie model based on linear elastic uncracked stress field. c) Resulting EPSF. d) Calculated reinforcement from resulting EPSF. Authorized reprint from Sept-Oct 2015 ACI Structural Journal, Vol. 112 No. 5, Title No. 112-S49 “Design versus assessment of concrete structures using stress fields and strut-and-tie models.”. Muttoni, et al. [55].

Rozvany [56] found it to be possible to derive optimal 2D-trusses from stressed plate structures. Making use of this, Fenton, et al. [57] presented a discrete truss optimization method using grammatical evolution. Grammatical evolution is an evolutionary computation, and it can represent a variable number of nodes and their locations on a continuum. The theory of the method is based on minimization of the self-weight of a structure, given a specified deflection limit. The method does not require any information concerning the desired form of solution other than the loads and the reactions (boundary conditions) involved. That is, the method does not employ the traditional ground-structure-based approach in which all possible

locations for nodes and the connection between them are known in advance and where an algorithm then selects the most appropriate configuration from the given list of nodes and connections. Instead, the method evolves the number and location of nodes which opens up for free searches that can lead to better solutions. Specifically, the method is appropriate for ill-defined problems without having knowledge of the structure of the final solution. Figure 36 shows the evolution of a simply supported truss structure.

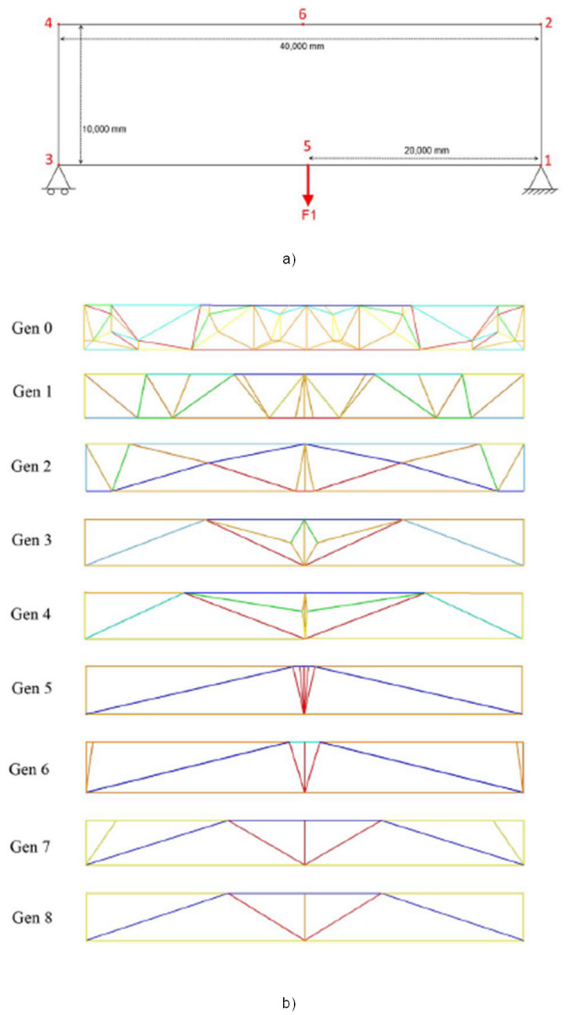

Figure 36
Evolution of a simply supported truss structure. a) Geometry for and load acting on the structure. b) Shows a number of solutions taken from the initial generations of an evolutionary run. As the generations progress the fittest solution become visible. Shades of blue indicate compression and shades of red indicate tension. Reproduced by permission. Copyright 2015 IEEE. Fenton, et al. [57].

In his thesis, Niketic [58] discusses the differences in the approach employed in designing and in assessing the load-bearing capacity of structural concrete members, using an elastic-plastic stress field (EPSF). Different strategies can be used to develop stress fields and strut and tie models suitable for the two stages. Many practical examples can be used to illustrate the idea of the gradual refinement of a model used for both design and assessment. The thesis also addresses compression softening and partial safety factors for steel and for concrete, respectively. The latter is because the theory of stress field model used simulates the behaviour of structural concrete more in detail than current codes do, according to the author. Figure 37 shows an example of a calculation using an EPSF. It is clear how the loads flow through the structure and give rise to compressive stresses in the concrete and tensile stresses in the reinforcement.

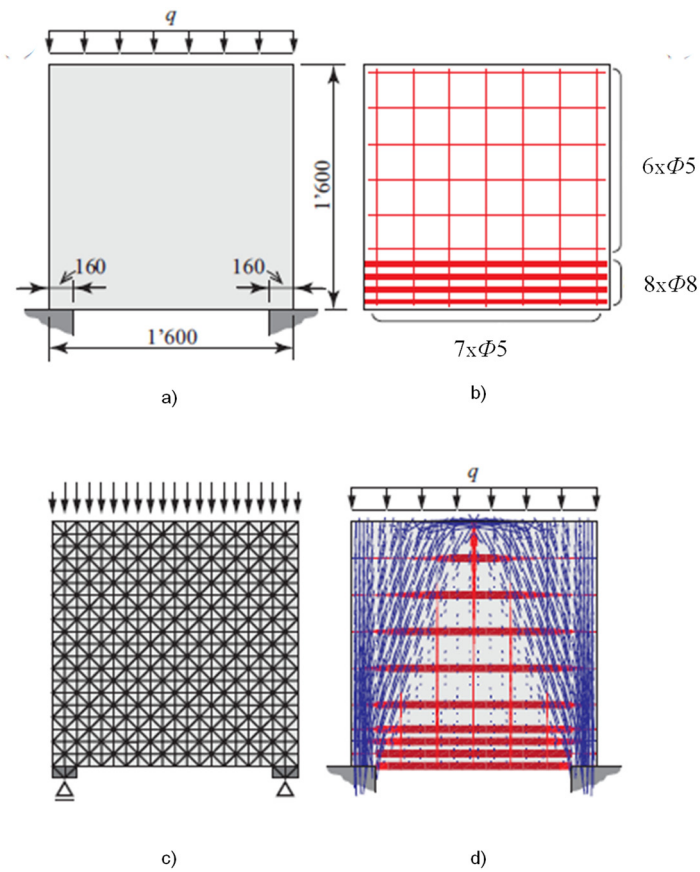

Figure 37
a) Geometrical properties. b) Reinforcement layout. c) FE mesh. d) Resulting EPSF. Shades of blue indicate compression and shades of red indicate tension. Reproduced by permission. Niketic [58].

2.7. Discussion

This chapter relates the purpose and aim of this dissertation to existing knowledge presented in previous chapters. The content of the chapter concentrates more on the conditions that apply and the results that can be expected when the methods referred to are applied.

As can be seen from the previous chapter, much work has been performed since the 1980s to systematize and automatize the development of truss models, strut and tie models and stress field models for the design and verification of structural concrete. None of the methods developed have led to any practical breakthrough for using strut and tie models and stress fields as design and verification tools, which in turn has resulted in a lack of commercial calculation programs in the area. Instead, linear and nonlinear FE-analyses are the tools employed the most today. The major reason for systematized methods based on strut and tie models and stress fields not being used to any great extent may be that current regulations do not deal with strut and tie models and stress fields as methods to describe various failure mechanisms of reinforced concrete in any broader sense. This can be expected to change in future regulations.

The FE method is a general and powerful method that can be used to evaluate nonlinear behaviour in discontinuity regions. It has many advantages, but also disadvantages, such as the interpretation of input and output, time aspects, the understanding of constructive behaviour and numerical problems. Often, the number of input parameters have a major impact on the end result and are thus potential sources of error.

Systematized methods based on strut and tie and stress field models are good alternatives to nonlinear FE-analyses. These are methods that emphasize the importance of being transparent, as opposed to the black box that FE-programs can be. In addition, they enable engineers to make use of their knowledge and to be involved in interpreting the results. Sometimes, the programs that handle strut and tie models and stress field models consist of compatible modules, such as databases, that can be used freely. The desire to be transparent leads to well-developed performance reports that are easy to evaluate.

What can be said then about where we are today? The question is: Do we have all the tools we need to understand the nonlinear behaviour in discontinuity zones and to effectively develop solutions that are safe, functional, optimal (regarding use of materials) and practical? Have we perhaps lost the original idea, that is, to explain the load-bearing function for reinforced concrete in a simple way that is easy to understand? Each of the methods developed and mentioned in chapter 2.6 has its

pros and cons and can be used either as a whole or in part. No method can be said to be completely optimal. Instead, each method is limited by certain conditions.

Schlaich, et al. [4] suggested that to be able to meet the serviceability requirements, design in discontinuity regions in the serviceability limit state should follow the linear elastic stress field. They also proposed that, in order to use a consistent approach and at the same time promote simplicity, one could use the same strut and tie model both in the ultimate limit state and in the serviceability limit state. Such a uniform design approach is still taken by designers today, although Schlaich explained that, if this was needed, the load-bearing capacity could be found without taken account of the elastic stress field. In such a case, the deformation that occurred and the deformation capacity would need to be taken into consideration. For deep beams with low reinforcement ratios, it has been shown, see fib Bulletin 61 [11], paper 16, chapter 3.2, that following the linear elastic stress field clearly underestimates the load-bearing capacity and, in the serviceability limit state it is unnecessarily conservative. This and the fact that it is not practical in all cases to arrange the reinforcement so that it follows the linear elastic tensile stress fields is a reason to consider the choice of stress field in both the ultimate limit state and the serviceability limit state.

Recently, extensive work has been done to develop tools to use in the design and verification of discontinuity zones. This has resulted in methods based on different conditions. Below, some of them mentioned earlier in the state of art are discussed.

Kostic [51] reduced the continuum to a discrete strut and tie model. The method does not deal with the deformation capacity or requirements of serviceability. The simplification of a continuum to a discrete strut and tie model is contrary to the physical reality involved. The stress-strain relationship for the compression of concrete and for the reinforcing steel is rigid-plastic, concrete having no tensile strength. The method can be effective for design, but the procedure described in the referenced paper need improvement related to the ductility demand and to the serviceability requirements.

Ruiz and Muttoni [53] presented a procedure that implemented the stress field method through use of the FE method. The procedure was based on use of the elastic-plastic stress field (EPSF) in the design and assessment of reinforced concrete structures. The concrete is assumed to be elastic-plastic and to be without tensile strength, the reinforcement being assumed to be elastic-plastic, with strain hardening, and carrying the tensile stresses and thus maintaining equilibrium. Since the concrete is assumed to have no tensile strength, the model requires distributed reinforcement for purpose of crack control. The materials are often presumed to have an unlimited deformation capacity, although this, in fact, is not the case. Using surface reinforcement of a small diameter as an active reinforcement together with a main reinforcement of large diameter can be a risk since the possibility exists of

the surface reinforcement reaching the ultimate strain earlier than the main reinforcement does. The procedure assumes, there to be full interaction between the concrete and the reinforcement. In fib Bulletin 65 [30], sec. 6.1.1 the bond-slip relationship is given. It can be seen here that there are two failure modes, pull-out or splitting, and that the bond-slip relationship is strongly influenced by reinforcement yielding, by transverse pressure and cracking along the bar, and if the load is cyclic, repeated or sustained. The procedure primarily refers to studies of the ultimate limit state, but research is being carried out for the automatic development of suitable reinforcement layouts allowing for optimizing some design criteria in the serviceability limit state, for example crack width. The impact on the result of the FE-analysis regarding load-bearing capacity and especially crack development when full interaction is assumed can be discussed. One parameter that can be decisive for the response is the element size. Its influence on the response depends on the assumed model of the interaction between concrete and reinforcement.

Lourenco [48] used complete material models in his method and could thus evaluate both the service behaviour and the deformation capacity involved. The interaction between the reinforcement and the concrete was simplified to a bond-slip in accordance with the tension chord model. The crack development could be followed, and the crack widths could be calculated. The stresses were redistributed, in a manner in line with the adaptive stress field model, through an energy minimization process that began from elements of three different types: ties, fan shaped struts and prismatic struts. This is a simplification of the structure being a continuum to being a truss structure. The adaptive variables can be node coordinates at which reinforcements and compressive struts meet. In order to obtain a true picture of the stress redistribution that takes place, account needs to be taken not only of the main reinforcement, but also of a uniformly distributed minimum reinforcement. This means distinguishing clearly between active (constructively utilised) reinforcement and passive (non-constructively utilised) reinforcement, i.e. determining how much of the passive reinforcement can be used as active. If all the reinforcement is used as being active, all the forces that influence the structure need to be taken into account, such as the restraint force, for example, since there is no margin.

Back to the question posed above, i.e.: Do we have all the tools we need to understand the nonlinear behaviour in discontinuity zones and to effectively develop solutions that are safe, functional, optimal (regarding use of materials) and practical? Perhaps the question should be reformulated somewhat, our asking instead: Do we now have all the knowledge that is necessary concerning the nonlinear behaviour of reinforced concrete in discontinuity zones? Leonhardt and Walther [22] conducted many tests on deep beams, already in the 1960s. Did their work present an answer to the question, and have the research performed after that been unnecessary?

The answer to the questions above is that there are still gaps in our knowledge of the matter and thus there is a need of added knowledge so to better understand the nonlinear behaviour that occurs in connection with discontinuity regions. There are many procedures and methods, based on different assumptions, that are applicable to design and verification. There must, however, be a basic understanding and perception of an expected result regarding the behaviour in service and ultimate states. Questions like:

- What parameters affect the stress redistribution and the deformation capacity within a structure?
- To what extent do the parameters affect the behaviour of a structure?
- What synergistic effects can there be between these parameters?

which are posed in connection with designing and analysing a certain structure and its parts using the strut and tie method or the stress field method are still not completely answered.

3. Deep beam studies

3.1. Introduction

Two major studies of deep beam modelling using FE-calculations have been conducted during the present research project. The deep beam, which is simply supported, is loaded on the top with a uniformly distributed load placed between the centres of the support, the ratio of height to span being 1.5, see Figure 38a. The purpose of the calculations is to study the gaps discussed in the previous chapter 2.7, the deformation capacity and the stress redistribution of the structure being of central interest.

Study 1 analyses, with use of nonlinear FE-analyses, the effects of each of six different reinforcement arrangements on the behaviour of the inner lever arm, and the stress- and crack development that takes place for an increasing load up to failure. Four of these six cases involve increased amounts of reinforcement being applied placed in one single layer. Regarding the other two cases, one case involves the main reinforcement being arranged in three layers instead of one, whereas the other case involves the main reinforcement being arranged in one layer that is supplemented by surface reinforcement. The reinforcement content is rather low in all of the cases.

Study 2 involves a design in which given loads in both the ultimate and the serviceability limit state are applied using different strut and tie models. The consequences of the different alternative strut and tie models and the reinforcement arrangements chosen are then studied and compared with the results of nonlinear FE-analyses for an increasing load up to failure. In addition, analyses of the results for the same reinforcement arrangements making use of various strut and tie models are carried out and compared with one another. On the basis of the results obtained, recommendations are made regarding the choice of strut and tie models and reinforcement arrangements.

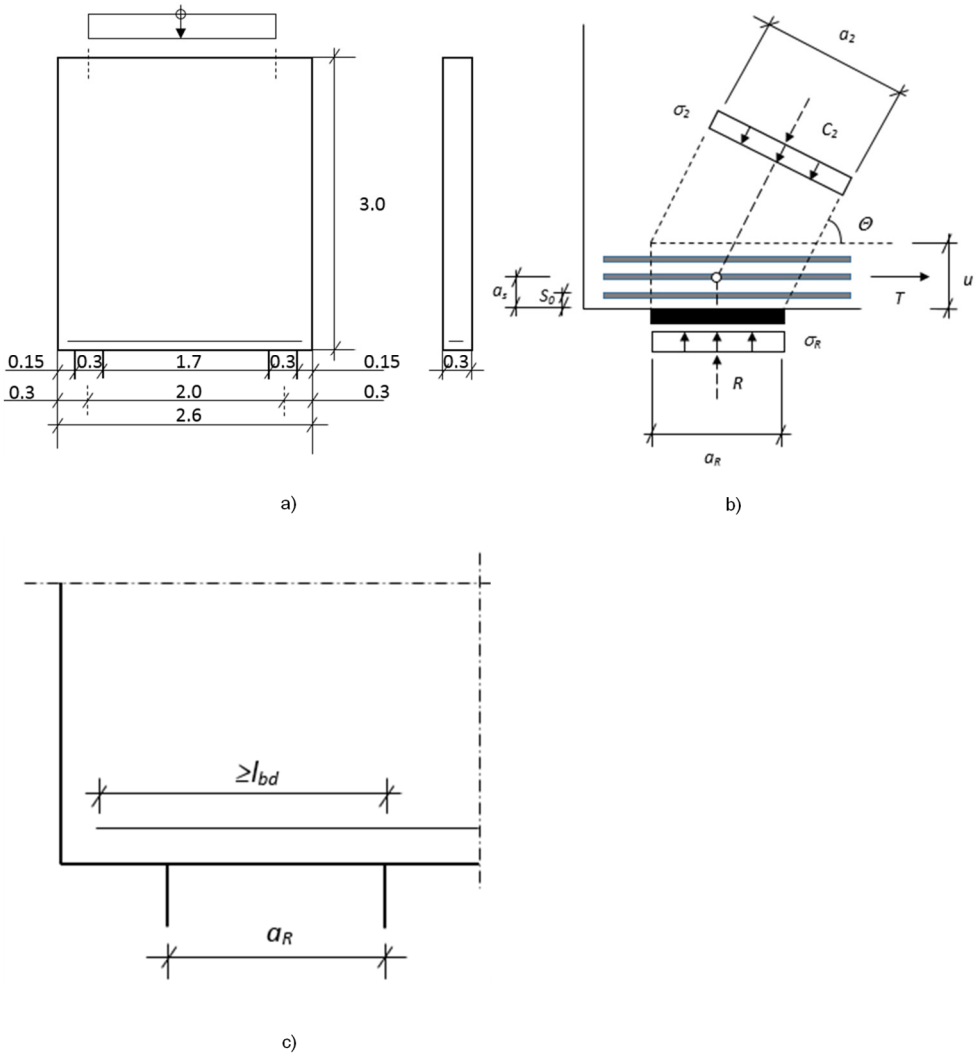

Figure 38
a) The geometry of and the load upon the deep beam. b) A typical support. R = Reaction force at the support. C_2 = Compression force in the inclined strut. T = Tension force in the tie. σ_R = Stress at the support. σ_2 = Stress in the inclined strut. c) The anchoring of the reinforcement in the analyses, the reinforcement being anchored one anchorage length, l_{bd}, behind the front edge of the support.

3.2. Overall and general conditions

The conditions that are applicable to both studies are presented here.

3.2.1. Studied deep beam

3.2.1.1. Geometry, support and load

The geometry of, and the load on the structure is shown in Figure 38a.

A geometry of a deep beam with a ratio of the height to the span of H/L=1.5 was chosen so as to allow for a large stress redistribution with an angle of up to 80 degrees between the inclined compressive strut and the tensile tie. The relation of H/L=1.5 means that the deep beam can be categorized as a very deep beam, one requiring a lesser amount of main reinforcement to withstand the bending moment in the midsection than in the case of an ordinary beam. The assumed geometry of the deep beam has affected the value of the design loads. It has also affected the chosen amount of reinforcement in the structure to have a low content.

The size of the supports was chosen in order to ensure that the stresses in the strut and tie connection in the current node at the support did not exceed the strength of the node. The support was also placed at a sufficient distance from the end of the structure so that an adequate anchorage of the reinforcement was possible without having to bend the reinforcement in any way. Both of the supports are fixed in the vertical direction, whereas in the horizontal direction the left support is fixed, the right support being free to move.

Figure 38b shows a typical support. The parameters in the figure are as follows:

- Θ = The inclination of a diagonal strut
- a_R = 0.3 m=The length of the support
- b_R = 0.3 m=The width of the support
- s_0 = 0.029 m=The distance from the bottom of the deep beam to the centre of the first reinforcement layer
- a_s = The distance from the bottom of the deep beam to the centre of the tie
- u = The width of the tie
- a_2 = The width of the inclined strut at the node

The parameter values not given were calculated on the basis of the parameter values that are given and the inclination of the diagonal strut in the case in question.

A uniformly distributed load is applied on the upper face of the deep beam. A load of this type was chosen since it was considered less governed in terms of the load paths it follows through the structure than a concentrated load with a load path that starts at the location of the load would be.

More data about the load is given in upcoming chapters.

3.2.1.2. Concrete and reinforcement

The reinforcement was chosen in order to obtain a clear indication of the effects of different arrangements. For this reason, a number of different cases were selected. The cases that were studied involved an increased degree of main reinforcement, a distribution of the main reinforcement over several layers and the inclusion of a surface reinforcement in addition to the main reinforcement.

The strength class of the concrete was C30/37, and the bars were of grade K500B steel, ribbed bars with a characteristic yield strength of 500 MPa and of ductility of class B, see the strength data given in Table 1. The type of the concrete and of the reinforcement chosen, corresponded to what is commonly employed in such structures.

Table 1
Strength data for the concrete and the reinforcement.

Concrete			Reinforcement	
f_{cm}[1] (MPa)	f_{ctm}[2] (MPa)	f_t[3] (MPa)	f_y[4] (MPa)	ϕ[5] (m)
38,0	2,9	540	500	0,008/0.004

[1] f_{cm} = The mean value of concrete cylinder compressive strength.

[2] f_{ctm} = The mean value of axial tensile strength of concrete.

[3] f_t = The tensile strength of reinforcement.

[4] f_y = The yield strength of reinforcement.

[5] ϕ = The diameter of the bars. For main reinforcement 0.008 m and for surface reinforcement 0.004 m.

The location of the reinforcement is presented in the following:

- C = 25 mm = The concrete cover from the bottom of the deep beam to the nearest bar
- $C1$ = 15 mm = The concrete cover from the side of the deep beam to the nearest bar
- $a_h \geq 15$ mm = The clear distance between the bars in the same layer
- $a_v = 42$ mm = The clear distance between the bars in the different layers

All the data are based on requirements presented in EN 1992-1-1 [2]. The thickness of the concrete cover fulfils structural class S1 and exposure class XC2, the

deviation being assumed to be 5 mm, see Section 4 in EN 1992-1-1 [2]. The clear distance between the bars is based on there being an 8 mm maximum size of an aggregate, see Section 8 in EN 1992-1-1 [2].

The reinforcement extends beyond the inner edge of the support by at least one anchorage length, l_{bd}, in which case it has a value of 0.40 m. This meets the requirements described in EN 1992-1-1 [2] regarding the anchorage of the tensile force, which corresponds to the tensile strength of the bars inside the inner edge of the support. The typical solution in terms of the anchorage of the reinforcement at the support is shown in detail in Figure 38c.

3.2.2. Nonlinear FE-model

3.2.2.1. Solution technique

The studies examined, among other things, the stress redistribution. The redistribution of stress occurs due to cracking and to plastic deformations. This meant that the entire loading process up to failure had to be followed.

A nonlinear FE-analysis can be performed as a load- or displacement-controlled static or quasi-static analysis. Static load has no acceleration and thus generates no forces of inertia. However, carrying out a static analysis can result in problems of convergence, so that the iteration process stops before the analysis is successfully completed. Performing a quasi-static analysis that includes inertial effects (though small) has a viscous effect and stabilizes the behaviour of the model, which can be of help in avoiding problems of convergence. In a quasi-static analysis, the load or displacement involved is applied slowly, simulating static behaviour, because it is important to minimise the kinetic energy, reducing the inertia effects, so that these do not appreciably affect how the structural system carries the external load.

It was shown that a quasi-static load-controlled or a static deformation-controlled analysis with an increase in the iterations and a decrease in the tolerances and increments that were involved overcame the problem of convergence, see chapter 3.6 where different methods of analysis for studying load versus displacement are compared and discussed in greater detail. In this study a quasi-static load-controlled solution was chosen, carried out by a dynamic implicit solver. At the first crack in the FE-analyses there was a maximum ratio of the kinetic to the strain energy of about 2.6 %, showing there to be a temporary imbalance in the equilibrium there, which points to a slight dynamic effect due to cracking. The low loading rate results in no major effects of inertia. The quasi-static approach can thus be considered as providing the equivalent of a static load. The program used in the study was BRIGADE/Plus [59], which is based on ABAQUS [60].

3.2.2.2. Structural model

The studies conducted have been limited to 2D-models of reality. This, because to provide a basic conception of the structural response unaffected of 3D-effects.

The geometry of the structure is in accordance with Figure 38a.

3.2.2.3. Material model

Concrete: The material model used for concrete was the Concrete Damage Plasticity Model, see ABAQUS [60], which is a plasticity- and continuum-based, damage model, the main failure mechanisms of the concrete being tensile cracking and compressive crushing. The model uses isotropic tensile and compressive plasticity to represent the inelastic nature of the concrete. In this study the loading was monotonic, without any unloading, there thus being no need of a damage parameter.

The stress-strain relationship for concrete under compression follows EN 1992-1-1 [2], sec. 3.1.5 (1). The relation of stress to crack width describing the tension softening response is represented by a bilinear curve, see Figure 39.

Values for the dilation angle, the eccentricity and the fracture energy were assumed to be those for $\psi = 38°$, see Jankowiak and Lodygowski [61], $\varepsilon = 0.1$, see ABAQUS [60], and $G_F = 75$ Nm/m^2, see CEB-FIP Model Code 1990 [6], sec. 2.1.3.3.2, Table 2.1.4. The values for the dilation angle and the fracture energy are discussed further under chapter 3.6.

Reinforcing steel: In the analysis the idealised stress-strain curve according to EN 1992-1-1 [2], sec. 3.2.7 (2) a) "with an inclined top branch" was used.

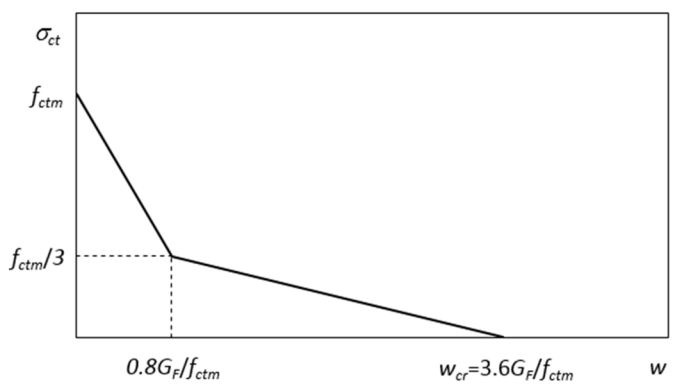

Figure 39
The tensile stress (σ_{ct})-crack width (w) relationship, where w_{cr} stands for stress-free crack-opening. The crack is fictitious as it has the ability to transmit tensile stresses up to a value corresponding to w_{cr}.

3.2.2.4. Load model

The deep beam was loaded with a uniformly distributed vertical pressure at the top of the specimen between the centres of support. The load was incremented at a low loading rate in small steps, to limit the kinetic energy in relation to the strain energy, according to a linear monotonically increasing function the loading rate being 135 kN/ms during a 20 s period up to failure or to a possible maximum load value of 2.7 MN/m. No cyclic loading was employed.

3.2.2.5. Boundary conditions

The model does not contain any structural elements in addition to those that were necessary for the studies that were planned. It was important that the modelling of the support and of the boundary conditions was done in such a way that it did not affect the response of the structure. Because of this, the support was modelled as being a part of the structure´s lower edge, on which the reaction was evenly distributed, and for which the rotation followed a reference point used to determine the boundary conditions. This provided a smooth transition between the edge of the support and the structure.

More specifically the support of the structure was modelled with use of a distributed coupling constraint for the bottom edge of the structure over the length of the support area (support length a = 0.3 m), see Figures 38 and 40a. This distributes the reaction force uniformly over the edge, resulting in the edge behaving as a loaded area, corresponding to a fictitious plate, having the length a and a width equal to the thickness of the deep beam. The area is constrained to a reference point, see Figure 40b, in which the boundary conditions, either fixed or free, are defined.

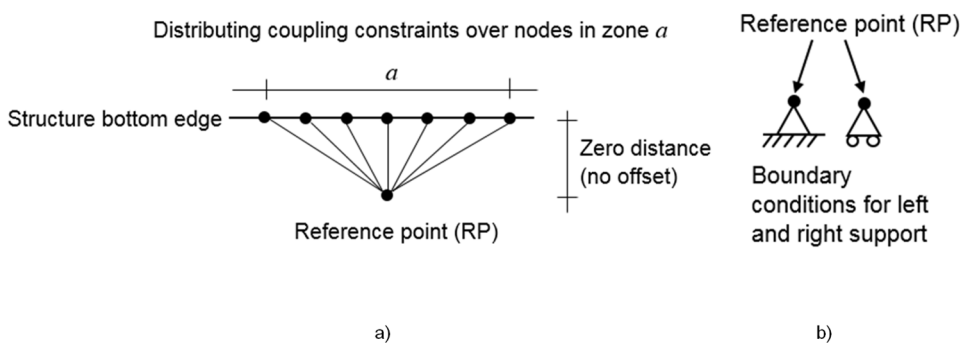

Figure 40
Boundary conditions. a) Definition of the support area. b) Definition of the reference point.

3.2.2.6. Concrete-reinforcement interaction

The conditions assumed to apply were those of monotonic loading with pull-out failure, no account being taken to the impact of the yielding of reinforcement on the stress-slip relationship of the bonds involved.

One way to describe the interaction between the concrete and the reinforcement is to assume a perfect bond with no slip. The perfect bond results in cracks in all the elements in the cracked regions. This is not the case if reinforcement-concrete slip is assumed. Then a crack localises to one element row. Due to the sliding, where the stress in the reinforcement is gradually transferred to the concrete, a second crack can only occur at a certain distance which corresponds to the concrete stress once again reaching tensile strength. Views are divided among researchers regarding whether it is possible to achieve the effect of the localisation of cracks by modelling a full interaction and using a fine element mesh or whether a bond-slip model for the interface is a prerequisite for localisation. It is clear, however, that full interaction is easier to model compared to a bond-slip model that can be complex.

In the present study the surface reinforcement (SR) was modelled in terms of there being full interaction (no slip) with the concrete. For the tensile reinforcement (TR) a simplified bond stress-slip relationship was employed, there being assumed to be a linear elastic relationship up to the maximum bond stress, $\tau_{max} = 0.45f_{cm}$, for a slip, $s_1 = 1.0$ mm, see Huang, et al. [62] and the fib Bulletin 10 [63], sec. 2.2.1.

This function was considered to be valid up to a maximum of 1 mm slip. The degree of slip was checked during the simulations, and the maximum value never exceeded the limitation for the validity of the function.

The concrete-steel interaction was modelled as being a force-slip spring (K_{spring}), see Equations (1) and (2), each element having a spring.

$$F_{spring} = 0.45 f_{cm} n \pi \phi l_e \tag{1}$$

$$K_{spring} = F_{spring} / s_1 \tag{2}$$

In the equations, F_{spring} = maximum force corresponding to a slip, $s_1 = 1.0$ mm, n = number of bars, ϕ = diameter of the bars, l_e = element length.

3.2.2.7. Elements and mesh

The concrete structure was modelled with use of 2D plane stress continuum elements. The form of the concrete elements is an important parameter in calculating the crack width, the best conditions for the calculation being assumed to be obtained

for the quadratic form of the elements. In all of the cases the concrete elements were modelled quadratically as being approximately 40 mm in size. However, the elements in the column just in front of the inner side of the respective support, were meshed with a slightly greater width of the mesh than the other elements, this was assumed to have no specific effect on the results.

In most of the simulations, 4-node bilinear plane stress quadrilateral elements with reduced integration and hourglass control were employed (CPS4R). This choice of elements was based on the principle of approximating the continuously unknown function of displacement with many elements with bilinear element functions, for example 4-node elements, instead of using fewer elements with higher order approximation, for example 8-node biquadratic elements. In some cases though, 8-node biquadratic plane stress quadrilateral elements having reduced integration were used instead (CPS8R) but without reducing the number of elements. The reason for using higher order elements was that a FE-analysis involving CPS8R-elements resulted in the desired yielding failure in the reinforcement, while a FE-analysis with low order CPS4R-elements instead resulted in a compressive failure of the concrete above the support before the reinforcement reached the yielding stress.

The reinforcement was modelled in terms of 2-node linear truss elements having only axial stiffness (T2D2), the reinforcement being simulated as being uniformly distributed over the thickness of the structure.

The bond-slip interaction between the concrete and the main reinforcement was modelled in terms of connector elements. A fictitious reinforcement bar with little rigidity and having full interaction with the concrete was arranged as being in the same position as the active reinforcement bar. The connector elements then connected the nodes for the fictitious and the active bars, the connection being defined with the current bond-slip function.

3.3. Specific conditions

The conditions that apply in the respective studies are presented here.

3.3.1. Study 1

The study is an analysis of different reinforcement arrangements using FE-analyses for an increasing load up to failure as described in section 3.2.2.4.

3.3.1.1. Reinforcement

The effects of six different reinforcement arrangements were studied, see Table 2. Five of them consisted of tensile reinforcement (TR) placed in a single layer at the bottom of the structure, in one of these five cases vertical and horizontal surface reinforcement (SR) also being provided. In one case the reinforcement was located in three successive layers.

Table 2
The reinforcement arrangements studied.

Case	Arrangement	Comment	Notation[1]
1	TR 8 ϕ8 mm		TR 8
2	TR 8 ϕ8 mm and SR ϕ4 mm s200 mm	SR arranged vertically and horizontally at a distance of 200 mm from each other	TR/SR
3	TR 10 ϕ8 mm		TR 10
4	TR 12 ϕ8 mm		TR 12
5	TR 3x4 ϕ8 mm	12 bars placed in 3 layers with 4 bars in each layer	TR 3x4
6	TR 14 ϕ8 mm		TR 14

[1] The notations will be used in referring to the respective cases.

3.3.1.2. Nonlinear FE-model

Table 3 refers to Study 1 and shows for the different cases what applies regarding:

- The assumed value for the dilation angle.
- Whether the regions of the entire height at the ends of the deep beam, and with a width, *b*, that includes the first row of elements in front of the support towards the midspan, see Figure 41, are assumed to have a linear elastic stress strain curve for the concrete or not.
- The type of meshed element used for the concrete.

The linear elastic assumption and the assumption regarding the value of the dilation angle are discussed in greater detail in chapter 3.6.

Table 3
Specific assumptions for the concrete regarding the dilation angles, the stress-strain relationships and the meshed elements.

Study 1			
Case	**Dilation angle (°)**	**Stress-strain[1]**	**Element**
1	38	N	CPS4R
2	38	N+L	CPS4R
3	38	N	CPS4R
4	38	N	CPS4R
5	38	N+L	CPS8R
6	45	N	CPS8R

[1] N = Nonlinear, L = Linear, N+L = Indicates that part of the structure has a linear stress-strain relationship.

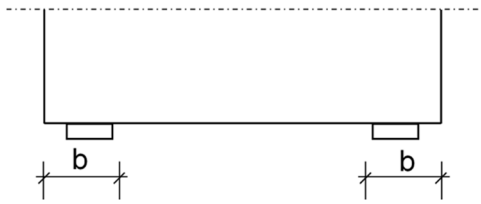

Figure 41
Indicates the width, *b*, at which the entire height of the deep beam, for some cases, is modelled with a linear elastic stress-strain curve.

3.3.2. Study 2

In the study a design is performed for given loads using different strut and tie models, the results being compared with those of nonlinear FE-analyses for an increasing load up to failure.

3.3.2.1. Load

The deep beam was designed for a load, $q_{STMfi} = 845$ kN/m, in the ultimate limit state. The choice of the load was a consequence of the geometry of the structure, a desire to limit the concrete compressive stresses and to obtain a given amount of reinforcement for a certain angle of the inclined compressive strut.

By choosing a load that met these conditions, it was possible to follow the nonlinear FE-analyses until the ultimate strain in the reinforcement was obtained.

3.3.2.2. Reinforcement

In the study, the amount and the arrangement of the reinforcement is a result of the design of the structure, not a condition, and is therefore presented in chapter 3.5. The area of the reinforcement is calculated for the tensile strength, f_t = 540 MPa. This is to be able to compare the result obtained from the strut and tie method with the result obtained from the non-linear FE analysis which uses the tensile strength in the material model.

3.3.2.3. Design with use of the strut and tie method

General

The deep beam was designed for a number of alternative strut and tie models having different angles between the inclined strut and the main reinforcement tie. The models were selected with regard to the minimum spacing between bars, the reinforcement being in multiple layers and the use of surface reinforcement.

Strut and Tie Models

Four different angles (60°, 69°, 73° and 76°) between the tie and the diagonal strut were studied. In addition, two alternative reinforcement arrangements were investigated. In the first alternative, instead of placing the bars in a single layer, the bars were placed in three layers. In the second alternative, the impact of utilising surface reinforcement was studied. This results altogether in there being 6 different cases, see Table 4.

The angles chosen, θ_c, are shown in Table 4. It is often recommended that the angle is set to 60° between an inclined strut and a single tie. The location of the compressive resultant for an angle of 76° approximately corresponds to the level of the compressive resultant for the uncracked concrete. This level was calculated in the study by use of a linear FE-analysis. The angles chosen result in a theoretical need of reinforcement. The reinforcement arrangements chosen, in turn, correspond to angles referred to here as theoretical angles, θ_t, these deviating slightly from the angles that were chosen. The theoretical angles involved will be presented in connection with the results. In using a surface reinforcement, two angles were chosen, one at each assumed tie. The lower tie simulates the main reinforcement, and the upper tie simulates the centre of gravity of the tensile surface reinforcement that is involved.

Table 4
The angle chosen and the basic conditions for the design used in each of the six alternative cases studied. Case 6 includes tensile surface reinforcement.

Case	Angle[1] (°)		Comments
	θ_{c1}	θ_{c2}	
1	60	-	The main reinforcement in a minimum number of reinforcement layers, using an angle of 60°
2	69	-	The main reinforcement in a minimum number of reinforcement layers, using an angle of 69°
3	69	-	Distribution of the main reinforcement over several layers, using an angle of 69°
4	73	-	The main reinforcement in a minimum number of reinforcement layers, using an angle of 73°
5	76	-	The main reinforcement in a minimum number of reinforcement layers, using an angle of 76°
6	76	73	The main reinforcement in a minimum number of reinforcement layers, using an angle of 76°, and utilising surface reinforcement, using an angle of 73°

[1] θ_{c1} and θ_{c2} = chosen angles between the main reinforcement and the lower diagonal strut and between the surface reinforcement and the upper diagonal strut, respectively.

Strength of struts, σ_{Rs}

Uncracked concrete:

$$\sigma_{Rs} = f_{cm} \tag{3}$$

Cracked concrete:

$$\sigma_{Rs} = 0.6\upsilon' f_{cm} = 0.6(1 - f_{cm}/250) f_{cm} \tag{4}$$

The calculated values are presented in Table 5.

Strength of nodes, σ_{Rn}

CCC-node (compression node without ties):

$$\sigma_{Rn} = k_1 \upsilon' f_{cm} = 1.0(1 - f_{cm}/250) f_{cm} \tag{5}$$

CCT-node (compression tension node with reinforcement provided in one direction):

$$\sigma_{Rn} = k_2 v' f_{cm} = 0.85(1 - f_{cm}/250) f_{cm} \quad (6)$$

Where $v' = (1\text{-}f_{cm}/250)$ is an efficiency factor that takes into account that the concrete does not have an ideal plastic response. The coefficients $k_1 = 1.0$ and $k_2 = 0.85$ are reduction factors for the compressive strength of the nodes. All factors are according to EN 1992-1-1 [2], sec. 6.5.

The calculated values are presented in Table 5.

Table 5
Strength of the struts and of the nodes, respectively.

Struts		Nodes	
Type	**σ_{Rs} (MPa)**	**Type**	**σ_{Rn} (MPa)**
Uncracked	38,0	CCC	32,2
Cracked	19,3	CCT	27,4

Design conditions

Struts: No calculation and control of the compressive struts was performed. All of them are considered to be uncracked, which means they are not decisive here. Instead, the connection of the compressive struts to the nodes is decisive.

Nodes: No calculation and control of the CCC-node at the top of the deep beam was performed. Instead, the width of the CCC-node, and consequently also the width of the compressive strut, at the upper edge of the deep beam was calculated and limited with respect to the strength of the CCC-node and included in the design conditions taken into account when selecting position of the compressive resultant.

Crack width: The crack width is calculated in accordance with EN 1992-1-1 [2]. In case 6 only the main reinforcement is used.

3.3.2.4. Design using nonlinear FE-analyses

Nonlinear FE-model

Table 6 refers to Study 2 and shows for the different cases what applies regarding:

- The assumed value for the dilation angle.
- Whether the regions of the entire height at the ends of the deep beam, and with a width, *b*, that includes the first row of elements in front of the support towards the midspan, see Figure 41, are assumed to have a linear elastic stress strain curve for the concrete or not.
- The type of meshed element used for the concrete.

The linear elastic assumption and the assumption made regarding the value of the dilation angle are discussed in greater detail in chapter 3.6.

Table 6
Specific assumptions for the concrete concerning the dilation angle, the stress-strain relationship and the meshed elements.

Study 2			
Case	**Dilation angle (°)**	**Stress-strain[1]**	**Element**
1	55	N+L	CPS8R
2	38	N	CPS4R
3	38	N+L	CPS8R
4	38	N	CPS4R
5	38	N	CPS4R
6	38	N+L	CPS4R

[1] N = Nonlinear, L = Linear, N+L = Indicates that part of the structure has a linear stress-strain relationship.

Compressive strength

The Concrete Damage Plasticity model used for concrete takes into account the effect of tensile stresses in the concrete by reducing the compressive strength, see Figure 42.

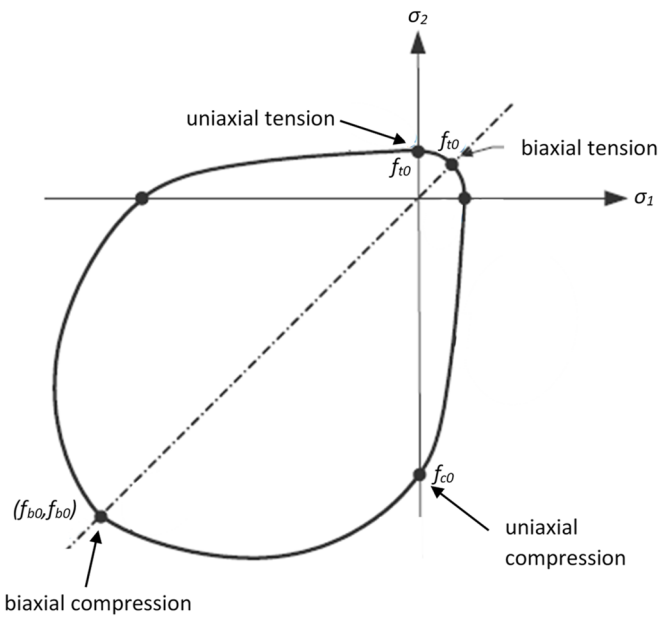

Figure 42
Yield surface in plane stress. Values of the ratio f_{b0}/f_{c0} for concrete are in the ranges from 1.10 to 1.16. σ_1 and σ_2 indicate the effective principal stresses. Based upon ABAQUS [60].

Design conditions

Compressed areas: In the nonlinear FE-analyses the compressive stresses were checked in the mid-span-area at the top of the deep beam and above the support-area. To facilitate the comparisons, the results of these checks are presented under the headings of struts or of nodes.

Crack width: The crack width is calculated as the maximum plastic strain times the length of the element at a level corresponding to the centre of the main reinforcement at the bottom of the deep beam.

3.4. Results and analyses for Study 1

Of the cases investigated, there were several that had a similar response, with a characteristic pattern. However, the case TR/SR for which there were special conditions in terms of a uniformly distributed surface reinforcement deviated from this pattern. The same is valid for the case TR 3x4 where the main reinforcement was located in three layers. In the following, the results for case TR 12 are presented as being representative of the typical response and a pattern deviating from this typical response is shown for case TR/SR.

Figure 43 shows the development of cracks and horizontal stress in the midspan section of the deep beam at five different load levels. The figure concerns case TR 12 but is also typical for the other reinforcement arrangements when the reinforcement is located in a single layer. The crack width in the figures is not shown in scale. The different load levels in Figure 43 are indicated in the load-displacement curve, see Figure 44. In the figure the load level at which the concrete cracks, q_{cr}, is presented instead of the load needed for reaching the tensile strength of the concrete, q_{ct}. The load values are the same.

As can be seen in Figure 43c, which shows the development of cracks at the end of the first crack period, corresponding to the load q_{cr1e}, two cracks, one larger (the first crack) than the other, start to develop at the load level at which the concrete cracks, q_{cr}. By crack period is meant here a stage at which the structure receives increased deformation under constant load conditions due to crack formation. The definition of the crack period is shown in Figure 44, where the load at the end both of the first crack period, q_{cr1e}, and of the second crack period, q_{cr2e}, is marked. The first crack continues to grow high up in the beam, along with several other cracks that grow to be less high. Nearly all of the cracks are formed before the load increases from q_{cr2e} after the second cracking period. There is no noticeable growth of the first crack when the load is increased from q_y (the load needed for reaching the yield strength of reinforcement) to q_t (the load needed for reaching the tensile strength of

reinforcement). The compressive zone is located high up in the deep beam, already after the second crack period.

The level of the compressive zone indicates that there is a marked stress redistribution taking place during the cracking process and a much smaller stress redistribution due to plasticity.

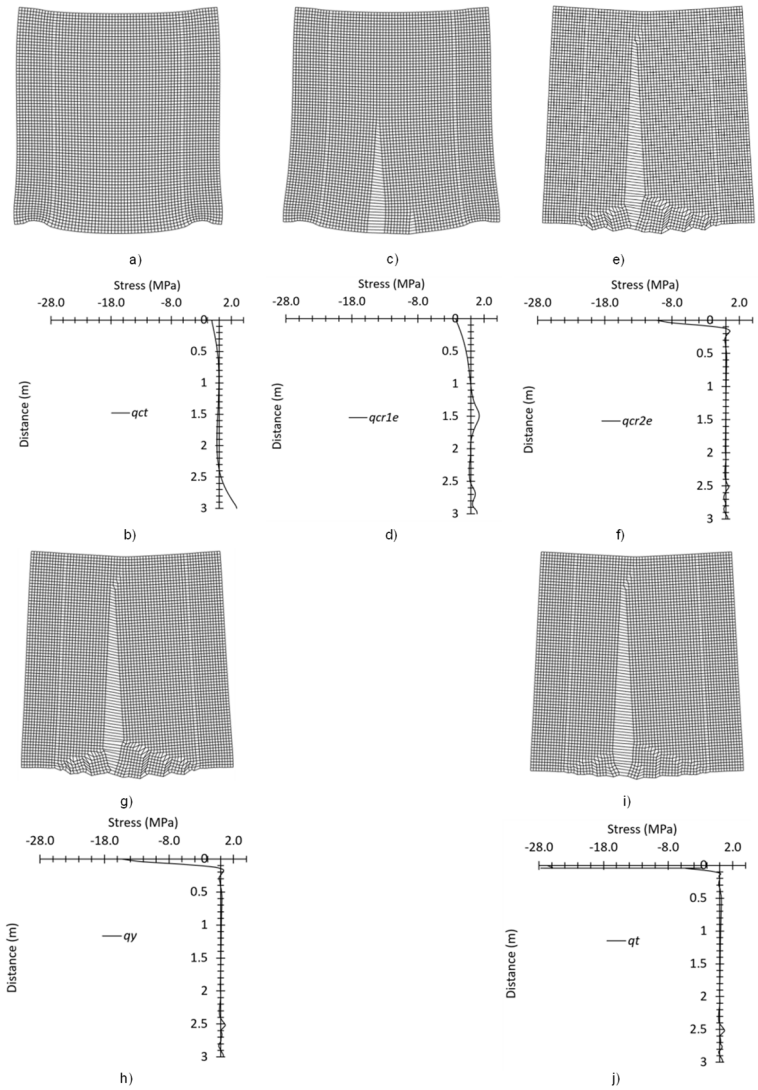

Figure 43
Development of cracks and of horizontal stress in the midspan section of the concrete structure in TR 12 at each of five different load levels. The load levels are for a) and b) q_{cr} (the load needed for reaching the tensile strength of concrete), for c) and d) q_{cr1e}, for e) and f) q_{cr2e}, for g) and h) q_y and for i) and j) q_t.

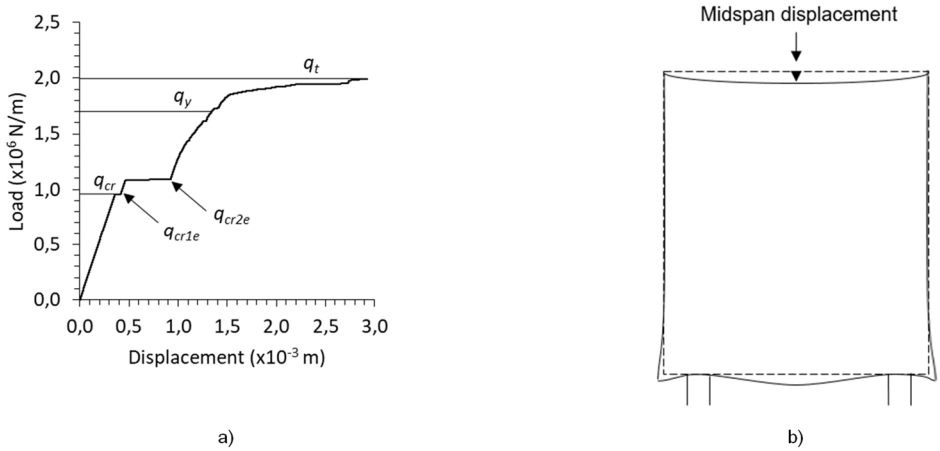

Figure 44
Load on the structure versus displacement in the midspan at the top of the structure for TR 12. The load levels q_{cr}, q_{cr1e}, q_{cr2e}, q_y and q_t are defined in the text. a) Load-controlled quasi-static analysis of a loading rate of 135 kN/ms (2.7 MN/m in 20 s). b) Definition of midspan displacement.

For the beam with both vertical and horizontal surface reinforcement located on each face, case TR/SR, a difference in the crack pattern compared with cases in which the reinforcement is located in a single layer can be seen. Figure 45, which concerns the case TR/SR, shows the development of cracks in the deep beam at six different load levels. The first crack is not located at the midspan section of the deep beam, but in one side of the beam, see Figure 45a. After the second cracking taking place two major cracks exist. When the reinforcement reaches the yield strength, a third and larger crack, near the midspan, starts to become prominent. With this crack pattern and the growth of the third crack, the reinforcement finally reaches its tensile strength and the deep beam collapses. The compressive zone is located high up in the deep beam, already at the end of the second cracking period, similar to cases in which no surface reinforcement is available.

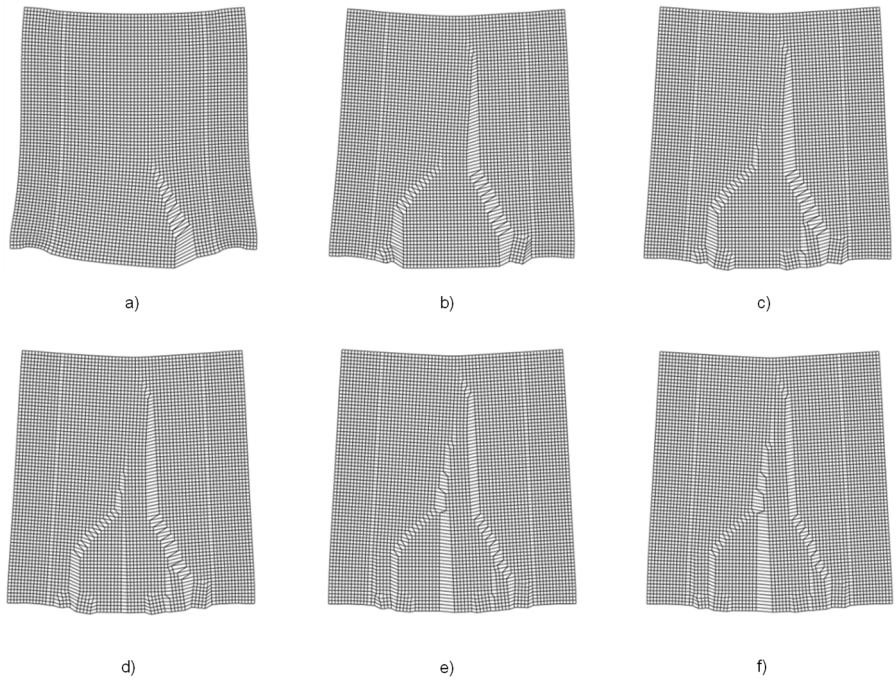

Figure 45
Development of cracks at six different load levels for specimen TR/SR. The symbols q_{cr3e} and q_{cr4e} indicate the load at the end of the third and of the fourth crack period respectively.The other symbols are defined in the text. The load levels are for: a) q_{cr1e}, b) q_{cr2e}, c) q_{cr3e}, d) q_y, e) q_{cr4e} and f) q_t.

The results shown in Figure 46 indicate that the distance to the compressive resultant changes suddenly when a crack occurs. The figure shows the distance from the bottom of the deep beam to the compressive resultant in the midsection versus the load on the deep beam for each of six different reinforcement arrangements. The compressive resultant has been calculated here as the sum of the concrete compressive stresses across the cross section. Minor concrete compressive stresses in the cracked state that are in line with the reinforcement have been neglected. The level marked with “Linear stress field” shows the distance from the bottom of the structure to the compressive resultant for the uncracked concrete. When using surface reinforcement (SR) and for the case TR 3x4, the second instantaneous increase in the distance to the compressive resultant occurs at a later stage during the cracking process than it does for TR 12 and TR 14.

Just as in Figures 43 and 45, Figure 46 also shows a marked stress redistribution during the cracking process and a small stress redistribution taking place due to plasticity. On the basis of the limited data available here, the use of surface reinforcement (SR) appears to result in a decrease in the stress redistribution during the cracking process.

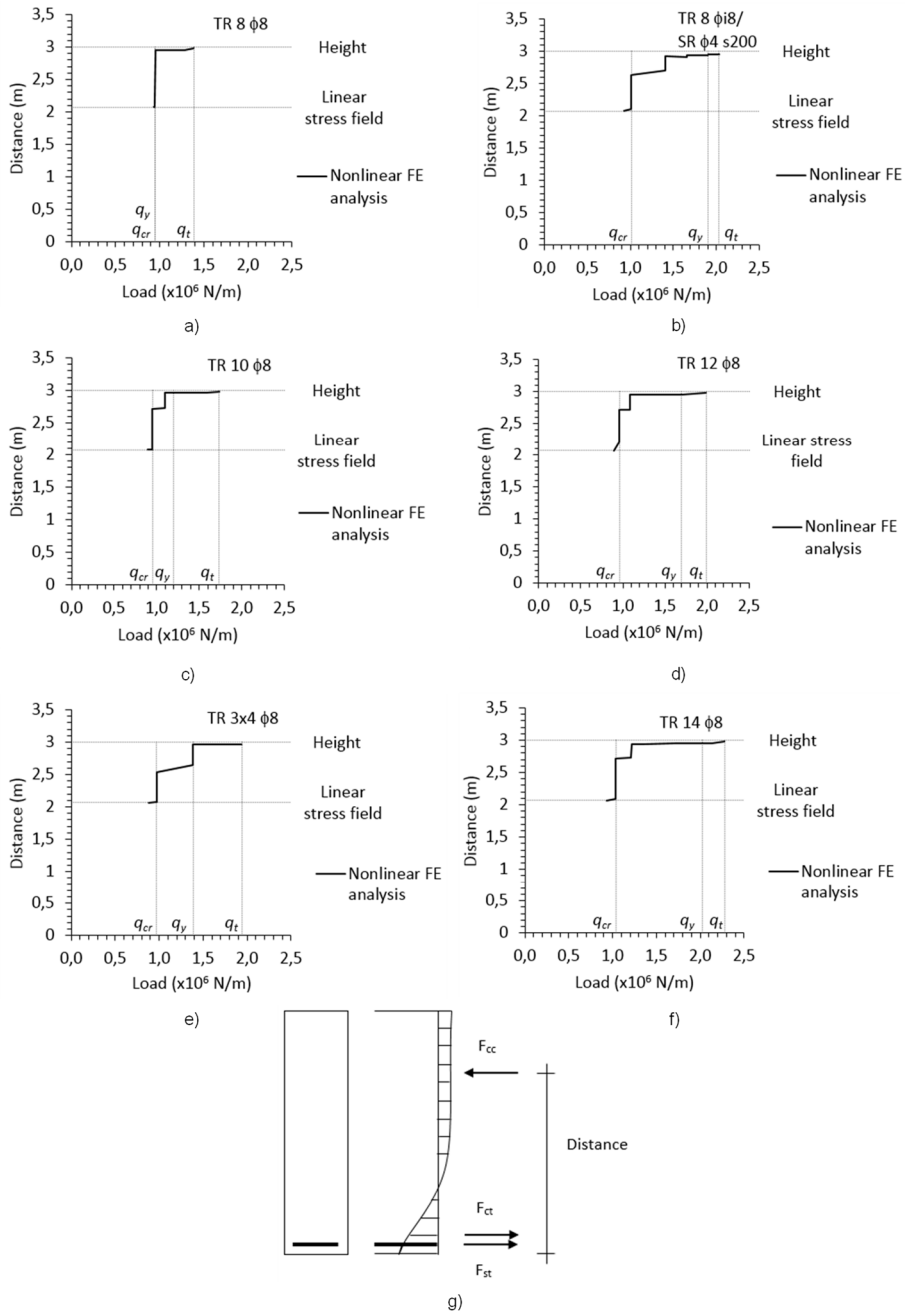

Figure 46
The distance from the bottom of the structure to the compressive resultant in the midsection versus the load on the structure for: a) TR 8, b) TR/SR, c) TR 10, d) TR 12, e) TR 3x4 and f) TR 14. g) definition of the distance.

Figure 47 shows the maximum stress in the reinforcement as a function of the load on the structure. In Figures 47a, c, d and f the maximum stress is located in the same section and layer. In Figure 47b the x-coordinate (see Table 7) at the location for the maximum stress varies when the load increases, and in Figure 47e the maximum stress occurs in different layers. Referenced Table 7 shows values and ratios for the different load levels that are implied for the different cases in Figure 47, as well as coordinates for the location of the maximum steel stress.

Table 7
Coordinates for the location of the maximum steel stress and values and ratios for the different load levels in the case of various reinforcement arrangements.

Case	x[1] (m)	Δx[2] (m)	q_{cr} kN/m	q_y kN/m	q_t kN/m	q_y/q_{cr}	q_t/q_{cr}	q_t/q_y	Comment[3]
TR 8	1.20	0.20	944	948	1387	1,00	1,47	1,46	
TR/SR[4]	0.92	0.08	1013	1901	2032	1,88	2,01	1,07	Element 30
	1.60	0.60							Element 47
TR 10	0.80	0.20	951	1197	1734	1,26	1,82	1,45	
TR 12	0.80	0.20	959	1700	1992	1,77	2,08	1,17	
TR 3x4[5]	1.40	0.40	973	1385	1937	1,42	1,99	1,40	Element 42
TR 14	1.08	0.08	1035	2028	2280	1,96	2,20	1,12	

1 x is the coordinate for the location of the maximum stress. Zero is at the centre of the fixed support. The coordinate indication coincides with the centre of an element.

2 Δx is the distance between the midspan and the location of the maximum stress.

3 Element 30 and 47 (e30 and e47 in Figure 47) indicate different mesh elements for the reinforcement located at the same layer (lag1 indicate layer 1 in Figure 47) in different sections. Element 42 (e42 in Figure 47) indicate the mesh elements for the reinforcement located at different layers (lag1 and lag3 indicate layer 1 and layer 3 respectively in Figure 47) in the same section.

4 For case TR/SR two different sections are decisive during loading.

5 For case TR 3x4 two different layers are decisive during loading.

Figure 47 also shows that for an increased reinforcement ratio the trend is a slower increase of the maximum steel stress up to the yield strength. Notable is also the small increase in load that is needed in order to increase the stress from the yield strength to the tensile strength. In the case of surface reinforcement (SR) there are three abrupt increases in stress in the tensile reinforcement (TR), these being rather uniformly distributed over the cracking state until the reinforcement begins to yield.

The results indicate that when the concrete cracks, the value of the sudden increase in the steel stress becomes less when the tensile reinforcement (TR) content becomes greater. This effect is also obvious for the specimen that has surface reinforcement (SR) and thus the ability to better distribute cracks. The development of the increase in load during plastic deformation, from yield strength to tensile

strength, is more difficult to comment on. Figure 46 indicates that the level of the inner lever arms in the midsection are already high when the yield strength is reached. The increase in load should therefore in principle only correspond to the ratio of f_t to f_y. However, this is not the case for most of the cases studied. One reason why the calculated value for the ratio of q_t to q_y does not become the same value as for the ratio of f_t to f_y may be because the location of the maximum stress is not in the midspan for the different specimens, that is, the stress in the reinforcement is lower at the midspan. Another reason may be that when the yield strength is reached in the sections adjacent to the midspan, then the inner lever arms in the adjacent sections to the midspan are probably smaller than it is in the midspan. An important aspect of the issue is also that the force in the reinforcement tends to be the same between the supports. After the reinforcement has reached the yield strength in a section, it flows and the stress increases in the reinforcement in adjacent sections until all of the reinforcement represented by the tie between the supports has reached the yield strength. The development of the increase in load during plastic deformation, from yield strength to tensile strength, are discussed in greater detail in chapter 3.6.

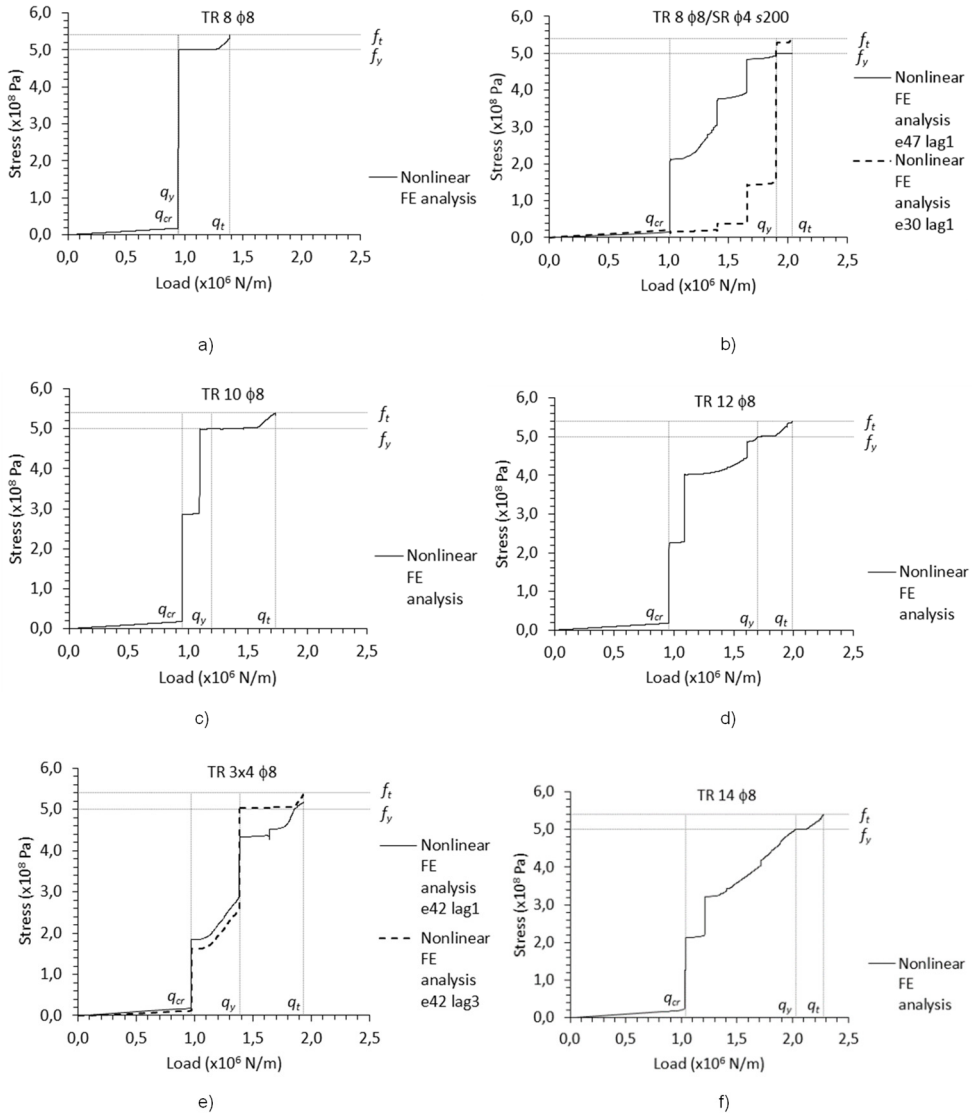

Figure 47
Maximum stress in the reinforcement as a function of the load on the deep beam for: a) TR 8, b) TR/SR (results for two different sections, see Table 7), c) TR 10, d) TR 12, e) TR 3x4 (the results for two different layers) and f) TR 14. The mesh elements 30, 42 and 47 (e30, e42 and e47), for the reinforcement, are defined in Table 7.

Figure 48 shows the crack width at the level of the bottommost reinforcement in the deep beam as a function of the load on the structure for specimen TR 12 at three different sections and for specimen TR 3x4 in one section.

The crack width, according to the nonlinear FE-analyses was determined as being equal to the maximum plastic principal strain multiplied by the length of the element. As can be seen in the figure, the crack width according to the nonlinear FE-analyses decreases when the reinforcement is arranged in three layers. This is in contradiction to the crack width, denoted here as w_{EC2fy}, calculated according to EN 1992-1-1 [2], sec. 7.3.4, for a steel stress equal to the yield strength.

EN 1992-1-1 [2], sec. 7.3.2, prescribes a minimum amount of bonded reinforcement in areas in which tensile stresses are expected in the case of limitations in crack width. Most of the cases in this study do not have reinforcement of this type. For the case involving surface reinforcement, the amount of reinforcement does not correspond to the minimum requirement for minimum reinforcement. Accordingly, more data is needed in order to draw conclusions regarding how an arrangement of the required reinforcement in one or more layers affects the crack width.

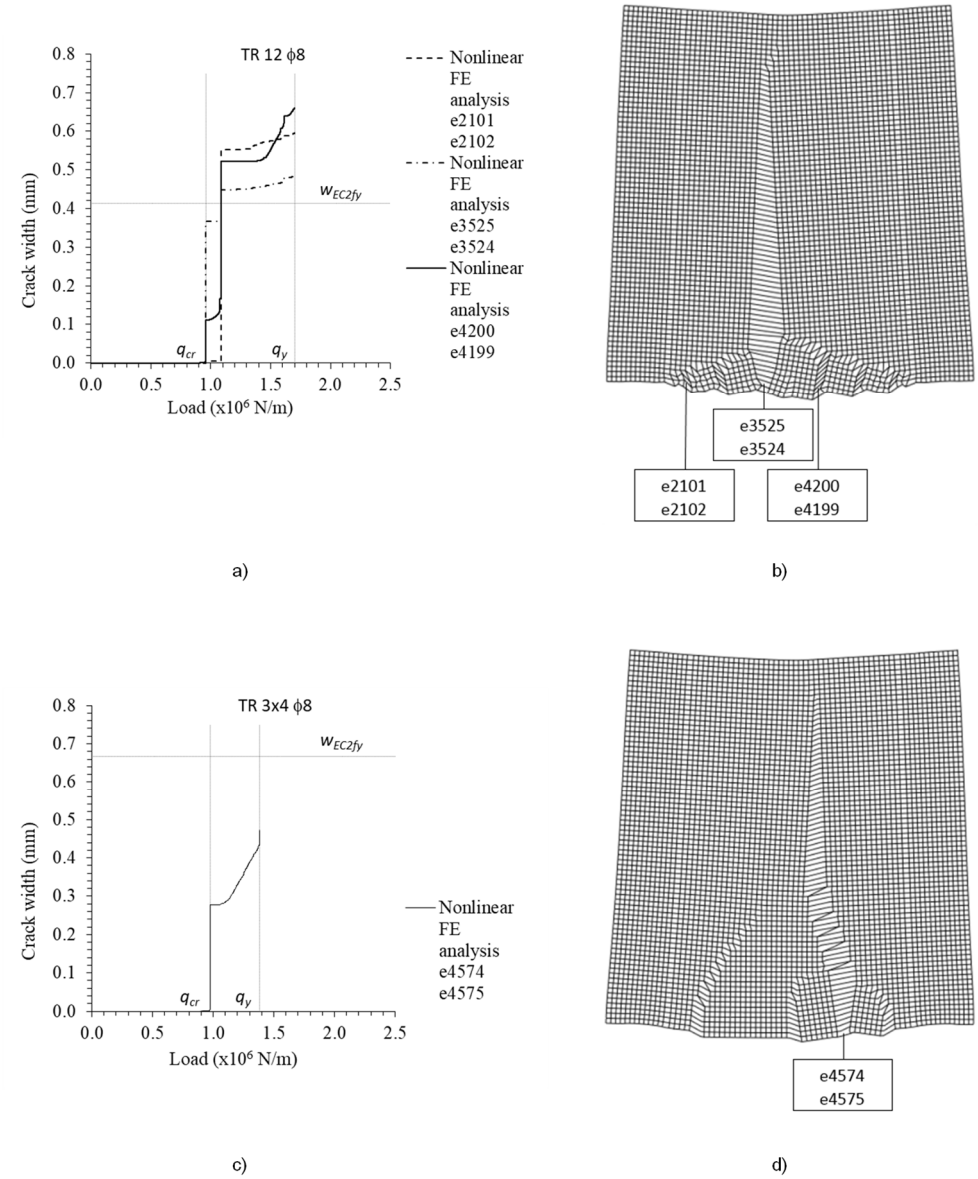

Figure 48
The crack width at the bottommost reinforcement in the deep beam as a function of the load on the structure, as determined by the nonlinear analysis. The figures also show in which sections the cracks that have been calculated are located. The figures apply to: a) and b) TR 12, c) and d) TR 3x4. The notation used here is the following: w_{EC2fy} = crack width according to EN 1992-1-1 [2], 7.3.4, as calculated for a steel stress equal to the yield strength.

3.5. Results and analyses for Study 2

In Study 2, both design and analysis of the load-bearing capacity was carried out with different strut and tie models in each case. The results obtained using the strut and tie method in regard to the design of compressive struts, tensile ties and nodes in the ultimate limit state and crack widths in the serviceability limit state are presented, along with the results of studies of the need of anchoring.

The different results obtained are compared with the responses obtained in nonlinear analyses of the deep beam and its different reinforcement arrangements. For each case, the strut and tie model involved is applied throughout the increase in load up to the ultimate load, i.e. the stresses and forces calculated using the strut and tie method are linear up to the load in the ultimate limit state.

When using the strut and tie method in the case of surface reinforcement, designated as case 6, the surface reinforcement exposed to tensile force is included in the load-bearing capacity together with the main reinforcement. The tensile surface reinforcement is assumed to be located within the distance, *a*, extending from the bottom of the deep beam up to a point at a given distance, *s*, below the compressive resultant. The distance, *s*, see Figure 49, corresponds to the minimum value of the distance from the top of the structure to the compressive resultant, or half of the inner lever arm for the main reinforcement, see Equation (7):

$$s = min(h - (TP + z_m); z_m/2) \tag{7}$$

Where:

- h = Height of the deep beam.
- TP = Distance from the bottom of the deep beam to the centre of the main reinforcement.
- z_m = Inner lever arm for the main reinforcement.

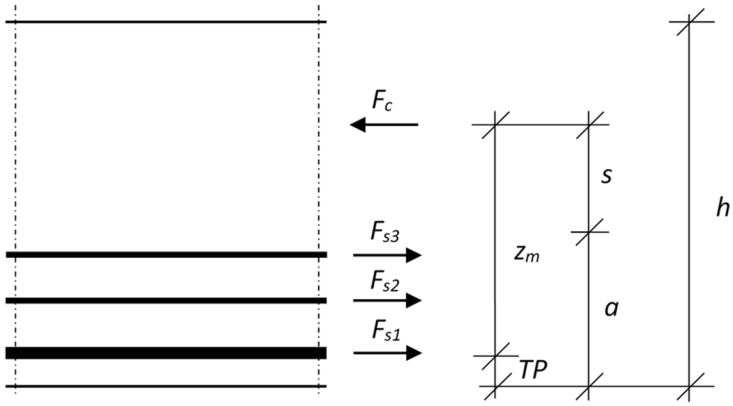

Figure 49
Definition of the distance, *s*, and the distance, *a*, within which the tensile surface reinforcement is assumed to be located. F_{s1}, F_{s2}, F_{s3} and F_c indicate the force in the main reinforcement, force in two layers of surface reinforcement and the compressive resultant respectively.

3.5.1. Ultimate limit state

3.5.1.1. Forces

An increase in the angle of the inclined compressive strut results in a decrease of the forces in the inclined and in the horizontal compressive struts and also in the tie for the same load, as can be seen in Table 8, where the forces in the various struts and ties, as defined in Figure 50, are presented for the different cases. The value of the angle can be regarded as a measure of the stress redistribution that occurs in the deep beam.

In Figure 50, the dashed and the solid lines represent compressive and tensile resultants, respectively, for the corresponding stress fields. In the figure, N stands for node, E for element, U for upper and L for lower.

Table 8
Forces in the ultimate limit state in different elements for the cases that were studied using the strut and tie method. The elements are defined in Figure 50.

Case	Forces (kN)					
	Element					
	E1	E2	E3	E4	E5	E6
1 θ_{c1}= 60°	845	976	489	489	845	976
2 θ_{c1}= 69°	845	905	326	326	845	905
3 θ_{c1}= 69°	845	905	326	326	845	905
4 θ_{c1}= 73°	845	888	271	271	845	888
5 θ_{c1}= 76°	845	872	217	217	845	872

Case	Element								
	E1	E2L	E2U	E3	E4L	E4U	E5	E6L	E6U
6 θ_{c1}= 76° θ_{c2}= 73°	845	873	888	271	217	54	845	873	888

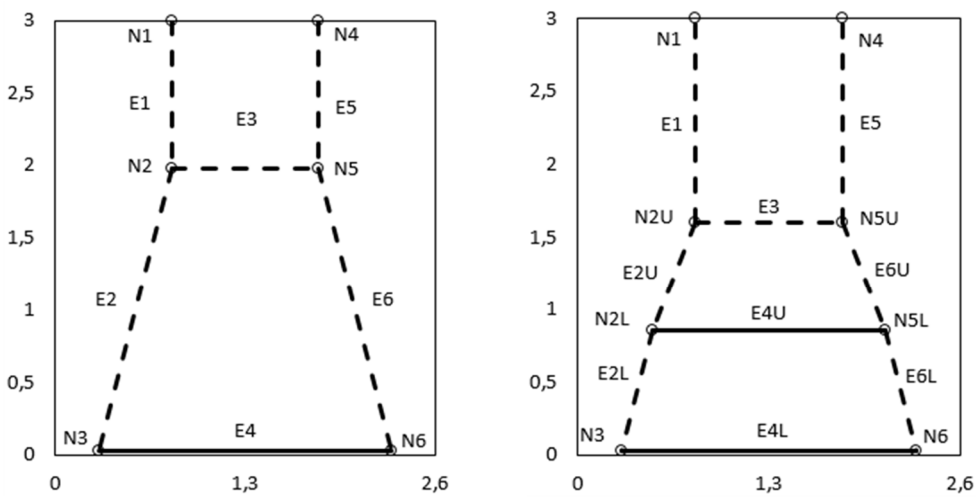

Figure 50
Typical element configurations for: a) Cases 1-5 and b) Case 6.

3.5.1.2. Ties

In Figure 51 the stress development in the main tie under conditions of increased load is presented. The figure shows results from calculations both with strut and tie models and nonlinear analyses of the different cases. According to the figure the angles of the inclined compressive strut that are assumed in the strut and tie models do not provide an ultimate limit load corresponding to that obtained when nonlinear analyses are performed. It is particularly notable that the cracking load exceeds the design load. For an angle corresponding to a linear elastic stress field, an angle of approximately 76 degrees (case 5), the strut and tie method indicates there to be an ultimate limit load of about 60% of the ultimate limit load according to a nonlinear analysis. This is seen in Table 9, in which the load-bearing capacity for the design using the strut and tie method is compared with the results of a nonlinear FE-analysis.

In case 6, the main reinforcement in case 5 is supplemented with a surface reinforcement. The nonlinear analysis for case 6 indicates that the ratio of q_{STMfi} to q_{NLfi} decreases, compared to case 5, see Table 9. The reason for this is that all the reinforcement, including the surface reinforcement, is used to carry the load.

The effect on the strut and tie model in case 6, using part of the surface reinforcement to carry the load, see Equation (7), is that the inner lever arm decreases. This is a consequence of the chosen angles of the inclined compressive struts and thus a measure of the stress redistribution. Case 6 thus requires less stress redistribution compared to case 5 for the same load-bearing capacity and in this way increases the possibility of meeting requirements in the serviceability limit state.

It is of interest to note in Figure 51 that the steel stress obtained with use of the strut and tie model chosen never falls below the steel stress as obtained by means of nonlinear analyses.

Table 9

The need of reinforcement in the ultimate limit state for a design load of q_{STMft} = 845 kN/m using the strut and tie method and the load-bearing capacity verified in a nonlinear FE-analysis.

Case	θ_t[1] (°)	F_s (kN)	Bars[2]	A_s (cm2)	TP[3,4] (m)	Z[5,6] (m)	q_{NLft}[7] (kN/m)	q_{STMft}/ q_{NLft} (-)
1	59.96	489	2x9 ϕ8	9.05	0.054	0.865	2860	0.295
2	68.92	326	12 ϕ8	6.03	0.029	1.297	1992	0.424
3	68.92	326	3x4 ϕ8	6.03	0.079	1.297	1937	0.436
4	72.19	271	10 ϕ8	5.03	0.029	1.557	1734	0.487
5	75.59	217	8 ϕ8	4.02	0.029	1.946	1387	0.609
6	75.59	217	8 ϕ8	4.02	0.029	1.557	2032	0.416
	72.19	54	2x4 ϕ4 s200 [8]	1.01	0.45			

[1] θ_t = Theoretical angles. Compare with the specifications in Table 4 of the angles chosen.

[2] Number and diameter of the bars.

[3] TP = Distance from the bottom of the deep beam to the centre of the main reinforcement.

[4] TP = Distance from the bottom of the deep beam to the centre of the surface reinforcement exposed to traction in case 6.

[5] z = Inner lever arm for the main reinforcement.

[6] z = Inner lever arm for the sum of the main and the surface reinforcement in case 6.

[7] q_{NLft} = Load-bearing capacity according to a nonlinear FE-analysis.

[8] Total amount of surface reinforcement exposed to tension.

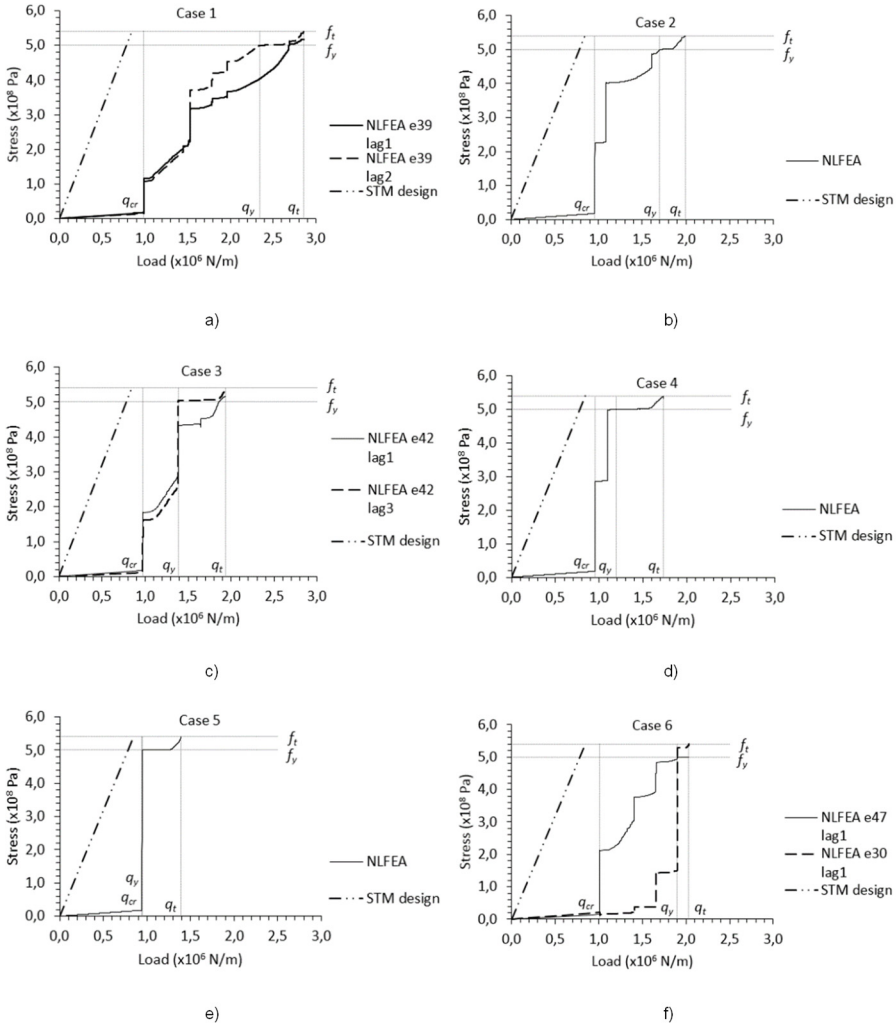

Figure 51
Stresses in the main reinforcement as a function of load for strut and tie models and in nonlinear analyses. The mesh elements 30, 42 and 47 (e30, e42 and e47), for the reinforcement, are defined in Table 7. The x-coordinate for the reinforcement element 39 (e39) in case 1 is x = 1.28 m. a) to f) show cases 1-6.

3.5.1.3. Struts

As previously mentioned, no check of the concrete compressive stresses in the compressive struts was performed in the strut and tie calculations.

In the nonlinear analyses, the values of the principal concrete compressive stresses in the midspan-area at the top of the deep beam were always below the concrete compressive strength used in the material model.

For the sake of comparison, the principal concrete compressive stresses at the top of the midspan as determined by nonlinear FE-analyses and the uniaxial concrete compressive strength for uncracked concrete are presented in Table 10.

Table 10
Principal concrete compressive stresses, σ_{Ss}, at the top of the midspan as determined by nonlinear FE-analysis compared to the uniaxial concrete compressive strength for uncracked concrete.

Case	σ_{Ss} (MPa)	σ_{Rs} (MPa)	OK[1]	Comments
1	30.2	38	Yes	2x9 ϕ8
2	27.6	38	Yes	12 ϕ8
3	25.4	38	Yes	3x4 ϕ8
4	25.6	38	Yes	10 ϕ8
5	22.1	38	Yes	8 ϕ8
6	24.5	38	Yes	8 ϕ8 2x4 ϕ4 s200[2]

[1] OK is denoted "Yes" if the condition $\sigma_{Ss} \leq \sigma_{Rs}$ is fulfilled.

[2] Total amount of surface reinforcement exposed to tension.

3.5.1.4. Nodes

For the CCT-node at the support, when the strut and tie method is employed, the concrete compressive stresses do not exceed the value of the concrete compressive strength in any case, as can be seen in Table 11.

Table 11
Concrete compressive stresses, σ_{Sn}, see Figure 52, in the CCT-node as determined by use of the strut and tie method compared to the concrete compressive strength for a CCT-node.

Case	Component	σ_{Sn} (MPa)	σ_{Rn} (MPa)	OK[1]	Comments
1	*R*	9.4	27.4	Yes	2x9 ϕ8
	S3-2	10.4	27.4	Yes	
	T3-6	15.1	27.4	Yes	
2	*R*	9.4	27.4	Yes	12 ϕ8
	S3-2	10.0	27.4	Yes	
	T3-6	18.7	27.4	Yes	
3	*R*	9.4	27.4	Yes	3x4 ϕ8
	S3-2	9.0	27.4	Yes	
	T3-6	6.9	27.4	Yes	
4	*R*	9.4	27.4	Yes	10 ϕ8
	S3-2	9.8	27.4	Yes	
	T3-6	15.6	27.4	Yes	
5	*R*	9.4	27.4	Yes	8 ϕ8
	S3-2	9.5	27.4	Yes	
	T3-6	12.5	27.4	Yes	
6	*R*	9.4	27.4	Yes	8 ϕ8
	S3-2	9.5	27.4	Yes	2x4 ϕ4 s200[2]
	T3-6	12.5	27.4	Yes	

[1] OK is denoted "Yes" if the condition $\sigma_{Sn} \leq \sigma_{Rn}$ is fulfilled.

[2] Total amount of surface reinforcement exposed to tension.

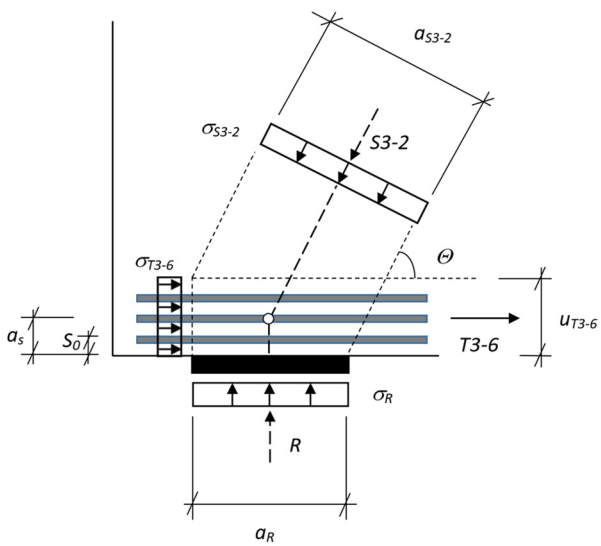

Figure 52
Components of the force of a node, *R*, *S3-2*, and *T3-6* and the associated stresses σ_R, σ_{S3-2} and σ_{T3-6}, respectively, acting on the node. The values for the different stresses are all presented in Table 11 under the name σ_{Sn}.

Concerning the nonlinear FE-analyses, the same applies to the principal concrete compressive stresses above the support-area as to those in the midspan-area at the top of the deep beam, that is, they do not cause any failure in the structure.

However, a comparison shows that in the nonlinear FE-analyses, the principal concrete compressive stresses above the support exceeded the concrete compressive strength corresponding to the value for a CCT-node when using the strut and tie method. This was true in all cases except for case 5, for which the value of the angle for the inclined compressive strut was highest. This can be seen in the results presented in Table 12. Nowhere, though, do the principal concrete compressive stresses exceed the value used for concrete compressive strength for uncracked concrete in a strut, but in this area, it is more applicable to compare with the concrete compressive strength for a CCT-node.

The result from the FE-analyses and how this is affected by the linear elastic assumption and the assumption made regarding the value of the dilation angle are discussed in greater detail in chapter 3.6.

Table 12
Principal concrete compressive stresses of the CCT-node as obtained by use of nonlinear FE-analysis compared to the biaxial concrete compressive strength for a CCT-node.

Case	σ_{Ss} (MPa)	σ_{Rs} (MPa)	OK[1]	Comments
1	33.0	27.4	No	2x9 ϕ8
2	31.5	27.4	No	12 ϕ8
3	29.8	27.4	No	3x4 ϕ8
4	28.5	27.4	No	10 ϕ8
5	17.1	27.4	Yes	8 ϕ8
6	29.9	27.4	No	8 ϕ8 2x4 ϕ4 s200[2]

[1] OK is denoted "Yes" if the condition $\sigma_{Ss} \leq \sigma_{Rs}$ is fulfilled.

[2] Total amount of surface reinforcement exposed to tension.

3.5.1.5. Anchoring

Figure 53 shows that the force in the reinforcement between the inner support edges is nearly constant at the time when the tensile strength is reached in the reinforcement. Thus, to curtail the reinforcement according to principles for an ordinary beam loaded with a uniformly distributed load where the moment and thereby the force in the reinforcement gradually decreases from a maximum value in the midspan to zero at the support is not appropriate here. Instead, all of the reinforcement needs to be anchored behind the inside of the support. The figure concerns case 1 but applies to deep beams in general.

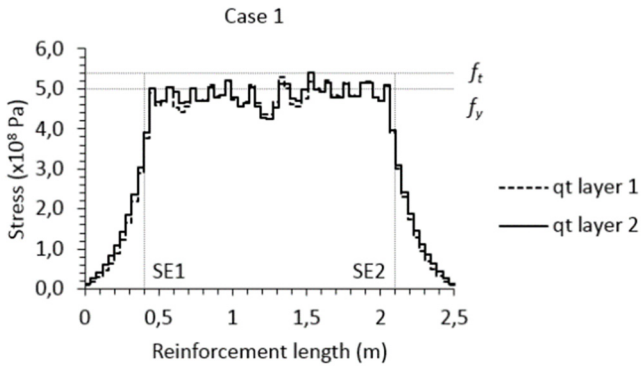

Figure 53
The stress distribution along the reinforcement for case 1 at the time when the tensile strength in the reinforcement is reached. SE stands for the inner support edge.

3.5.2. Serviceability limit state

3.5.2.1. Crack width

The crack width in the different cases was calculated using the strut and tie method and was then compared with the crack width obtained using a nonlinear FE-analysis. The load that resulted in yielding of the main reinforcement, using the strut and tie method, was assumed to correspond to the load in the serviceability limit state. For the strut and tie method the stresses were assumed to be linear up to the ultimate limit load, the yielding load being calculated then by interpolating it against the ultimate limit load using the ratios f_y and f_t. This gives a yielding load that is assumed to correspond to the serviceability limit state:

$$q_{STMf_y} = q_{STMf_t} f_y / f_t \tag{8}$$

$$q_{STMf_y} = 845 \cdot 500/540 = 782\ kN/m$$

The load resulting in yielding of the main reinforcement in the nonlinear FE-analyses is consistently larger than the load that causes yielding using the strut and tie method, as can be seen in Figure 54, which shows the crack widths as a function of the load on the deep beam. The crack widths obtained with use of the two different methods, the strut and tie method and nonlinear FE-analysis, presented in Table 13, are thus calculated for different load levels. The same applies to the comparison performed below. It can be noted in the results of the nonlinear FE-analyses shown

in Figure 54 that the concrete structure cracks at a higher load value than that assumed to correspond to the design load in the serviceability limit state when using the strut and tie method. Generally, when using the strut and tie method, it has not been taken into account whether the concrete structure is cracked or not.

Table 13
The calculated crack width, w_{EC2fy}, in the serviceability limit state for a design load of q_{STMfy} = 782 kN/m, using the strut and tie method, and a verified crack width, w_{NLfy}, obtained in a nonlinear FE-analysis for a load equal to the load resulting in yielding of the main reinforcement.

Case	w_{EC2fy} (mm)	w_{NLfy} (mm)	w_{EC2fy}/ w_{NLfy} (-)	q_{NLfy} (kN/m)	q_{STMfy}/ q_{NLfy} (-)	Comments
1	0.456	0.530	0.860	2342	0.334	2x9 ϕ8
2	0.413	0.660	0.626	1700	0.460	12 ϕ8
3	0.667	0.471	1.417	1385	0.565	3x4 ϕ8
4	0.449	0.691	0.649	1197	0.654	10 ϕ8
5	0.499	0.666	0.750	948	0.825	8 ϕ8
6	0.499	0.653	0.765	1901	0.412	8 ϕ8 2x4 ϕ4 s200

Figure 54a, case 1, where the reinforcement is located in two layers, shows that the strut and tie model gives approximately similar values for the crack width calculated for the reinforcement-yielding load as the nonlinear analysis. The ratio of the reinforcement-yielding loads for the two respective methods is 0.33, as can be seen in Table 13.

For case 2, Figure 54b, where the number of reinforcement bars is less than in case 1 and where the reinforcement is located in one layer the crack width calculated on the basis of a nonlinear analysis is larger than the crack width calculated with the strut and tie method. This can be compared with the result presented in Figure 54c, case 3, where the reinforcement is located in three layers. In the latter case the crack width is smaller when calculated on the basis of a nonlinear analysis, than when it is calculated on the basis of the strut and tie method.

The relationship of the crack width to one another in the two cases, case 2 and 3, calculated for the yielding load, using the strut and tie method in the one case and nonlinear analysis in the other, is 0.626 and 1.417, respectively, see Table 13. A larger value for the crack width calculated with use of the strut and tie method in case 3 compared with case 2, is expected since, although the amount of reinforcement is the same, in case 3 it is distributed over a larger effective tension area. The nonlinear FE-analysis shows it to be favourable to arrange the reinforcement in several layers, however, at the expense of a decreased load resulting in yielding in the reinforcement. See the values in Table 13 for the yielding load, which is 1700 kN/m and 1385 kN/m for case 2 and case 3, respectively.

In the cases in which the reinforcement is arranged in a single layer, cases 2, 4 and 5, (Figures 54b, 54d and 54e) the two methods show approximately the same relationship between the crack widths, the strut and tie method having the smaller values. As regards the relationship between the reinforcement-yielding loads for the three cases, this varies, being 0.46, 0.65 and 0.83, respectively.

Case 5, Figure 54e, has a small reinforcement ratio and the reinforcement yields directly when the concrete cracks. In this case there is one distinct crack that is more marked than the others. The difference in comparison to case 6, Figure 54f, containing the same main reinforcement as in case 5, utilising the existing surface reinforcement that is exposed to tensile stress, and having a higher load for the reinforcement-yielding, is apparent. In case 6 further cracks are formed during the period between when the concrete cracks and the reinforcement yields. Nearly the same value for the crack width, yet for a higher load, is reached in case 6 by the end of the increase in load in terms of a nonlinear FE-analysis as compared to case 5, but the crack development there is more gradual. This result is not unexpected, since all the reinforcement that occurs in the structure is utilised, which for case 6 includes the surface reinforcement, this also affecting the reinforcement ratio.

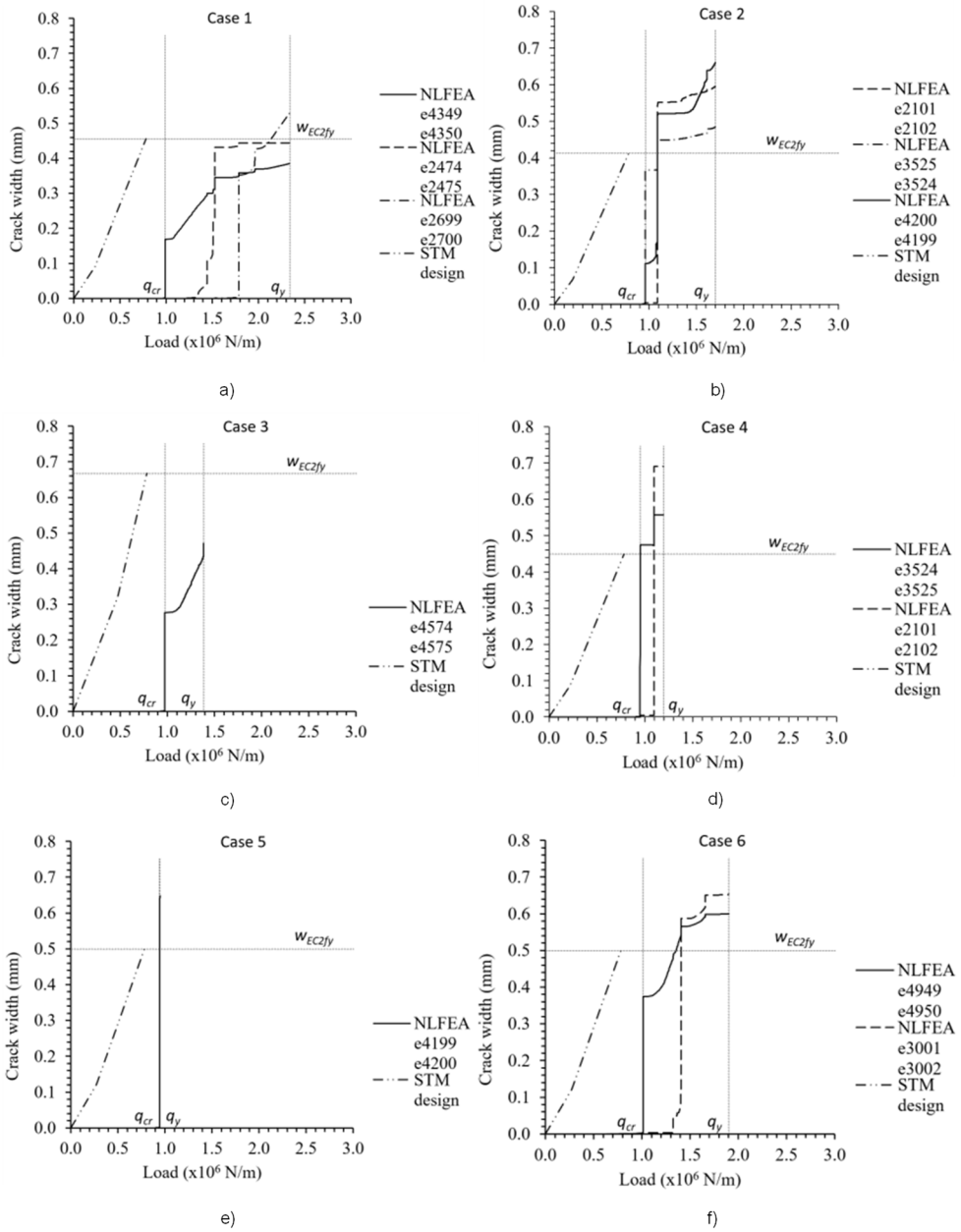

Figure 54
Crack width as a function of load, based on use of strut and tie models and nonlinear analyses. The designations with e and a number refer to mesh elements in the concrete for which the crack width momentarily has its highest value during the loading up to the yield strength is reached for the reinforcement. The crack development for cases 2 and 3 is shown in Figure 48. Case 2, with one larger crack and several smaller cracks, is typical for cases 4 and 5 and case 3, with several larger cracks, is typical for case 1 and case 6 (see Figure 45). a) to f) showing cases 1-6.

The results so far refer to studies of the amount of reinforcement needed for a given design calculated for various assumed strut and tie models and reinforcement arrangements. The consequences of the different choices made are then compared with results of nonlinear FE-analyses, using the same reinforcement. It was also of interest to analyse and compare the load-bearing capacity available in connection with a given amount of reinforcement, assuming various strut and tie models. Figure 55 shows the maximum stress in the reinforcement as a function of the load on the structure for each of the various reinforcement arrangements studied. The reinforcement arrangements investigated are the same as before, and for each of these six cases the following four strut and tie models are studied:

- The same as used for the design load, STM design.
- A model using an inclination of 60° between the main reinforcement tie and the diagonal strut, STM 60.
- A model using the linear stress field, STM linear.
- A model consisting of a horizontal strut and a CCC-node that utilises the maximum concrete compressive strength of the component, STM fcm.

From the figures it is apparent that the choice of an inclination corresponding to 60° between the diagonal compressive strut and the horizontal tie underestimates the load-bearing capacity. A strut and tie model utilising the ultimate strength of the compressive horizontal strut results in a value of the load-bearing capacity that matches fairly well results of the nonlinear analysis. It can also be seen that it underestimates the stress for a given load in certain areas. A strut and tie model following the linear elastic stress field overestimates for a given load the stress in the reinforcement.

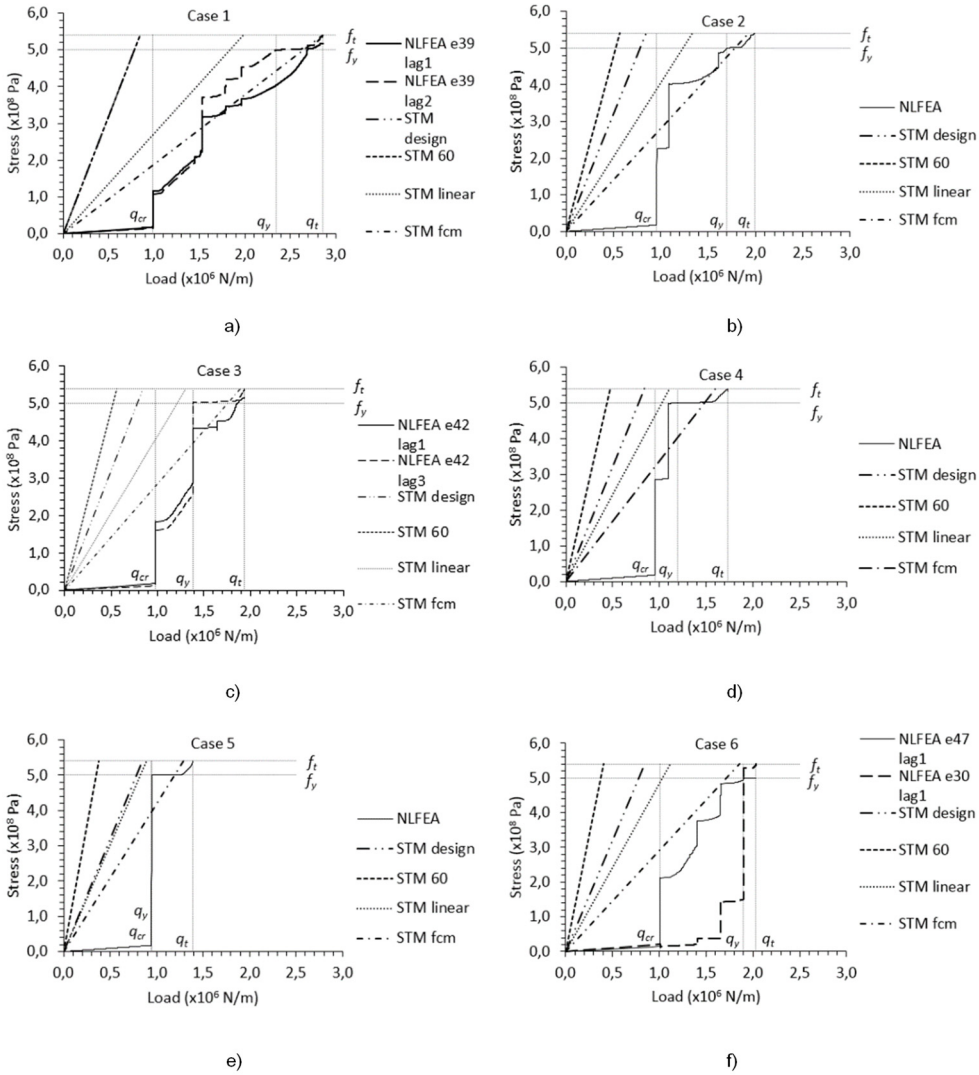

Figure 55
Stresses in the main reinforcement as a function of load. a) to f) showing cases 1-6.

Figure 55, showing the stress in the reinforcement as a function of load on the structure for the different load cases, for different strut and tie models, and for nonlinear analyses, can also be used to evaluate the development of the crack width. The evaluation is based then on the fact that calculations of the crack width depend upon the stress in the reinforcement.

Based on the results presented in Figure 55, the following can be concluded:

- A linear elastic stress field for the strut and tie models can be used for calculating the crack width. As can be seen from the figures, the stresses in the reinforcement are always overestimated as compared with results of nonlinear analysis.
- The stress field redistribution is strongly dependent upon the amount and the arrangement of the reinforcement. On the bases of these conditions and the relationship between the design loads in the serviceability limit state and the ultimate limit state, it is possible, in calculating the crack width, to choose a stress field that is more redistributed than the linear elastic one, and still overestimate the stresses in the reinforcement.

The crack development can also be studied by means of crack width calculations. Here comparisons are also affected, of course, by any deviations between a crack width calculation performed in connection with a nonlinear analysis and one performed in accordance with EN 1992-1-1 [2] using the strut and tie method. Figure 56 shows the crack width as a function of the load on the structure for the same cases and strut and tie models as in Figure 55. The crack widths are studied up to a load corresponding to f_y in the most strained main reinforcement.

The difference that can be seen in Figure 56 when it is compared with Figure 54 is that the calculated crack width, w_{EC2fy}, obtained using the strut and tie method, can be assumed to be valid for different values of the load, resulting in the value f_y in the most strained main reinforcement. This has to do with the question of how much one can allow the stress field to be redistributed, i.e. that here the same amount and arrangement of the reinforcement, and the same crack width result in different load-bearing capacities in the serviceability limit state due to the choice of the inner lever arms.

In the figures one can note the following:

- An inclination of 60° of the diagonal compressive strut using the strut and tie model always overestimates the crack width as compared with a nonlinear analysis at the same load.
- Using a linear stress field enables the crack width to be estimated rather well. How well depends upon the load levels and the reinforcement arrangements.
- Utilising f_{cm} for the horizontal compressive strut, in the strut and tie model, underestimates in most cases the crack width as compared with a nonlinear analysis at the same load.

It is also apparent from the figures showing the stress in the main reinforcement that the deep beam has a high cracking load. For an inclination of 60° of the diagonal compressive strut the load-bearing capacity does not exceed the cracking load. The

fact that the crack load is high can be appropriate to bear in mind when designing and analysing deep beams.

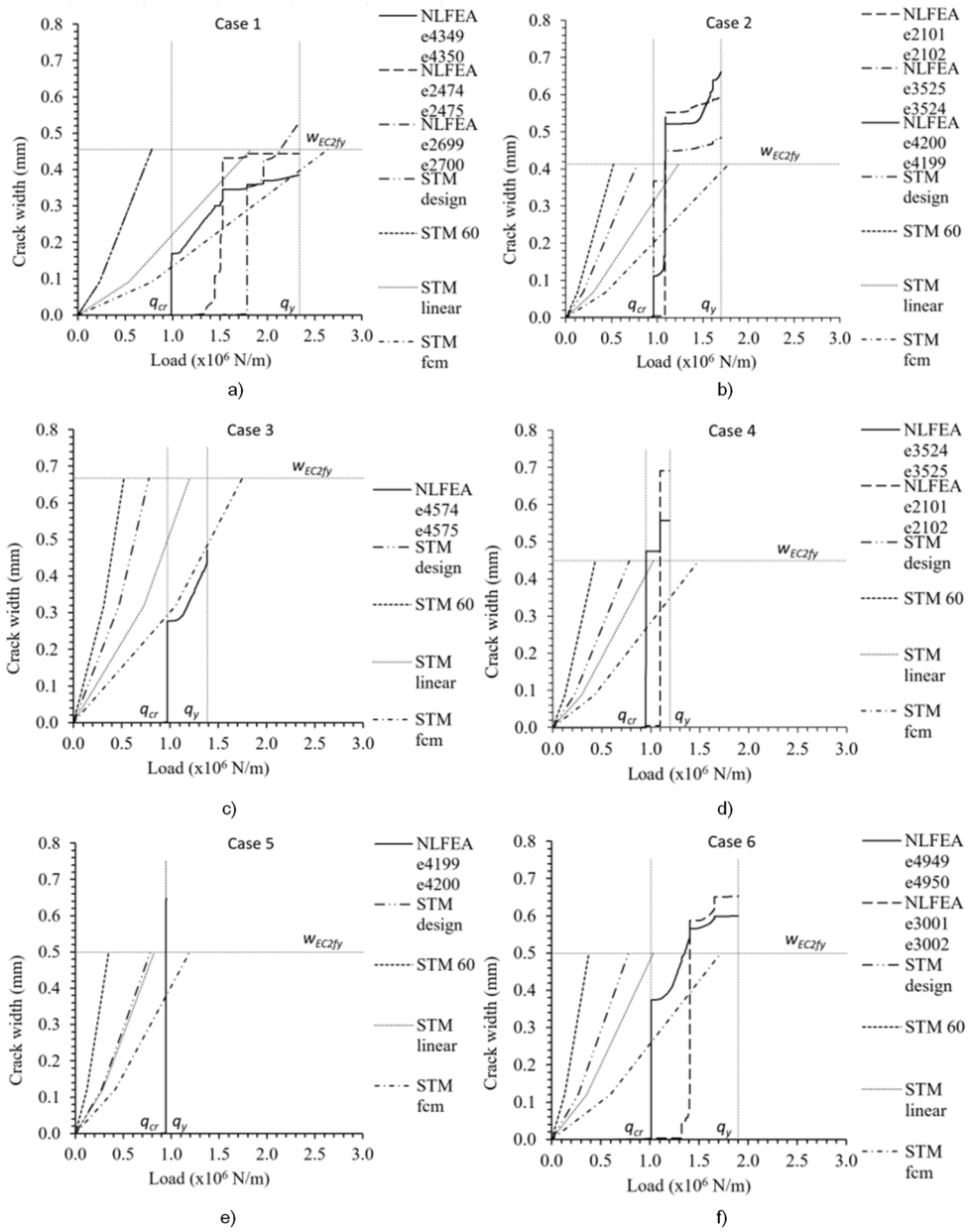

Figure 56
Crack width as a function of load. a) to f) showing cases 1-6.

3.6. Discussion, assumptions and results

This chapter discusses assumptions made and results obtained in more detail.

In the studies, quasi-static analyses were performed. This is a choice that can be discussed. Figure 57 shows the effects on the load-displacement relation of different ways of analysing the deep beam. As can be seen in the figure, the curves for quasi-static analysis at a loading rate of 135 kN/ms (2.7 MN/m in 20 s) and of static deformation-controlled analysis coincide for a load that is less than the cracking load and for a load above the load for reaching the yield strength. During the cracking process there is a certain discrepancy between the two curves. Quasi-static analysis with a loading rate of 67.5 kN/ms (2.7 MN/m in 40 s) and static load-controlled analysis both end up showing premature failure. In the case of quasi-static analysis (40 s) it stops with a failure that occurs before the reinforcement has reached its ultimate strain and in the case of the static analysis it does not converge. On the basis of these results, quasi-static analysis (20 s) was chosen.

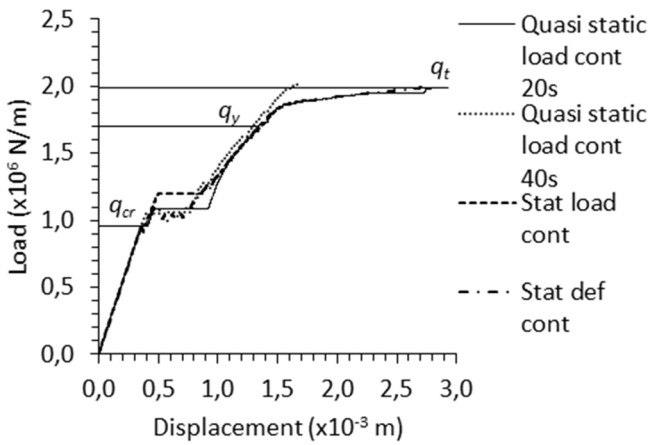

Figure 57
The impact on the relationship of the load on the structure to the displacement in the midspan at top of the structure of TR 12 with use of four different methods of analysis. The different methods of analysis involved are load-controlled static analysis, deformation-controlled static analysis and quasi-static analysis for each of two different loading rates. The values for q_{cr}, q_y and q_t relate to a quasi-static load-controlled analysis (20 s).

The assumed value of the fracture energy, G_F, for concrete C30, in these studies is 75 N/m. According to the fib Bulletin 65 [30], sec. 5.1.5.2, the fracture energy can be estimated to be $G_F = 73 \cdot f_{cm}^{0.18} = 140$ N/m for $f_{cm} = 38$ MPa. The reason for the choice of this value of the fracture energy, G_F, is that it is generally accepted and well established. The magnitude of this parameter can clearly have an effect on the crack width as determined by nonlinear FE-analysis. It is assumed, however, that

the relationship between the crack widths of different specimens is not significantly affected by the fracture energy.

In the investigation, a yield failure in the reinforcement was desired. The ratio of the height to the span and the desire to have a yield failure resulted in failure loads of high load value. High load values gave rise to high compressive stresses at the support, with the risk of compression failure. To prevent a compression failure at the support from occurring before there was a yield failure in the reinforcement, the material model for the concrete had to be adjusted in some of the cases that were studied. This was needed in cases 2 and 5 in Study 1 and for cases 1, 3 and 6 in Study 2. In these cases, having a larger reinforcement content compared to the other cases, a shear-like failure emerged from the bottom of the deep beam at the inner edge of the support. In order to avoid failures of this type, which are considered to be unmotivated, and to be able to follow the analyses until yielding of the reinforcement occurs, a linear material model was assumed for the part of the concrete structure that is beyond the inside of the support edge, and for the first of the element columns located in front of the inside of the support edge.

Another way of increasing the compression failure load is to adjust the dilation angle in the material model of the concrete. In models based on plasticity, the expansion in volume due to shear forces is described as one of dilation, higher values of the dilation angle resulting in higher shear resistance of the cracked concrete. The default value of the dilation angle in the Concrete Damage Plasticity Model is 38°, which is considered as describing the behaviour of normal grade concrete under high confining pressures, see Jankowiak and Lodygowski [61]. Initially, the dilation angle was assumed to be the default value, 38°, in the nonlinear analyses. The shear capacity affects the compression failure, and it turned out that a high value of the dilation angle counteracted the unwanted failure that occurred in the structure adjacent to the support. In several tests, see Malm [64], it has been found that for a structure with a low degree of confinement and axial plastic strain the dilation angle is more than 50°. Since such conditions apply in the present studies, it was assumed that a higher value was motivated. For case 6 in Study 1 and case 1 in Study 2 (involving maximum reinforcement in the two studies) an adjustment of the dilation angle to a value of 45° and 55°, respectively, was made. The adjustment of the dilation angle to 45° for case 6 in Study 1 proved to be sufficient to obtain a yielding failure in the reinforcement, so that an adjustment of a part of the concrete structure to a linear material was not necessary. The above-mentioned assumptions concerning the dilation angle are not considered to affect the outcome of the studies. On the other hand, it is important not to ignore the possibility of an undesirably brittle concrete crushing failure of a reinforced deep beam for which both the value of the ratio of height to span and the reinforcement content are high.

The deep beams in these studies have a low reinforcement ratio, as shown by the fact that the yield strength in the reinforcement of case TR 8 was reached immediately when the concrete cracked. The results confirm what previous research suggests of there being a "considerable redistribution […] due to cracking" in deep beams in the case of low reinforcement ratios, see fib Bulletin 61 [11], paper 16, sec. 3.2, Leonhardt and Walther [22], Lourenco and Almeida [65] and Kempengren [66]. Otherwise, the common idea is that the stress redistribution that occurs is due largely to plasticity. Whether an increase in the reinforcement ratio would be an example of a circumstance that affects the behaviour of the stress redistribution in that direction is unclear since deep beams with high reinforcement ratios are not included in the present studies.

One visible effect of an increase in the reinforcement ratio in the cases that were studied is a more continuous increase in stress in the reinforcement. This is apparent from the curve in Figure 47 showing the stress in the reinforcement as a function of the load, which indicates there to be less prominent discontinuities during the cracking process until yielding of the reinforcement takes place when the reinforcement ratio increases. This is not surprising, since the steel stress that occurs when the concrete cracks is less when the reinforcement area increases. A low level of steel stress during this period, which corresponds to the service state, is also favourable with regard to crack widths.

An increase in load was found to occur after the reinforcing steel yields. It is of interest in Study 1 to compare the relationship between q_t and q_y with the ductility factor $k = 1.08$ (the ratio of the tensile strength to the yield strength of the reinforcing steel) according to EN 1992-1-1 [2], Annex C, Table C.1, Class B, used in the material model of the reinforcing steel in the FE-analyses. The comparison shows how much of the increase in load from q_y to q_t is due to stress redistribution (the value for the inner lever arm becoming greater), compared to an increase in load due to strain hardening of the reinforcement. The relationship q_t/q_y can be seen in Table 7. An important matter to consider here is that the maximum steel stress does not take place in the midsection of the deep beam. There has been no investigation though, of how the results for the crack section (where the steel stress is at a maximum value) and for the midsection relate to one another. The present study shows the value of the ratio q_t/q_y to approach the value of the ductility factor $k = 1.08$ when the reinforcement content increases. Thus, the possibility of increasing the load on the structure above the yield strength is due more to an increase in strength of the reinforcement than a larger value of the inner lever arm. However, as stated before, to draw conclusions whether the load increase from q_y to q_t is due to stress redistribution or strain hardening is uncertain.

In the studies performed, the stress development in the reinforcement was studied for case 2 (12 ϕ8) in Study 2, from yield strength to tensile strength in more detail,

see Figure 58. The figure shows that when the reinforcement in the most stressed section, e27 (element 27), has reached the yield strength, then the stress in the reinforcement increases in some of the adjacent sections, for example e32 (element 32), up to the yield strength, before the stress in the reinforcement in the most stressed section continues to increase up to the tensile strength. If we compare Figure 58d which applies to case 2 (12 ϕ8) in Study 2 with Figure 53 which applies to case 1 (2x9 ϕ8) in Study 2, it appears that the stress distribution in case 1 (2x9 ϕ8) in Study 2 is more evened out, that is, the reinforcement has reached the yield strength in more sections than in case 2 (12 ϕ8) in Study 2, before the tensile strength is reached in the reinforcement in the most strenuous section. There are thus many indications that the entire tie rod is involved in the process up to failure as the tension in the reinforcement increases from the yield strength to the tensile strength. Questions about how different factors affect the stress distribution in the tie during the load increase, as the stress in the reinforcement increases from yield strength to tensile strength, need to be studied in more detail to better understand and to be able to predict the behaviour of the plastic redistribution. It should be recalled that the present study concerns a deep beam with a low reinforcement content. At higher reinforcement contents, the development of the stress distribution at increased load may look different.

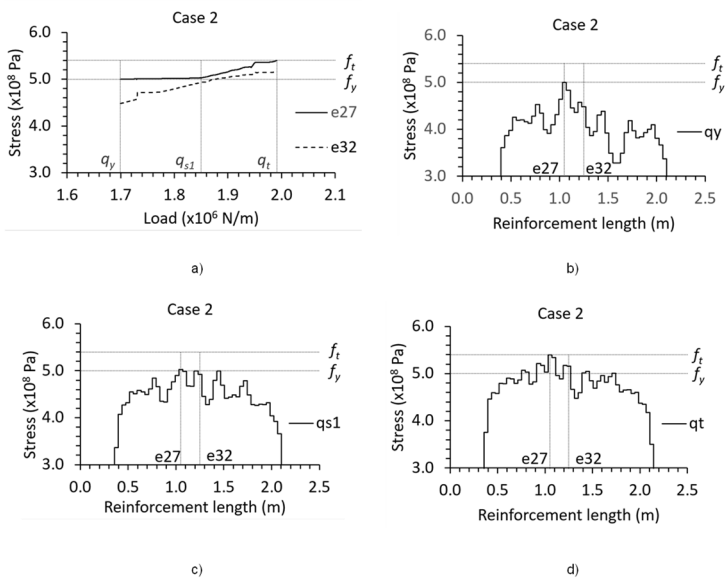

Figure 58
Stress development in the reinforcement in case 2, from yield strength to tensile strength. a) stress development in the reinforcement for a load corresponding to the yield strength in the most stressed section of the reinforcement to a load corresponding to the tensile strength in the most stressed section of the reinforcement. b) stress along the reinforcement at a load corresponding to the yield strength in the most stressed section of the reinforcement. c) stress along the reinforcement at a load corresponding to q_{s1}. d) stress along the reinforcement at a load corresponding to the tensile strength in the most stressed section of the reinforcement.

The impact and the development of the inner lever arm during increasing load on the basis of the reinforcement content and the reinforcement arrangement related to the relationship between q_y and q_{cr} and between q_t and q_y, was shown in Figure 46 and tabulated in Table 7. Leaving the discussion concerning the theoretical background for the development of the plastic redistribution and just looking at the relations for the different load levels it can be noticed that for the cases that were studied in Study 1, an increase in the reinforcement ratio was found to result in a higher ratio of q_y to q_{cr}, whereas the inner lever arm in each case already nearly utilises the compressive strength of the concrete at the top of the deep beam when the reinforcement yields. That is, the inner lever arm basically does not increase in value after the reinforcement yields. It can also be seen that the increased reinforcement ratio leads to a lesser increase in load between yielding and the tensile strength of the reinforcement. This increase in load gradually approaches the value of the ductility factor, its thus being caused decreasingly by the stress redistribution (compare TR 8, TR 10, TR 12 and TR 14). For the cases where the increase in load is higher than the ductility factor this points to an increase in the value of the inner lever arm from yielding until the final stress increase (from load level q_y to load level q_{s1} in Figure 58a), in the most strained section and layer of the reinforcement starts. This is not the case, however, as discussed above. The same tendency regarding the impact and the development of the inner lever arm is obtained when the main reinforcement is supplemented by surface reinforcement (compare TR 8 with TR/SR). A distribution of the main reinforcement over a greater number of layers leads, on the other hand, to effects that are the opposite of what is described above (compare TR 12 with TR 3x4). As mentioned above, a greater reinforcement content can result in a different development of the inner lever arm with an increase in load.

One of the specimens in Study 1 contains surface reinforcement, the effect of which is evident from the results obtained. If the crack pattern shown in Figure 45 is compared with the typical appearance of a specimen without surface reinforcement, as shown in Figure 43, it is obvious that the surface reinforcement contributes to a more even distribution of the cracks. During the cracking process, the inner lever arm shows a more continuous increase, and less prominent discontinuities, until yielding of the reinforcement takes place. This effect is also noticeable in TR 3x4 when one compares it with TR 12, its being beneficially affected by surface reinforcement and also by the distribution of the reinforcement at the bottom of the deep beam over a greater number of layers. A similar effect, see Figure 47, can be noted in the development of maximum stress during the cracking process until yielding of the reinforcement takes place, however less for TR 3x4. The figure in question shows a more continuous increase in stress in the reinforcement, as well as less prominent discontinuities.

However, placing the reinforcement in multiple layers at a concentrated node is a contradiction to the recommendation to have a concentrated tie in order to enable a sharp bending of the load path to take place. But the compressive stresses in the node need to be limited to the concrete compressive strength in the node, which means that the node area may need to be increased. One way to do this is to have the reinforcement located at the bottom in multiple layers, the number of layers being limited to just satisfying the stress limitation of the node. The results of Study 1 indicate that placing the reinforcement in multiple layers at the bottom of the structure also has a positive effect through its reducing the crack width.

Figure 55 shows that the stress field redistribution is strongly dependent upon the amount and the arrangement of the reinforcement. The figure also shows that it is possible, in calculating the crack width, to choose a stress field that is more redistributed than the linear elastic one, and still overestimate the stresses in the reinforcement. Figure 59 shows that when using a strut and tie model with a stress redistribution of 15 percent, compared to a strut and tie model that follows the linear elastic stress field, the stresses in the reinforcement still exceed the result obtained for the stresses in the reinforcement in a nonlinear analysis. The figure applies to case 4, in Study 2, which is the most critical of the cases.

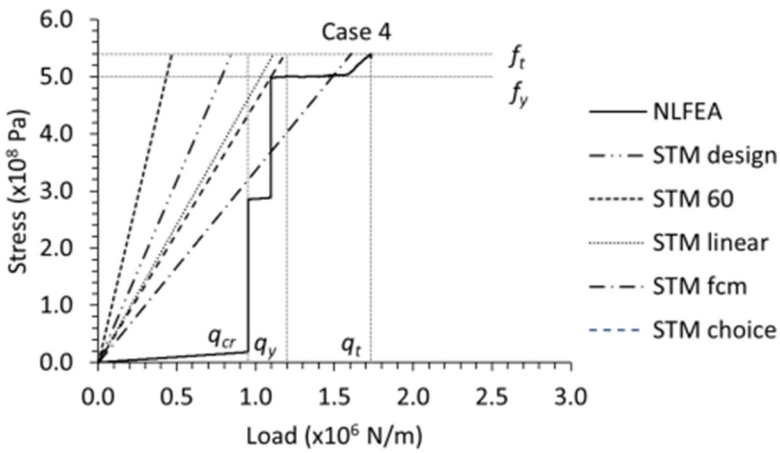

Figure 59
Stresses in the main reinforcement as a function of load for case 4. "STM choice" shows the line for a strut and tie model using a chosen stress redistribution of 15 percent.

The inner lever arm for the chosen stress redistribution, z_{choice}, is calculated according to Equation (9).

$$z_{choice} = z_{linear} + perc(z_{fcm} - z_{linear}) \,/\, 100 \tag{9}$$

Where:

- z_{linear} = Inner lever arm for the linear elastic stress field.
- z_{fcm} = Inner lever arm utilising the concrete compressive strength in the horizontal strut at the top of the deep beam.
- *perc* = The chosen stress redistribution for the strut and tie model given in percent.

In Figure 55, it is visible that for case 1, with an increased amount of main reinforcement, and especially for case 6, where the surface reinforcement is used as a load-bearing reinforcement, it is possible to choose a larger stress redistribution than 15 percent. Case 6 corresponds more to what applies to reinforced structures in practice as there is always a requirement for surface reinforcement. Based on the discussion above, in order to determine the stress in the reinforcement used to calculate the crack width in the serviceability limit state, a strut and tie model that not follows the linear stress field can be used. It can then be recommended to use a stress redistribution corresponding to an increase in the inner lever arm, compared to the one for the linear elastic stress field. The increase can cautiously be chosen to be 25 percent of the difference between the inner lever arm for the maximum stress redistribution, that is full utilisation of the compressive capacity of the concrete, and the inner lever arm for the linear elastic stress field.

An even larger stress redistribution might be possible, but this requires data from more studied cases. To take advantage of these higher values of the stress redistribution several factors need to be considered, such as:

- Reinforcement amount and arrangement.
- The relationship between the utilised stress redistribution for the design load in the ultimate limit state and the maximum available stress redistribution.
- The relationship between the design load in the serviceability and ultimate limit states.
- The degree of stress redistribution due to cracking.
- The continuity of the increased stress redistribution due to cracking
- The relationship between the stress redistribution due to plasticity and that due to cracking.

4. Conclusions

In this chapter some general conclusions based both on the state-of-the-art chapter and the research presented in the thesis, are presented. Conclusions based on studies made on specific situations related to the research question will also be presented.

4.1. General conclusions

- Comparative calculations with programs with automatically developed stress fields and strut and tie models can serve the purpose of checking the results from a nonlinear FE-analysis when there are limited opportunities for experimental verification.
- Based on the present study it could be recommended, for the sake of optimal utilisation, that one uses various strut and tie models in the ultimate and serviceability limit state that do not follow the linear elastic stress field. To be able to comment on other geometries and reinforcement arrangements not studied here, further research is needed.
- When using the Concrete Damage Plasticity Model in nonlinear FE-analysis the value of the dilation angle can be set manually. A high value of the dilation angle, which is realistic for a deep beam, results in a stronger resistance to shear failure and counteracts the risk of an unrealistic premature failure in the model due to high compressive stress at the supports. The above should be kept in mind when studying stress redistribution and crack development for an increasing load up to failure in the horizontal reinforcement constituting the tie at the support.
- The studies presented here show that considering the surface reinforcement to be active has a non-negligible effect on the load bearing capacity. If the surface reinforcement is considered to be active, then it is important that the load model covers all the loads that affect the structure, and that the boundary conditions describe all of the conditions that can be present, such as constraint, for example. Otherwise, the contribution may be overestimated.

4.2. Specific conclusions

The specific conclusions stated here apply for the specimens that were studied in the thesis. The answers to some of the questions overlap, which means that the answers to some of the questions can also be read under other questions.

Research questions

To what extent can one deviate from the linear elastic stress field in the discontinuity region while still fulfilling the functional requirements involved and avoiding premature failure?

- A strut and tie model with an inclination of 60°, or an inclination following a linear elastic stress field for the diagonal compressive strut, underestimates the load-bearing capacity in the ultimate limit state and overestimates the stress in the main reinforcement.
- A strut and tie model with a horizontal compressive strut which utilises the compressive strength provides a load-bearing capacity in the ultimate limit state that is more than 90 % of the load-bearing capacity obtained in a nonlinear analysis of the structure. For an increasing load up to the failure load and at certain load levels the same strut and tie model underestimates the stresses in the main reinforcement compared to a nonlinear analysis of the structure.
- It is important to check the principal compressive stresses that are present above the support and in the mid-span at the top of the structure, so as to reduce or eliminate the risk of a crushing failure taking place before the stress field that has been chosen has developed through stress redistribution.

How large can the degree of stress redistribution due to cracking and plastic deformation be?

- Already before the reinforcement yields, the distance from the bottom of the structure to the compressive resultant in the midsection almost reaches its maximum value due to the stress redistribution caused by cracking.
- The stress redistribution due to plastic deformation is negligible.

What are the conditions for choosing different stress field for design in the ultimate and serviceability limit state?

- Using the linear elastic stress field underestimates the load-bearing capacity in the ultimate limit state. In the serviceability limit state, the linear elastic stress field results in an overestimation of the stress in the reinforcement. The recommendation is therefore, that the ultimate limit state and the serviceability limit state should be dealt with, in terms of optimal utilisation,

by use of different strut and tie models in the two different limit states and that they do not follow the linear elastic stress field.

- A strut and tie model that does not follow the linear stress field can be used to determine the stress in the reinforcement used to calculate the crack width in the serviceability limit state. Based on the work presented in this thesis it is recommended to use a stress redistribution corresponding to an increase in the inner lever arm, compared to the one for the linear elastic stress field. The increase can cautiously be chosen to be 25 percent of the difference between the inner lever arm for the maximum stress redistribution, that is full utilisation of the compressive capacity of the concrete, and the inner lever arm for the linear elastic stress field. A larger stress redistribution might be possible, but this requires data from more studied cases.

  Several factors need to be considered when using a strut and tie model not following the linear elastic stress field in the serviceability limit state, such as:

  - Reinforcement amount and arrangement.
  - The relationship between the utilised stress redistribution for the design load in the ultimate limit state and the maximum available stress redistribution.
  - The relationship between the design load in the serviceability and ultimate limit states.
  - The degree of stress redistribution due to cracking.
  - The continuity of the increased stress redistribution due to cracking
  - The relationship between the stress redistribution due to plasticity and that due to cracking.

  The full influence of these factors on the result and hence the possibility to use a higher value of the stress redistribution, than the 25 percent mentioned above, has not been thoroughly investigated in this work due to time limitation.

  Regarding the ultimate limit state, more data is required to be able to comment on which factors determine the conditions for deviating from the linear elastic stress field.

What effects do geometry, material, reinforcement content and reinforcement arrangement, respectively, have on the stress redistribution and crack development that takes place?

- There is a trend towards a more continuous increase in stress in the reinforcement, and less prominent discontinuities during the cracking process up to yielding of the reinforcement when the tensile reinforcement ratio is increased and when use is made of surface reinforcement. A similar tendency, though less pronounced, applies if the main tensile reinforcement is distributed in more than one layer at the bottom of the deep beam.
- Surface reinforcement and the distribution of the main tensile reinforcement at the bottom of the deep beam over more than one layer contributes to a more even distribution of the cracks, thus reducing the risk of a single large and concentrated crack.
- A favourable effect on the crack width can be obtained by distributing the main tensile reinforcement at the bottom of the deep beam over more than one layer.

In chapter 1.3 a number of research questions is presented. The work presented in this thesis does not present answers to all the questions. Restrictions due to the geometry studied in the thesis made it difficult to study the stress redistribution due to plastic deformation in the ultimate state. In order to present more general conclusions concerning stress redistribution due to cracking and plastic deformation more studies of various geometries, reinforcement ratios and reinforcement arrangements is required.

5. Further research

In this last chapter, suggestions and motivations for future research are presented.

5.1. Topics related to the present research

- Further comprehensive examinations of the effects of geometry, material, reinforcement ratio and reinforcement arrangements in other geometries than the presented deep beam. This in order to be able to provide recommendations and guidelines on how to apply strut and tie methods for both the design and verification of D-regions, taking into account of various requirements and fulfilling the required deformation capacity.

  Motivation: In existing documents, such as Eurocode SS-EN 1992-1-1, there is a lack of guidance about under which conditions and to what extent one can deviate from a linear elastic stress field in the ultimate and serviceability limit states. Comprehensive examinations and knowledge of the effects of geometry, material, reinforcement ratio, and reinforcement arrangements on the stress redistribution and deformation capacity for various D-regions, in this case deep beams, are a prerequisite for being able to provide adequate rules in this area.

5.2. Other topics within the subject area

- Investigations of stress redistribution, deformation capacity and crack formation conducted on other discontinuity regions than simply supported deep beams.

  Motivation: There is no standard solution for stress redistribution in discontinuity regions. Each discontinuity region is unique and follows its own rules as to how its stress fields develop with increasing load up to an ultimate load.

- Studies of how corrosion affects stress redistribution, deformation capacity and crack development in discontinuity regions.

  Motivation: This research is particularly called for since various studies have shown the inclination for shear cracks to develop to be affected by corrosion. Possible effects on the stress redistribution, deformation capacity and crack development in discontinuity regions can be of interest when analysing the load bearing capacity of existing structures.

- Comparisons of practical tests with results obtained for stress redistribution, deformation capacity and crack development using nonlinear FE-analyses in connection with different concrete material models.

  Motivation: Different models concerning approaches to cracking can be used in a nonlinear analysis, such as:

  - Discrete crack approach.
  - Smeared crack approach.
  - Embedded crack approach.

  Results from simulations using finite element analysis are essential in providing recommendations concerning the choice of strut and tie models that fulfil requirements applying to an ultimate and serviceability limit state. Because of the huge scatter between finite element model predictions and real test data, it is important to have knowledge of any possible differences of the effects on stress redistribution, deformation capacity and crack development obtained of any concrete material model that is used.

- A survey of the effects associated with whatever reinforcement/concrete interface model one employs in the finite element analytic research, on stress redistribution, deformation capacity and crack development. In connection with this, any impact of the choice of FE-mesh on the concrete-reinforcement interaction, is also examined.

  Motivation: In the present study a simplified bond-slip function for the concrete-reinforcement interaction, examined in terms of a linear relationship, was used, see also Huang, et al. [62] and fib Bulletin 10 [63], as well as new developments concerning bonds reported in MC2010, chapter 6, fib Bulletin 65 [30]. The evaluation of bond resistance is complex and is influenced by many parameters, such as, the geometry of the concrete section, material characteristics and stress state, see fib Bulletin 72 [67]. The size of the FE-mesh is also a parameter that may influence the modelling of the bond resistance and the results concerning the behaviour of the concrete.

- Examining the effect of damage on stress redistribution, deformation capacity and crack development due to cyclic loading.

  Motivation: Damage due to cyclic loading will affect the elastic stiffness of the concrete and the bond-slip function for the concrete-reinforcement interaction. Following effects on stress redistribution and on crack development together with other possible effects of damage due to cyclic loading, should be examined.

- Exploring the results of stress redistribution, deformation capacity and crack development when using 3D-modelling in nonlinear FE-analyses.

  Motivation: Examples of applications of the strut and tie method are often presented as 2D-models. There are also examples in 3D-designs using the strut and tie method, although these are more unusual. One of the reasons for this is the basic idea of the strut and tie method, being an easy-to-use method that can simulate the stress field at the ultimate load. One of the issues that needs to be investigated when the strut and tie method is used in connection with 3D-models is how to model the node areas.

- Developing a framework for, and show on the application of, the strut and tie method in the quality assurance of linear and nonlinear FE-analyses.

  Motivation: There is a need of the quality assurance of linear and nonlinear FE-analysis. Especially the results of nonlinear analysis are strongly affected by the assumptions regarding models for materials, for bond between reinforcement and concrete and for element mesh, for example. The strut and tie method is a suitable method for the interpretation and evaluation of many results concerned with verifying safety as well as function.

6. References

[1] T. Ekström, P.-J. Gustafsson, M. Hallgren, M. Hassanzadeh, R. Malm, L.-O. Nilsson, and S. Thelandersson, "Granskning av beräkningar i betongkonstruktioner," 2016:259, 2016.

[2] EN 1992-1-1, *Eurocode 2: Design of concrete structures - Part 1-1: General rules and rules for buildings*, 2005.

[3] J. Schlaich and D. Weischede, "Manual for detailing of concrete structures," *CEB Bulletin 150,* Paris, Jan. 1982.

[4] J. Schlaich, K. Schaefer, and M. Jennewein, "Toward a Consistent Design of Structural Concrete," *PCI Journal,* vol. 32, pp. 74-150, 1987.

[5] fib Bulletin 66, *Model code 2010 : final draft, volume 2*. Lausanne, Switzerland: International Federation for Structural Concrete (fib), 2012.

[6] CEB-FIP Model Code 1990, *Design of concrete structures*: Thomas Telford, 1993.

[7] K. Schaefer, "Nodes, Section 4.4.4 in Structural Concrete, Vol. 2, 1 edition," *fib Bulletin 2,* 1999.

[8] K. Schaefer, "Deep beams and discontinuity regions, section 7.3 in Structural Concrete, Vol. 3, 1 edition," *fib Bulletin 3,* 1999.

[9] FIP Report, *Practical Design of Structural Concrete. FIP-Commision 3 "Practical Design", Sept. 1999*: SETO, London, 1999.

[10] fib bulletin 16, *Design examples for the 1996 FIP recommendations Practical design of structural concrete*, 2002.

[11] fib Bulletin 61, *Design examples for Strut-and-Tie models* 2011.

[12] K.-H. Reineck, *Examples for the Design of Structural Concrete with Strut-and-Tie Models, ACI SP-208*: ACI, Farmington Hills, 2002.

[13] W. Ritter, ""The Hennebique Construction Method" ("Die Bauweise Hennebique")," *Schweizerische Bauzeitung,* vol. Bd.XXXIII, pp. 41-61, 1899.

[14] E. Mörsch, *Der Eisenbetonbau-Seine Theorie und Andwendung (Reinforced Concrete Construction-Theory and Application)*, 3rd ed.: Stuttgart, Wittwer, K., 1908.

[15] E. Mörsch, "Der Eisenbetonbau-Seine Theorie und Andwendung (Reinforced Concrete Construction-Theory and Application)," vol. 1, 5th ed: Stuttgart, Wittwer, K., 1922.

[16] CEB-FIP, *Model Code for Concrete Structures: CEB-FIP International Recommendations*, 3 ed.: Comité Euro-International du Béton, 1978.

[17] M. P. Collins and D. Mitchell, *Prestressed Concrete Structures*, 1997.

[18] H. Wagner, "Ebene Blechwandträger mit sehr dunnem Stegblech (Metal Beams with Very Thin Webs)," *Zeitschrift fur Flugtechnik und Motorluftschiffahr,* vol. 20, 1929.

[19] D. Mitchell and M. P. Collins, "Diagonal Compression Field Theory-A Rational Model for Structural Concrete in Pure Tension," *ACI Journal,* vol. 71, pp. 396-408, Aug. 1974.

[20] M. P. Collins, "Towards a Rational Theory for RC Members in Shear," *Journal of the Structural Division , ASCE,* vol. 104, pp. 649-666, Apr. 1978.

[21] F. J. Vecchio and M. P. Collins, "The Modified Compression Field Theory For Reinforced Concrete Element Subjected to Shear," *ACI Journal,* March-April 1986.

[22] F. Leonhardt and R. Walther, *Wandartiger träger, DAfStb Heft 178*: Wilhelm Ernst & Sohn, Berlin, 1966.

[23] F. Leonhardt and E. Mönnig, *Vorlessungen uber Massivbau - Zweiter Teil, Sonderfälle der Bemessung im Stahlbetonbau*, 2 ed.: Springer-Verlag, Berlin, Heidelberg, New York, 1975.

[24] P. Marti, "Basic Tools of Reinforced Concrete Beam Design," *ACI Journal,* vol. 82, pp. 46-56, Nov.-Dec. 1985.

[25] A. Muttoni, J. Schwartz, and B. Thurlimann, *Design of Concrete Structures with Stress Fields*: Birkhäuser, 1996.

[26] K. Schaefer, "Nodes, Section 4.4.4 in Structural Concrete, Vol. 2, 2 edition," *fib Bulletin 52,* 2010.

[27] K. Schaefer, "Deep beams and discontinuity regions, section 7.3 in Structural Concrete, Vol. 3, 2 edition," *fib Bulletin 54,* 2010.

[28] J. E. Breen, "Why Structural Concrete? p. 15-26," in *Structural Concrete, IABSE Colloquium, Stuttgart march 1991, Volume 62*, 1991.

[29] K. Schaefer, J. Schlaich, and M. Jennewein, "Strut and tie modelling of structural concrete," in *Structural Concrete, IABSE Colloquium, Stuttgart march 1991, Volume 62*, 1991.

[30] fib Bulletin 65, *Model code 2010 : final draft, volume 1*. Lausanne, Switzerland: International Federation for Structural Concrete (fib), 2012.

[31] fib Bulletin 100, *Design and assessment with strut-and-tie models and stress fields: from simple calculations to detailed numerical analysis*, 2021.

[32] M. P. Bendsoe and O. Sigmund, *Topology Optimization - Theory, Methods and Applications*: Springer, Berlin, Heidelberg, 2003.

[33] Eurocode Software AB, "Strut and Tie - User manual," ed, 2020.

[34] M. Schlaich, "Computerunterstutzte Bemessung von Stahlbetonscheiben mit Fachwerkmodellen," Diss. , ETH Zurich, Bericht 1, Professur fur Informatik, Oktober 1989.

[35] R. Hajdin, "Computerunterstutzte Bemessung von Stahlbetonscheiben mit Spannungfeldern," Diss, Nr. 9167, ETH Zurich, Institut fur Baustatik und Konstruktion, 1990.

[36] K. Ruckert, "Design and analyses with strut-and-tie models - computer - aided methods," in *Structural Concrete, IABSE Colloquium, Stuttgart march 1991, V.62*, 1991, pp. 379-384.

[37] K. Ruckert, "Computer Aided Methods for the Design of Structural Concrete," in *IABSE Workshop, New Dehli*, 1993.

[38] K. Ruckert, "Computer-unterstutztes Bemessen mit Stabwerkmodellen (Computer aided design with strut-and-tie models)," *BuStb 89 (1994), Heft 12,* pp. 319-325, 1994.

[39] W. Sundermann and P. Mutscher, "Nonlinear Behaviour of Deep Beams, p. 385-390," in *Structural Concrete, IABSE Colloquium, Stuttgart march 1991, Volume 62*, 1991.

[40] W. Sundermann, "Tragfähigkeit und Tragverhalten von Stahlbeton-Scheibentragwerken," Diss., Institut fur Tragwerksentwurf und -konstruktion, Univ. Stuttgart, 1994.

[41] Y. M. Xie and G. P. Steven, "A simple evolutionary procedure for structural optimization," *Computers & Structures,* vol. 49, pp. 885-896, 1993/12/03/ 1993.

[42] M. P. Bendsoe, A. Ben-Tal, and J. Zowe, "Optimization methods for truss geometri and topology design," *Structural optimization* vol. 7, pp. 141-159, 1994.

[43] D. A. Kuchma and T. N. Tjhin, "Advances and Challenges to Design by the Strut-and-Tie method," in *Open Paper Session at the ACI Fall Convention 2000 in Toronto, Canada*, 2000.

[44] D. A. Kuchma and T. N. Tjhin, "Computer-Based Tools for Design by Strut-and-Tie Method: Advances and Challenges," *ACI Structural Journal, September-October,* 2002.

[45] G. Elia, F. Palmisano, A. Vitone, and C. Vitone, "An interactive procedure to design Strut-and-Tie models in reinforced concrete structures using the "Evolutionary Structural Optimisation" method," in *Proceedings of the 4th ASMO-UK/ISSMO conference, Newcastle-upon-Tyne, UK July* 2002.

[46] H. M. Salem, "The Micro Truss Model: An Innovative Rational Design Approach for Reinforced Concrete," *Journal of Advanced Concrete Technology,* vol. 2, No. 1, February, pp. 77-87, 2004.

[47] M. S. Lourenco, J. F. Almeida, and N. Nunes, "Nonlinear Behaviour of Concrete Discontinuity Regions," *fib Congress 2006,* 2006.

[48] M. S. Lourenco, "Adaptive Stress Field Models for Structural Concrete," PhD dissertation, IST, Lisbon, 2010.

[49] P. Marti, M. Alvarez, W. Kaufmann, and V. Sigrist, "Tension Chord Model for Structural Concrete," *Structural Engineering International,* vol. 8, No. 4, 1 November 1998, pp. 287-298, 1998.

[50] A. Vitone, F. Palmisano, and C. Vitone, "Load Path Method (LPM) in Detailing Design," in *Proceedings of the 2nd fib congress, Naples June 5-8*, 2006.

[51] N. Kostic, "Computer-Based Development of Stress Fields " in *6th International PhD Symposium in Civil Engineering, Zurich, August 23-26*, 2006.

[52] F. Biondini, F. Bontempi, and P. G. Malerba, "Ricerca di Modelli Strut-and-tie mediante prograam-mazione Lineare," *Studi e Ricerche No, 17,* pp. 121-156, 1996.

[53] M. F. Ruiz and A. Muttoni, "On Development of Suitable Stress Fields for structural Concrete," *ACI Structural Journal, V. 104, No. 4, July-Aug,* pp. 495-502, 2007.

[54] A. Muttoni, M. F. Ruiz, F. Niketic, and M.-R. Backes, "Assessment of Existing Structures based on Elastic-Plastic Stress Fields," École Polytechnique Fédérale de Lausanne (EPFL) Laboratoire de construction en béton (IBETON),2016.

[55] A. Muttoni, M. F. Ruiz, and F. Niketic, "Design versus assessment of concrete structures using stress fields and strut-and-tie models," *ACI Structural Journal,* vol. 112, pp. 605-615, 2015.

[56] G. I. N. Rozvany, "A critical review of established methods of structural topology optimization," *Struct. Multidiscip. Optim.,* vol. 37, no. 3, pp. 217-237, 2009.

[57] M. Fenton, C. McNally, J. Byrne, E. Hemberg, J. McDermott, and M. O'Neill, "Discrete planar truss optimization by node position variation using grammatical evolution," *IEEE Transactions on Evolutionary Computation,* vol. 20, pp. 577-89, 08/ 2016, © 2015 IEEE.

[58] F. Niketic, "Development of a consistent approach for design and assessment of structural concrete members using stress field and strut and tie models," PhD dissertation, Ecole Polytechnique Federale De Lausanne, 2017.

[59] BRIGADE/Plus. BRIGADE/Plus, User´s Manual, Version 6.1 [Online].

[60] ABAQUS. Abaqus 6.14 Online Documentation [Online].

[61] T. Jankowiak and T. Lodygowski, "Identification of parameters of concrete damage plasticity constitutive model," *Foundations of Civil and Environmental Engineering, No. 6,* pp. 53-69, 2005.

[62] Z. Huang, B. Engström, and J. Magnusson, "Experimental and analytical studies of the bond behaviour of deformed bars in high strength concrete," presented at the Fourth international symposium on the utilization of high strength concrete/high performance concrete, 29-31 may 1996, Paris, France, 1996.

[63] fib Bulletin 10, "Bond of reinforcement in concrete," 2000.

[64] R. Malm, "Predicting shear type crack initiation and growth in concrete with non-linear finite element method," Doctoral thesis, Department of Civil and Architectural Engineering, Royal Institute of Technology (KTH), 2009.

[65] M. S. Lourenco and J. F. Almeida, "Adaptive stress field models: Assessment of design models," *ACI Structural Journal,* vol. 110, pp. 83-94, 2013.

[66] K. G. Kempengren, "Non-linear FE-Analysis of stress redistribution in a deep beam," in *High Tech Concrete: Where Technology and Engineering Meet - Proceedings of the 2017 fib Symposium*, 2017, pp. 1200-1208.

[67] fib Bulletin 72, "Bond and anchorage of embedded steel reinforcement in fib Model Code 2010," *Structural Concrete,* vol. 16, pp. 45-55, 2015.

About the author

Kent Kempengren has more than 35 years of experience in design and verification of bridges and tunnels in concrete and steel in the fields of new structures, improvements and repairs of existing structures and load bearing classification. He participates in the SIS technical committee TK 556 "Concrete Structures" which is working on revising Eurocode 2, parts 1 to 4. His research concerns design and verification using the strut and tie method (STM), specifically stress redistribution in relation to needed and available deformation capacity. STM will be an increasingly important tool for practicing engineers for checking and understanding results obtained from nonlinear FE-analyses of reinforced concrete structures.

Kent spends his free time in his weekend cottage on Österlen in the beautiful surroundings near Knäbäckshusen and Stenshuvud National Park with his family.

Printed by Media-Tryck, Lund 2023 NORDIC SWAN ECOLABEL 3041 0903

Lund University
Faculty of Engineering
Department of Building & Environmental Technology
Division of Structural Engineering
Report: TVBK-1057
ISBN: 978-91-87993-23-7
ISSN: 0349-4969
ISRN: LUTVDG/TVBK-22/1057-SE

LUND UNIVERSITY

9 789187 993237